Gezamenlijke opleiding UHasselt en KU Leuven

2020•2021

Faculteit Industriële Ingenieurswetenschappen

master in de industriële wetenschappen: energie

Masterthesis

A pilot project to introduce renewable energy and reduce environmental pollution by using a solar collector in Kenya

PROMOTOR :

Prof. dr. ir. Wim DEFERME

PROMOTOR :

dr. Michael J. SAULO

Kjel Van Schijndel, Leon Vandenberghe

Scriptie ingediend tot het behalen van de graad van master in de industriële wetenschappen: energie, afstudeerrichting elektrotechniek

2020•2021

Faculteit Industriële Ingenieurswetenschappen

master in de industriële wetenschappen: energie

Masterthesis

A pilot project to introduce renewable energy and reduce environmental pollution by using a solar collector in Kenya

PROMOTOR :

Prof. dr. ir. Wim DEFERME

PROMOTOR :

dr. Michael J. SAULO

Kjel Van Schijndel, Leon Vandenberghe

Scriptie ingediend tot het behalen van de graad van master in de industriële wetenschappen: energie, afstudeerrichting elektrotechniek

Foreword

In October 2019, during a class taught by Prof. Dr. Ir. Wim Deferme, we were told about his yearly recurring projects around durable energy in Africa. The project during our master year was already getting form and would involve providing the kitchen of the Technical University of Mombasa of renewable energy. Leon and I were interested in the project and after long hesitation, we signed up for this adventure. During the next year we prepared ourselves for this adventure and the project in faraway Kenya.

We had about 3 months to build a solar collector system. After 3 years of studying behind school desks, it was finally time to use our theoretical knowledge in practice.

This master's thesis was made possible by amongst others, non-profit organization Students For Energy in Africa. For that, we would like to thank this organization for organizing these annual recurring energy projects. Without the organization, this amazing adventure would never have happened. Also the financial support by the organization gave us an extra push in realizing the project. Prof. Dr. Ir. Wim Deferme and Mrs. Karine Evers played a major role in guiding us through the project on both the content, the preparation and the administration. A big thank you for that! We would also like to thank all members of the non-profit organization for supporting and helping us during our waffles sale.

We would also like to thank the people at the Technical University of Mombasa. In particular Prof. Dr. Michael J. Saulo for guiding us into the unknown Kenya and always being available to help us, even with the smallest problem. In addition to our supervisor, the other individuals within the university took care of us and looked after us in various ways. Therefore a heartfelt thank you or to put it in Kiswahili: "Asante Sana!"

Furthermore, without the financial help of VLIR-UOS and Uhasselt in the form of a grant and a budget for the project, we could never have participated and the project would never have been possible. We would like to thank Dr. Els Wieërs and Ms. Karine Evers for guiding us through the application for this Erasmus grant.

Finally, we would like to thank our family, friends and all the individuals who have supported us in the preparation and during our unforgettable experience. As well as everyone who has supported the project financially by means of donations or ordering waffles at our waffle sale!

THANK YOU!

Content table

List of tables

List of figures

Abstract

In the Technical University of Mombasa, 3 meals are prepared daily for about 2000 students. A combination of firewood and LPG is used as the energy source for cooking. For these meals large amounts of boiling water are needed. This not only results in high energy costs, but the use of fossil fuels also creates an unsafe working environment for the kitchen staff and has a large ecological impact. The main goal is to reduce the energy costs for boiling water by 65%. This will be done in an ecological and ergonomic way, using a solar collector.

Based on a literature study, it was decided to use a flat plate solar collector with an internal matrix structure and a glycol solution as intermediate fluid. The system was also designed to use natural convection, such that no external pumps are needed for the flow of the glycol. This concept was drawn in a 3D drawing package and simulations were performed on the design to get a better idea of the size and operation of the installation. The simulations showed an energy saving of 55% on average. As a next step in the project, the installation was built in cooperation with local technicians whereby knowledge transfer took place in both directions.

Finally, measurements were performed on the installation and they correspond well to the simulations made beforehand. The installation provides an average energy saving of 55%. In this way, the main objective has not been achieved but progress has been made on the ecological and ergonomic fronts.

Abstract in Dutch

In de Technische Universiteit van Mombasa worden dagelijks 3 maaltijden bereidt voor zo een 2000 studenten. Als energiebron voor het koken wordt een combinatie van brandhout en LPG gebruikt. Voor deze maaltijden zijn grote hoeveelheden kokend water nodig. Dit zorgt niet enkel voor hoge energiekosten, maar het gebruik van fossiele brandstoffen zorgt ook voor een onveilige werkomgeving voor het keukenpersoneel en heeft een grote ecologische impact. Het hoofddoel is om de energiekosten om water te koken te verminderen met 65%. Dit zal gebeuren op een ecologische en ergonomische manier, gebruik makend van een zonneboiler.

Aan de hand van een literatuurstudie werd besloten gebruik te maken van een vlakke plaat zonneboiler met een interne matrix structuur en een glycol-oplossing als tussenvloeistof. De installatie is ook ontworpen om gebruik te maken van natuurlijke convectie.

Dit concept is uitgewerkt in een 3D tekenpakket en hierop zijn simulaties gebeurd om een beter beeld te krijgen van de omvang en de werking van de installatie. Uit deze simulaties komt een energiebesparing van gemiddeld 55%. De installatie werd later opgebouwd in samenwerking met lokale technici waarbij kennisoverdracht in beide richtingen heeft plaatsgevonden.

Ten slotte blijken de metingen op de installatie goed overeen te komen met de vooraf gedane simulaties. De installatie zorgt dus voor een gemiddelde energiebesparing van 55%. Hiermee is het hoofddoel niet bereikt maar er is wel vooruitgang geboekt op ecologisch en ergonomisch vlak.

1. Introduction

1.1 Situation

This master's thesis was provided by the non-profit organization Students for Energy in Africa [1] (S.E.A.), under the supervision of Prof. dr. ir. Wim Deferme. This non-profit organization realizes annually recurring projects in function of sustainable energy in Africa. These projects are executed by students of UHasselt/KU Leuven in collaboration with the local population. The projects concern the sustainable use of energy sources and have the greater aim of promoting sustainable energy and further distributing similar installations throughout Africa. This way, fossil fuel usage can be reduced throughout Africa. In the previous projects of the non-profit organization S.E.A. several sustainable installations have already been realized such as a windmill, solar panels installation, solar collector [2] and biogas production.

This year's project proposal [3] is written by Prof. Dr. Ir. Wim Deferme (UHasselt/KU Leuven), together with Dr. Michael Juma Saulo (TUM) and will be implemented at the Technical University of Mombasa (Figure 1) [4] (TUM) in Kenya. It is the only Technical University in Kenya situated near the coast.

Figure 1: Main Building Technical University of Mombasa [5]

Of course, for the preparation of the large quantities of food, a lot of boiling water is needed. For this purpose, large kettles are filled with water at room temperature. In order to bring the water to a boil, 70% of the energy is provided by burning wood while the remaining 30% is provided using LPG. In Kenya it is customary to eat hot food 3 times a day. Therefore, in the kitchen (Figure 2) of TUM hot food is prepared 3 times a day.

Figure 2: Inside the main kitchen at Technical university of Mombasa

1.2 Problem definition

The large quantities of meals require large quantities of boiling water. This water is heated in large kettles that can hold up to 50 liters. It can easily take more than one hour to bring the water in such a kettle to a boil. Consequently, a large amount of firewood and LPG is needed, which results in high energy costs. This energy cost has a major impact on the university.

In addition to the energy costs, the use of wood as fuel produces a lot of smoke. Also harmful gasses are released through the use of both wood and LPG. This creates an unpleasant working space for the staff in the kitchen, which even can be unsafe.

Because wood is still mainly used as a source of energy for cooking and heating in Kenya, it also contributes greatly to deforestation in the country. In addition to deforestation, burning wood and LPG creates flue gases that are harmful to the environment. Thus, the current setup is not only economically suboptimal, but it is also ecologically suboptimal.

1.3 Objectives

The main objective of this master thesis is to reduce the energy costs of the kitchen in the TUM by 20%. This will be done by replacing the wood and LPG with a renewable energy source.

It is important that only local materials and workers are used. This way, the local economy is stimulated and the population will be educated about sustainable energy sources so that the installation can be applied in other places. An additional requirement is that the installation must be easy to maintain so that the employees of TUM can maintain it themselves. This means that preferably no complex electronics are used, such as automatic controls.

The solution for this project is already broadly defined. The heating of water for cooking will be divided into two processes. First, the water is pre-heated using a solar collector (Figure 3). This collector consists of panels with copper or aluminum pipes, on which sun rays fall. Solar energy will heat up the intermediate fluid in these pipes. If the storage tank is placed higher than the collectors, the intermediate fluid in the system will automatically flow around by natural convection. This will cause the entire tank to heat with no extra energy needed to pump the intermediate fluid around.

Figure 3: Example solar collector [6]

This pre-heated water will then, in the second phase, be brought to boiling point using biogas. This biogas will be extracted from green waste from the TUM and surrounding restaurants, hotels and markets. With this green waste, a fermentation process will be started to create biogas. The digestate from this fermentation process can also be used as fertilizer afterwards. This project will be executed by Tobias Corthouts and Daan Vanhoudt and will not be discussed further. This thesis therefore only focuses on building the solar collector system.

The main objective by May 2021 is to heat the 250 liters of water to a temperature of 70 °C and in this way reduce the energy consumption by 40%. Together with the project on the biogas installation, the energy consumption could be further reduced. Ultimately, the aim is to eliminate wood and LPG as an energy source. An additional objective is to transfer the knowledge about solar collectors to the local population and students. For this purpose, an energy center will be built so that the system can serve as an educational tool in the engineering major 'renewable energy'. The energy center will not be discussed since the TUM is responsible for it.

1.4 Methods

The master thesis is divided into two phases, a preparatory phase and a construction phase. The first phase takes place in semester 1, in Belgium. In this phase, the design is worked out theoretically as far as possible.

First, with a literature study the different types of solar collectors can be determined. The working principle and different advantages and disadvantages are put side by side for each type. Based on this study, the most promising concepts of solar collectors are selected. The selection criteria are complexity, cost and maintenance. The most suitable concept will be determined using a SWOT analysis.

Once the concept is chosen, the sizing can start. This is done using the available data communicated from the university in Mombasa. These data include the cooking hours, the water consumption and the cooking temperature. The size of the installation is then determined based on these data. After this, the installation is drawn in a 3D software package. This way, a visual representation can be provided to everyone involved.

Based on the 3D design and dimensioning, simulations are carried out in Python to determine the output of the solar collectors throughout the day. By executing the simulations, the number of solar collectors is determined in order to achieve the desired temperature. Using the 3D design, a bill of materials can be drawn up, which specifies the materials and quantities needed. This bill of materials is then sent to the local supervisor, who can make a cost estimate.

In the second semester, the installation will be built at the TUM. In the first weeks of the second semester, adjustments will be made to account for differences in the actual situation from the situation used in the simulations. After this, the building of the installation can begin. The installation is then extensively tested to ensure that it functions as it should and adjustments can be made to improve the installation. Local workers will be assigned to help building the installation. This way, they also learn about the construction of a solar collector system. This will make it possible for the project to be implemented in similar situations, such as local schools.

2. Literature study

2.1 Introduction

A solar collector consists mainly of a piping system which fluid flows through. Due to incoming solar rays, the fluid in the piping starts to heat up. Depending on the type of solar collector, an intermediate fluid and a heat exchanger may be used or not. In an indirect system, an intermediate fluid is used which never leaves the piping of the solar collector. This intermediate fluid loses its absorbed heat through a heat exchange to a water storage. In a direct system on the other hand, the water flows through the solar collector and is directly heated by the incoming solar rays. This way, no intermediate fluid and heat exchanger are needed.

The following sections will first discuss the differences between a direct and an indirect system. Then natural convection is explained. This is a mechanism used in certain types of solar collectors. After this, the different types of solar collectors are explained. And lastly, a SWOT-analysis is conducted on the discussed types to find the most promising design in our situation.

2.2 Direct or indirect system

A subdivision can be made between types of solar collectors depending on whether it is a direct or an indirect system or, more simply, whether or not an intermediate fluid and heat exchanger are used. With a direct system, no intermediate fluid and heat exchanger are used. In this last case, the water to be heated flows through the collector part of the installation itself. This water is thus heated directly from room temperature. In an indirect system, on the other hand, an intermediate fluid and heat exchanger are used. In this case, the intermediate fluid flows through the collector section, which will cause the fluid to heat up. This heat is then given off to the water via a heat exchanger which heats the water and cools the intermediate fluid. The intermediate fluid is then sent through the collector again to heat up. Because the intermediate fluid can never cool further than the water in the storage tank, the temperature of the fluid in the collector section can become considerably higher than that in a direct system.

Figure 4 below shows a schematic representation of a direct and an indirect system. The left figure is the indirect system where the heat exchanger is clearly shown. The cold water enters at the bottom of the vessel and the hot water leaves the vessel at the top. Through the heat exchanger the intermediate fluid flows, the heat of this liquid is transferred to the vessel with water. The right image is the direct system where the water flows through the collector and ends back up in the vessel with water. The hot water from the panels now mixes with the water that is in the vessel. In this way, the vessel starts to heat up.

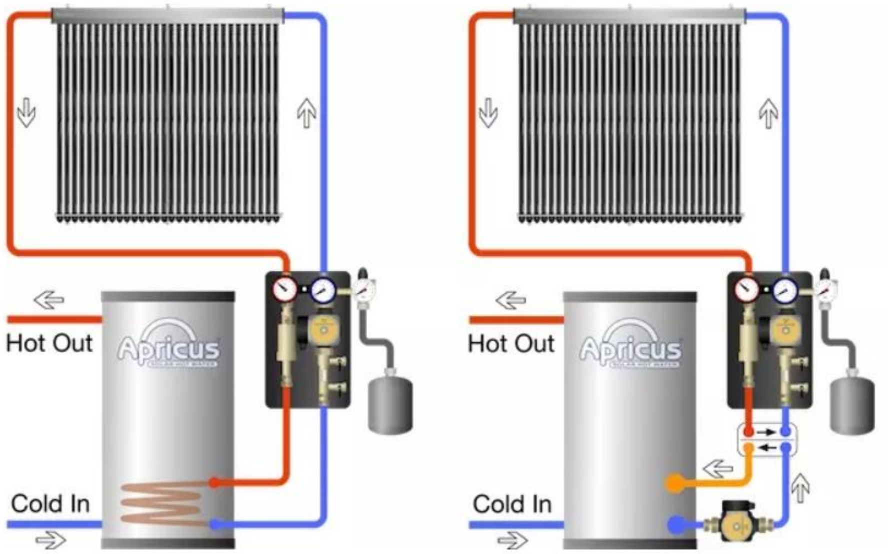

Figure 4: Difference between direct and indirect system [7]

There are several possibilities for the intermediate fluid in an indirect system. Two of which are most commonly used. The first fluid is pure water. Because water is frequently available, this is a cheap solution. When using water, replacing the intermediate fluid is also cheap. The main disadvantage of using water is the limited temperature range. Because water already freezes at the relatively high temperature of 0 °C, water is not suitable for cold climates. If the water freezes in the collector, this could lead to large pressure increases and even cracks in the pipes. However, this will not be a problem for the climate for which this thesis is designing a solar collector. In addition to the freezing of water, boiling at 100 °C also poses a hazard. As the water begins to evaporate, this can again lead to a large increase in pressure which can cause leaks. In addition to the danger of leaks, steam in the pipes also causes poor flow. This should definitely be taken into account for the climate where the installation is going to be build.

Another liquid commonly used in solar collectors is a glycol solution. By mixing glycol with water, the freezing point drops and the boiling point of the liquid rises. For example, a commonly used solution of 30% glycol and 70% water will result in a freezing point of -14 °C and a boiling point of 104.4 °C. This already gives a little more room for exceptional hot and cold days.

In the calculation below, a brief comparison is given between water and a 30% glycol solution as an intermediate fluid. It is assumed that 25 liters of liquid flows through the piping of a collector, both when using water and when using the glycol solution. The glycol solution consists of 30% pure glycol and 70% water. To make a realistic calculation, a temperature difference of 40 °C is assumed. The fluid starts with a temperature of 20 °C and ends at a temperature of 60 °C.

Water

Specific heat of water (C_P) = $4.1842 \frac{kJ}{kgK}$

Water density (ρ) = $984.96 \frac{kg}{m^3}$

Volume = 25 liters = 0.025 m^3

Absorbed heat (Q) = $V * \rho * C_P * \Delta T$

$$Q = 0.025\, m^3 * 984.96 \frac{kg}{m^3} * 4.1842 \frac{kJ}{kgK} * 40\, K = 4121.27\, kJ$$

Glycol solution

Specific heat of glycol (C_P) = $2.21 \frac{kJ}{kgK}$

Glycol density (ρ) = $1109.99 \frac{kg}{m^3}$

Specific heat of glycol solution:

$$0.3 * 2.21 + 0.7 * 4.1842 = 3.591 \frac{kJ}{kgK}$$

Glycol solution density:

$$0.3 * 1109.99 + 0.7 * 984.96 = 1022.47 \frac{kg}{m^3}$$

Absorbed heat (Q) = $V * \rho * C_P * \Delta T$

$$Q = 0.025\, m^3 * 1022.47 \frac{kg}{m^3} * 3.591 \frac{kJ}{kgK}$$

In this equation, the heat taken up for water will be equal to 4121.27 kJ and for the glycol solution it will be 3671.69 kJ. From this it can be deduced that less energy is required to heat up the glycol solution as much as pure water. Thus, the glycol solution will heat up faster than the water at the same energy input. This will result in a higher temperature difference between the intermediate fluid and the water in the storage tank, allowing the heat from the intermediate fluid to be released more easily.

2.2.1 Water quality

It is important to study the water quality when a direct system or an indirect system with water as intermediate fluid is used. A poor water quality can have a negative effect on lifespan of the solar collector. The most important parameter is the hardness of the water. Making use of hard water will result in a buildup of lime in the piping of the solar collector and will result in a worse heat absorption, lower mass flow and eventually in blockages.

For this purpose, the hardness of water in Bilzen, Belgium and Mombasa, Kenya will be compared.

The average hardness of tap water in Bilzen is 138 mg/l dissolved salts [8]. In Mombasa, no tap water is used for cooking. The water used comes from wells. The average hardness of well water in Mombasa is 262 mg/l dissolved salts [9]. This value is so high because Mombasa is a coastal state and water from the sea typically has a high salt concentration.

Water in Belgium usually passes through a water softener to further reduce the hardness of the water used in the household. This typically results in a reduction of the hardness by a factor of 10 [10]. This would result in an average hardness of around 13.8 mg/l. The water in Mombasa on the other hand is directly used from the well for cooking.

If the hardness of the water used in a solar collector is compared between Bilzen and Mombasa, the water in Mombasa is a factor 19 higher than the water used in Bilzen. This will result in a much faster buildup of lime in the solar collector in Mombasa.

2.3 Natural convection

Natural convection is a phenomenon where there is going to be a natural movement of a gas or a fluid. So this theory is applicable to liquids and gasses. For this thesis, the theory of natural convention is only applied to the fluids inside the solar collectors.

Table 1 shows that the density of water at a temperature of 20 °C is equal to 998.29 kg/m³. If the temperature is increased, the density will decrease, as is clearly seen in the table. The density of water at 100 °C is equal to 958.05 kg/m³. If this is compared with the density at 20 °C, then de density has decreased by 4%. This decrease in density is related to the expansion coefficient. As the temperature increases the coefficient of expansion causes the substance to expand. If a substance expands, there is going to be less mass per unit volume and that is exactly what density means. The coefficient of expansion is different for each substance, for water it is 0.21 $\frac{10^{-3}}{K}$ while for methanol it is 1.1 $\frac{10^{-3}}{K}$ [11].

Table 1: Density values for different temperatures [12]

External pressure: 1 atm = 101 325 Pa

Temperature °C	Density kg/m³	Temperature °C	Density kg/m³	Temperature °C	Density kg/m³
0 (ice)	917.00	33	994.76	67	979.34
0	999.82	34	994.43	68	978.78
1	999.89	35	994.08	69	978.21
2	999.94	36	993.73	70	977.63
3	999.98	37	993.37	71	977.05
4	1000.00	38	993.00	72	976.47
5	1000.00	39	992.63	73	975.88
6	999.99	40	992.25	74	975.28
7	999.96	41	991.86	75	974.68
8	999.91	42	991.46	76	974.08
9	999.85	43	991.05	77	973.46
10	999.77	44	990.64	78	972.85
11	999.68	45	990.22	79	972.23
12	999.58	46	989.80	80	971.60
13	999.46	47	989.36	81	970.97
14	999.33	48	988.92	82	970.33
15	999.19	49	988.47	83	969.69
16	999.03	50	988.02	84	969.04
17	998.86	51	987.56	85	968.39
18	998.68	52	987.09	86	967.73
19	998.49	53	986.62	87	967.07
20	998.29	54	986.14	88	966.41
21	998.08	55	985.65	89	965.74
22	997.86	56	985.16	90	965.06
23	997.62	57	984.66	91	964.38
24	997.38	58	984.16	92	963.70
25	997.13	59	983.64	93	963.01
26	996.86	60	983.13	94	962.31
27	996.59	61	982.60	95	961.62
28	996.31	62	982.07	96	960.91
29	996.02	63	981.54	97	960.20
30	995.71	64	981.00	98	959.49
31	995.41	65	980.45	99	958.78
32	995.09	66	979.90	100	958.05

Densities will vary for certain temperatures. Because the density of water at 100 °C is lower than that of 20 °C, the hot water will tend to float upward. So in a container of water, the cold water will be found at the bottom because the density is higher and the hot water will be found at the top of the container because the density is lower. Important to mention is that this is only valid if the water is warmer than 4 °C. When water gets cooled down from 4 °C, it will also expand which will make the density go down. However, temperatures lower than 4 °C will never occur in our case so this doesn't cause a problem.

The same thing will happen with a glycol-solution. As seen in Table 2, the density of the solution will go down with increasing density. This will happen with every mass fraction. This means that natural convection will also happen when making use of a glycol-solution.

Table 2: Density of glycol-solution for different mass fractions and temperatures [13]

Density - ρ - (kg/m³) (lb/ft3)												
Mass Fraction of Ethylene Glycol in Solution	Temperature - t - (°C) (deg F)											
	-48	-35	-25	-14	-8	-4	0	20	40	60	80	100
0							1000	998	992	983	972	958
0.1						1019	1018	1014	1008	1000	992	984
0.2					1038	1037	1036	1030	1022	1014	1005	995
0.3				1058	1056	1055	1054	1046	1037	1027	1017	1007
0.4			1080	1077	1075	1073	1072	1063	1052	1041	1030	1018
0.5		1103	1100	1096	1093	1092	1090	1079	1067	1055	1042	1030
0.6	1127	1124	1120	1115	1112	1110	1107	1095	1082	1068	1055	1042

Figure 5 shows a schematic drawing of natural convection during the boiling process of water. In the cooking pot, there is an amount of cold water to start off. By using the gas stove, the liquid is heated. The red arrows show the flow of the hot liquid moving upward. At the same time, the cold liquid is pushed down and starts to heat so a natural flow occurs. This keeps going until the temperature of the liquid is the same everywhere or in other words, the water starts boiling. From then on, there is no difference in density and the natural flow stops automatically.

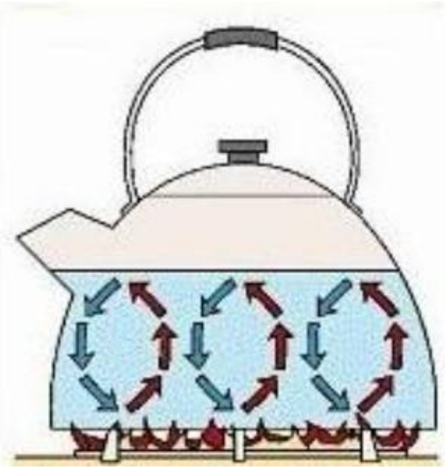

Figure 5: Schematic representation of natural convection [14]

2.4 Solar collector based on the focal distance

2.4.1 The principle

Figure 6 below shows the operating principle of the focal point.

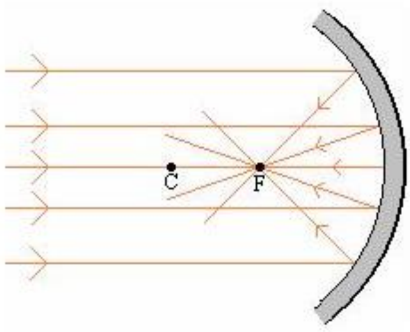

Figure 6: Illustration of a focal point [15]

If a hollow mirror is used and light rays fall on it, these light rays will be reflected towards the focal point. This focal point is indicated on Figure 6 as the letter F. The deflection of these light rays is caused by the shape of the mirror. To do this, the mirror must be perfectly shaped so that all light rays strike in at the focal point. If the mirrors are not perfectly formed then the light rays incident at the point where there is a deformation and will not deflect to the focal point.

The drop in efficiency is proportional to the degree of deformation of the mirror. Under perfect conditions, the light rays converge to the focal point. At this focal point, a certain heat is combined. If an object is placed in the focal point then the heat at the focal point is going to heat up the object. The temperature in the focal point can theoretically reach up to 350 °C. In practice, this value will be lower due to contamination of the mirrors and deviating shape of the mirrors.

The background knowledge of the focal length in Figure 6 underlies the design in Figure 7. Here several mirrors are going to be placed side by side, all of them have a concave shape so that the sun rays are directed inward. In the focal point of these mirrors a pipe is placed. This is an indirect system so an intermediate fluid flows through these pipes and because the pipe is in the focal point this fluid starts to heat up. A circulation pump is used to pump the fluid through the pipes.

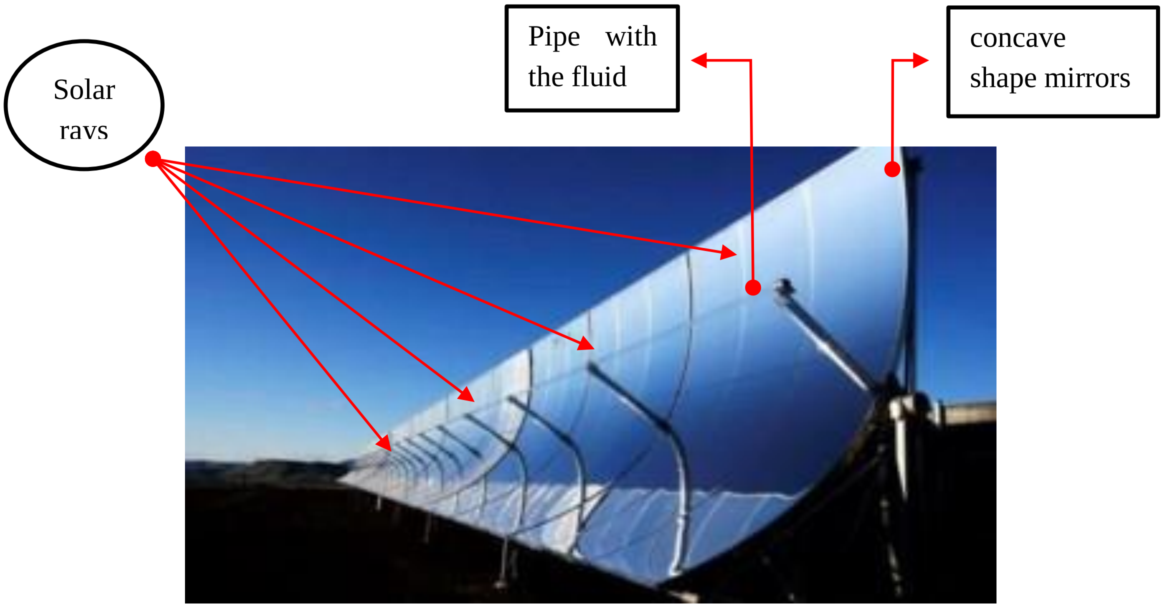

Figure 7: Solar collector based on the focal distance [16]

2.4.2 The theoretical design

Based on the figure above, calculations can be done for dimensioning this solar collector. In these calculations, the focal distance is calculated last. Before the focal distance is calculated directly, intermediate calculations have to be done [17], [18].

At the beginning of the calculations, an outer diameter of the pipe through which the liquid will flow is chosen. Based on this outer diameter, the absorber area is calculated (Formula 1).

$$A_{abs} = \frac{\pi * D_{abs}^2}{4} + \pi * D_{abs} * l \quad (1)$$

Where:

1. A_{abs} : Absorber area,
2. D_{abs} : Outer diameter,
3. l : The length of the pipe.

Based on the absorption area, the aperture area can be determined from the concentration ratio. This ratio (Formula 2) represents the ratio of the aperture area to the absorption area.

$$C = \frac{A_a}{A_{abs}} \tag{2}$$

Where:

1. C : The concentration ratio,
2. A_a : The aperture area,
3. A_{abs} : The absorption area.

Based on the surface area, the inside diameter can be determined. This inner diameter is determined by Formula 3.

$$A_a = \frac{\pi * D_a^2}{4} \tag{3}$$

Where:

1. A_a : The aperture area,
2. D_a : The inner diameter.

Then the half-acceptance angle can be determined (Formula 4). This angle is defined as the angle between which a light source can incident and still be absorbed. Figure 8 gives a clarification of this angle. The dotted line of this angle passes through the focal plane, so it is needed to determine the focal length.

$$C = \frac{1}{\sin^2(\phi)} \tag{4}$$

Where:

1. C : The concentration ratio,
2. ϕ : The half-acceptance angle.

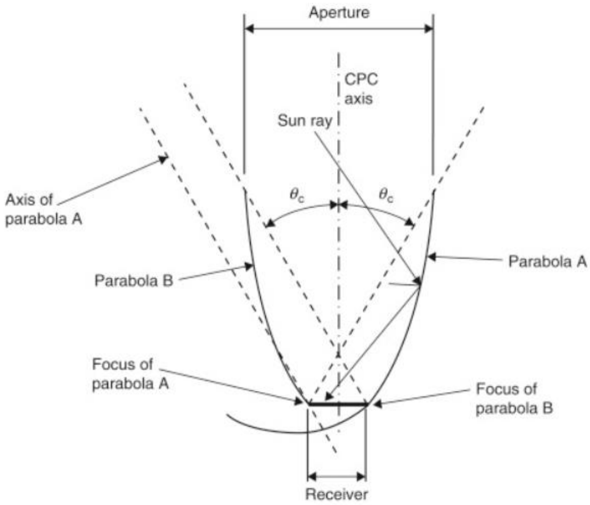

Figure 8: Clarification of the half-acceptance angle [19]

The rim angle gives the maximal angle between the end of the mirror and the center line of the collector. Figure 9 gives a clarification of this angle, it is denoted by φ_r. At the maximum moment this angle is equal to 90°, due to the half-acceptance angle, the rim angle is going to decrease (Formula 5).

Thus:

$$\varphi_r = 90° - \theta_c \tag{5}$$

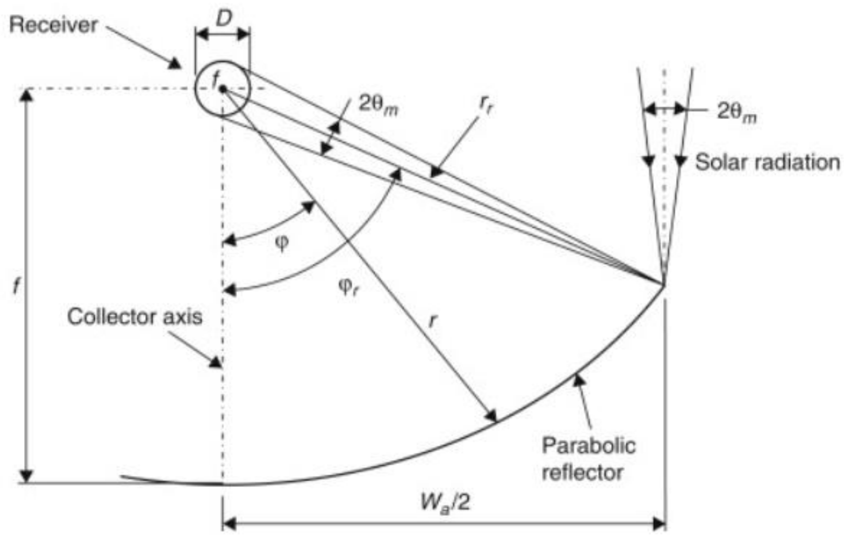

Figure 9: Clarification of the rim angle [20]

Finally, the focal length can be determined by formula 6.

$$\frac{f}{D_a} = \frac{1 + \cos(\varphi_r)}{4 * \sin(\varphi_r)} \tag{6}$$

As a check, the rim angle can also be calculated in another way (formula 7). For this calculation, the focal length must be known.

$$\tan\left(\frac{\varphi_r}{2}\right) = \frac{D_a}{4f} \tag{7}$$

2.4.3 The efficiency

The efficiency of a solar collector based on the focal point can be divided into two types of efficiencies. First is the thermal efficiency and second is the optical efficiency [21].

Thermal efficiency

The thermal efficiency (formula 8) is the ratio of the heat captured by the pipe system to the total heat falling on the system.

$$\eta_t = \frac{Q_u}{Q_s} \tag{8}$$

Where:

1. η_t : The thermal efficiency,
2. Q_u : The useful energy,
3. Q_s : The total incident energy.

Both quantities for the energy can be further developed. Figure 10 gives a graphical representation of the heat arrows that can occur in the parabolic mirror.

The solar rays incident on the system can be described by formula 9.

$$Q_s = I_s * A_a \tag{9}$$

Where:

1. Q_s : The heat from the sunrays,
2. I_s : The solar radiation,
3. A_a : The aperture area.

The heat collected by the tubes can be described by formula 10.

$$Q_u = Q_r - Q_l \tag{10}$$

Where:

1. Q_u : The incident heat on the concentrator aperture,
2. Q_r : The reflected heat,
3. Q_u : The heat losses to the atmosphere.

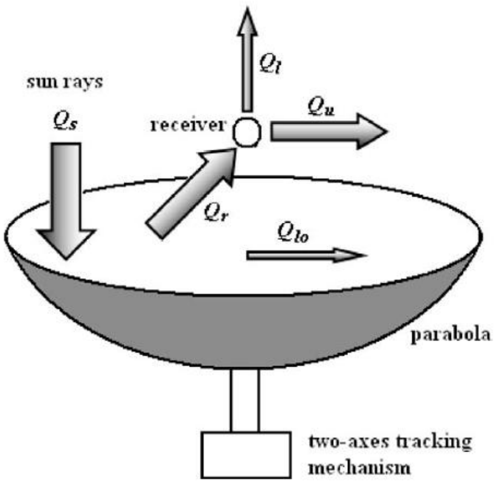

Figure 10: Graphical representation of the heat arrows in the parabolic mirror [21]

In addition, a number of efficiencies can be drawn up based on Figure 10. The optical efficiency (formula 11) is the ratio of reflected rays to incident rays.

$$\eta_o = \frac{Q_r}{Q_s} \tag{11}$$

Where:

1. η_o : The optical efficiency,
2. Q_r : The reflected rays,
3. Q_s : The incident rays.

The receiving efficiency (formula 12) gives the ratio of the heat received by the pipe to the reflected heat.

$$\eta_r = \frac{Q_u}{Q_r} \tag{12}$$

Where:

1. η_r : The receiving efficiency,
2. Q_u : The received heat,
3. Q_r : The reflected heat.

Formulas 8, 10, 11 and 12 can now be combined so that the thermal efficiency can be further elaborated.

$$\eta_t = \frac{Q_u}{Q_s} = \frac{Q_r}{Q_s} * \frac{Q_u}{Q_r} = \eta_o * \eta_r = \eta_o * \frac{Q_r - Q_l}{Q_r} = \eta_o * \left(1 - \frac{Q_l}{Q_r}\right) \tag{13}$$

The final thermal efficiency is described in formula 14.

$$\eta_t = \eta_o * \left(1 - \frac{Q_l}{\eta_o * Q_s}\right) = \eta_o - \frac{Q_l}{Q_s} \tag{14}$$

Optical efficiency

The optical efficiency is the ratio of reflected solar rays to incident solar rays as described in formula 11. This efficiency depends on the type of materials used. This can be considered a disadvantage because if the shape deviates, Q_r will decrease and η_o will decrease as well.

Therefore, there are a number of losses that will cause a reduction in efficiency. The types of losses are described below:

1. Cosine loss,
2. Shading loss,
3. Reflectivity loss,
4. Transmission and absorption loss,
5. Spillage loss.

The cosine loss is expressed in the form of an angle. This angle is the angle of the dish with respect to the sun. If the dish is perfectly oriented towards the sun this coefficient is going to be equal to 1 and no losses are going to occur. But if the dish has a small rotation of 10° then this factor will be equal to 0.9848 and there will be a loss of 1.52%. This loss can be solved by using a tracking system. This tracking system follows the sun and is going to ensure that the dish always points perfectly in the direction of the sun, this way there will be no losses [21].

The shading loss is going to occur because the tube system creates a shadow in the dish. Because of this shadow, no sun rays can reach that spot. This is going to cause a loss. Because the opening of the dish is much larger than the shadow by the tubes this loss will be only ± 1%.

The reflected loss is a loss that is going to occur when solar rays fall on the dish. Not all of the sun's rays are reflected and some will be lost. This loss has an order of magnitude of 6 to 10% so that 90 to 94% of the sun rays are reflected. This efficiency depends on the type of material used. If the dish has a perfect surface, the efficiency will be around 94%. But if there is dust or dirt due to the weather conditions then this factor goes down to 90%.

The transmission and absorption loss is a loss that occurs from the reflected rays to the object in focus. The reflected rays go by transmission to the object, in this case the object is the pipe system. If they use an object where the transmission happens ideally and the object is isolated from the outside environment, then the transmission coefficient will be equal to 1. Such an object is also called a black body. The pipe system is not an ideal object, so the transmission will not be ideal and there will be a loss of 7 to 12%.

The spillage loss is a waste of the solar rays. These solar rays do not reach the opening of the dish and will cause an additional loss of ± 3%.

All these factors can be brought together into 1 formula (Formula 15) that incorporates all these losses.

$$\eta_o = \Lambda * \tau * \alpha * \gamma * \cos(\theta) \tag{15}$$

Where:

1. $\cos(\theta)$: The cosine loss,
2. Λ : The shading loss,
3. τ : The reflectivity loss,
4. α : The transmission and absorption loss,
5. γ : The spillage loss.

If a tracking system is used, then the cosine loss is not going to occur and it will not be taken into the formula. This way, the previous formula can be rewritten:

$$\eta_o = \Lambda * \tau * \alpha * \gamma \tag{16}$$

Lastly, the effects of the flowrate on the outlet temperature will be discussed.

The temperature of the liquid that flows out of the pipe is around the boiling point of water. Because one pipe is used, the flow rate is going to be low. This is because the liquid needs time to warm up. If the flow rate is to high then the fluid does not have time to go to the desired temperature and the efficiency of the design will drop. Figure 11 below shows the variation in temperature for different flow rates. If the flow rate is 0.36 L/min, the temperature of the fluid at the end of the pipe is going to be equal to 45 °C. However, this is a large difference from the 62 °C where a flow rate of 0.2 L/min is used [22].

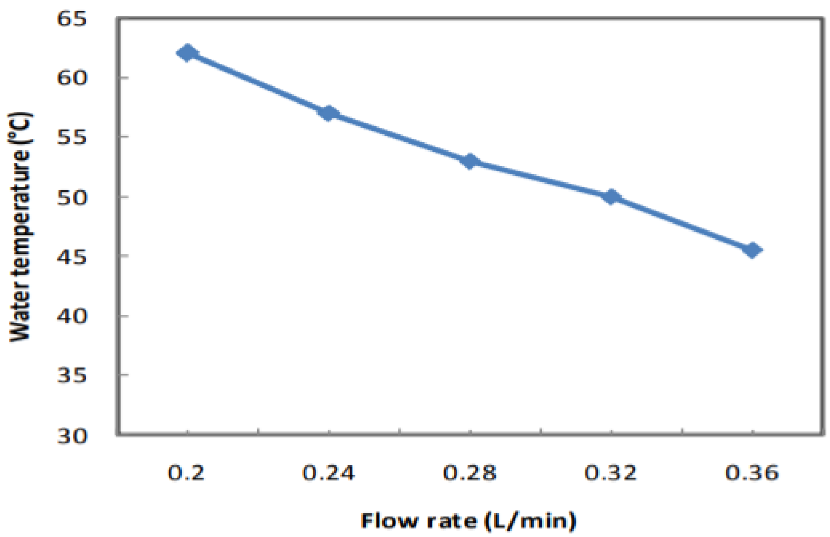

Figure 11: Impact of the flow rate on the temperature [22]

Then the intermediate liquid is pumped to a storage vessel. The heat from the liquid is transferred to the large amount of water. Depending on how long the fluid flows through the storage vessel and the size order of the vessel, the water is going to get a certain temperature. The circulation of the pipes through the storage vessel is a closed system. In this process the fluid does not come into direct contact with the water. Heat transfer occurs only by convection from the fluid to the pipes to the water.

2.4.4 The advantages and disadvantages

There are a number of advantages and disadvantages with this method. First, this design is a simple mechanism because the underlying theory is based on a simple principle. Theoretical values for the temperature at the focal point are around the boiling point, the practical values are shown in Figure 11. despite this, the design has a difficult construction, this is because the mirrors must have a perfect shape so that the sun rays end up at the focal point. As mentioned above, the flow rate must be low so that high temperatures can be achieved at the tip. The mirrors create an additional cost due to the difficult manufacturing process to get the mirrors the shape they need to work efficiently

The advantages of the focal solar collector:

- Simple mechanism,
- Temperatures are around the boiling point (theoretically).

The disadvantages of the focal solar collector:

- Difficult construction,
- Large installation,
- Low flow (0.2L/min) rate for high temperature.

2.5 Spherical solar collector

2.5.1 The principle

The figure below (Figure 12) shows the shape of a solar collector based on a spherical shape. The solar collector is constructed with a system of tubes. These tubes are coiled and shielded by a dome. The tubes are rolled up and the total solar collector is much more compact than the solar collector based on the focal point. At the bottom of the solar collector, cold water enters, this water is going to be warmed up by the solar rays falling on the dome. The water is now going to slowly flow upwards and gradually get warmer. Finally, at the top of the solar collector, the hot water flows out. This is an indirect solar collector so no intermediate fluid and heat exchanger are used.

Figure 12: Solar collector based on a spherical shape [23]

2.5.2 The theoretical design

The solar collector consists of a couple of components which each have their function.

The first and most important component is the water tube. This tube will hold the water during the heating process. It is important this tube is made from a flexible material since it will be coiled up inside the collector. The material of the tube does also need a low thermal resistance to improve the heat absorption of the water.

The second one is the stand for the tube. It has the form of a spiral staircase and is designed to hold the tube in position. A hard plastic is usually used for this since it is cheap to produce and does the job.

The third one is the dome. It is half a sphere that fits over the tubing. Its function is to protect the tubing from dust and weather conditions to improve the lifespan of the collector. This dome should of course be made from a clear material so the solar rays still reach the tubing.

And the last one is the mounting plate. The stand with the tubes and the dome are connected to this plate to create one piece. This plate can also be used to connect the collector to angled surfaces.

This type of solar collector is designed to heat pools. The idea of the collector is that it can easily be mounted after the filter installation. This way, no extra circulation pump is needed which reduces the cost. This is also why the tubing in the collector has a rather high diameter since it needs to accept the same mass flow as the filter of the pool. The suggested setup can be seen in Figure 13.

Figure 13: Suggested setup spherical solar collector [24]

2.5.3 The efficiency

The efficiency of the spherical solar collector can again be divided into two parts. First the thermal efficiency and second the optical efficiency.

The thermal efficiency can be calculated from the heat absorbed by the water and the heat provided by the sun. The absorbed heat can be calculated using the following formula:

$$Q_u = m * c_p * (T_o - T_i) \tag{17}$$

Where:

1. Q_u : The absorbed heat by the fluid inside the tubes,
2. m : The mass flow of the fluid inside the tubes,
3. c_p : The specific heat of the fluid inside the tubes,
4. $(T_o - T_i)$: Difference in temperature between hot and cold side inside the tubes.

The incoming heat can be found using the solar radiation and the total area of the spherical solar collector.

$$Q_i = I * A_t \tag{18}$$

Where:

1. Q_i : Total incoming heat,
2. I : Solar radiation,
3. A_t : Total area spherical solar collector.

The thermal efficiency can now be found using the following formula:

$$\eta = \frac{Q_u}{Q_i} \tag{19}$$

Formula's 17 and 18 can be filled in formula 19 to give us formula 20 which gives the thermal efficiency.

$$\eta = \frac{m * c_p * (T_o - T_i)}{I * A_t} \tag{20}$$

The optical efficiency on the other hand, is dependent on the position of the sun. For every solar position, an illuminated area can be derived. When the position of the sun is right above the collector, this illuminated area is maximal so the optical efficiency will be 100%. The illuminated area is found by taking the area of the spherical solar collector projected on a plane perpendicular to the solar position.

If the maximal projected area is equated to 1, the efficiency is directly shown by this area for every solar angle. Figure 14 shows the optical efficiency for the different solar angles.

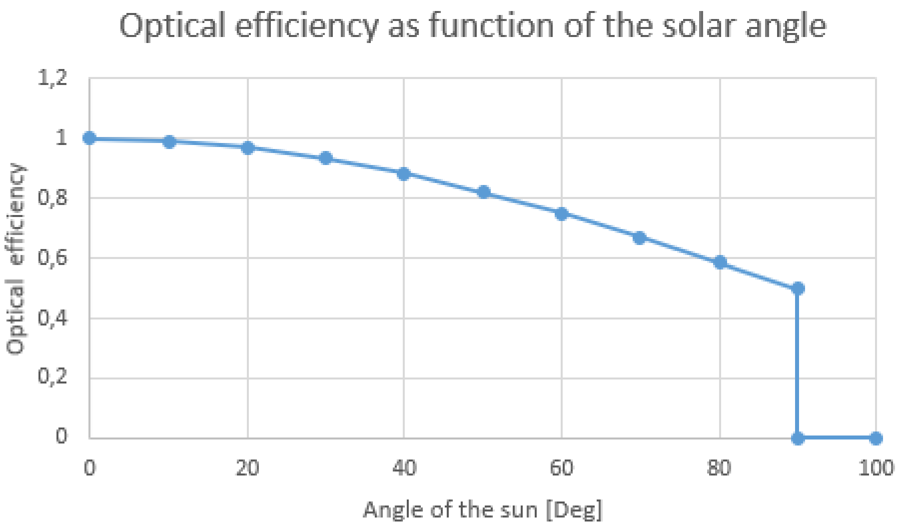

Figure 14: Optical efficiency as function of the solar angle

With an angle of 0 degrees, the sun is directly above the collector. Now the projected area is at the maximum. As the sun descends, so does the efficiency until it reaches an angle of 90 degrees with an efficiency of 50%. At this point, the sun is positioned right above the horizon. With an angle greater than 90 degrees, the sun sets. Now no solar rays reach the collector anymore and the efficiency drops to 0%.

2.5.4 The advantages and disadvantages

The shape of this solar collector is a big difference in the pros and cons. The compact shape of the solar collector means that it takes up half as much space. In addition, only a pump is going to be needed to pump the cold liquid upwards. The tubing is coiled so the flow rate is 4 times higher. This design will also be 70% cheaper because compared to the previous design no expensive mirrors are needed.

Because the tubes are not flat, the sun's rays cannot give off their full energy everywhere. If the sun is straight above the solar collector, the solar rays can reach the tubes over the entire dome. If the sun has a deviation and is not straight above the solar collector, a shadow will be created. This conclusion can be expressed in figures, if the sun has a 45° deviation from the perpendicular of the solar cylinder, a shadow will be created and the efficiency will drop by 20%. The temperature difference between inlet and outlet is 20 to 30 degrees Celsius. These are very low values which is why this design is often used in heating a swimming pool and not for building a solar heating system.

The advantages of the spherical shape solar collector:

- 50% cheaper,
- 4 times more water output,
- Simple design,
- Smaller circulation pump.

The disadvantages of the spherical shape solar collector:

- Efficiency depending on the position of the sun;
- Low temperature difference: 20-30 degrees Celsius.

2.6 Flat plate solar collector

2.6.1 The principle

The principle of the flat plate solar collector is again based on a piping structure where water will flow through. As the name suggests, the piping is encased in a flat plate.

For the heating process, the fluid enters the solar collector at the bottom. The incident solar rays heats up the tubes in the collector. The heat from the tubes flows further into the fluid inside the tubes. In this way the fluid is going to heat up. The flat plate solar collector can be carried out as both an indirect as a direct system. Depending on the version, an intermediate fluid and heat exchanger may or may not be used.

The flat plate solar collector also can be executed with or without circulation pump. When not making use of a circulation pump, natural convection is used to make either the water or the intermediate fluid flow through the collector.

Lastly, there also are different structures possible for the piping itself. Most common are the matrix- and the hose structure. This will be discussed later on.

The flat plate solar collector is a versatile type of collector because so many design choices can be made to suit the needs of the client.

2.6.2 The theoretical design

A flat plate solar collector is composed of a flat box in which the piping structure is placed. Figure 15 clearly shows the construction of a flat plate solar collector [25]. It consists of several layers. The bottom layer (1) is the housing of the collector. This housing is used for mounting the collector on the roof. Above that layer is an insulating material (2). This insulation serves to ensure that the heat stays inside the collector. The tubing (3) is the third layer, through which the liquid flows that is heated by the incoming solar rays. The second last layer is an absorbent plate (4). This plate is treated with a special coating that will ensure that the solar rays enter the solar collector are absorbed. The heat that the plate has collected is then going to be given off to the pipe system. On top of the absorbing plate there is a protective plate (5), this plate will provide protection against weather conditions such as: rain, hail, snow...

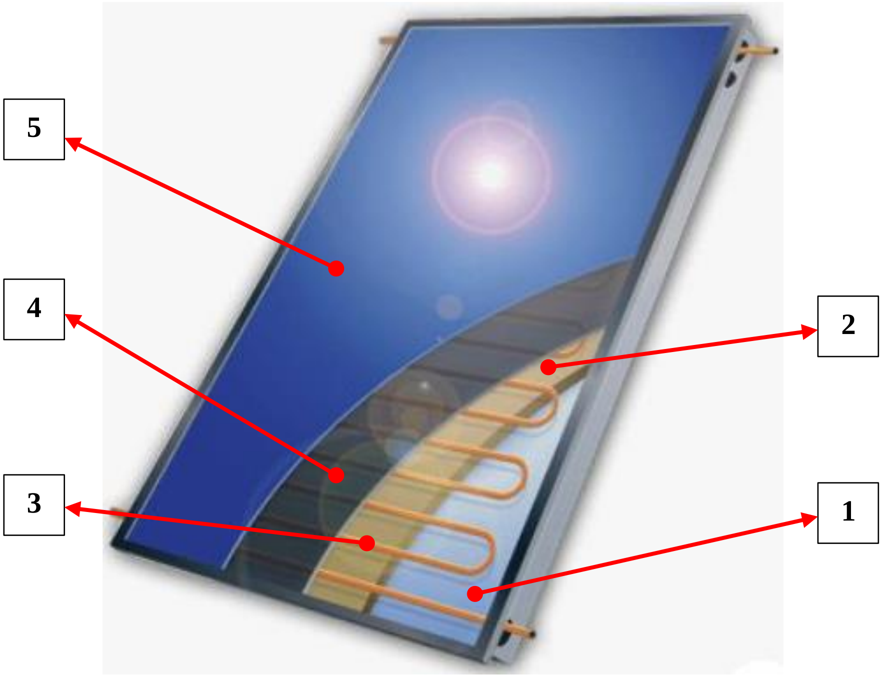

Figure 15: Illustration and construction of a flat plate solar collector [25]

When natural circulation is used instead of a circulation pump, the storage tank has to be placed higher than the collector. A possibility is to place the storage vessel together on the sloping roof (Figure 16). Then there is an additional advantage that the storage vessel can warm up due to the solar rays falling on the vessel. This allows the water in the tank to warm up slightly.

In this setup, no circulation pump is needed but a pump to refill the vessel will be needed if no pressured water is available. This still gives an advantage against making use of a circulation pump since the pump to refill the tank is only active when hot water is used whereas the circulation pump is active during the whole day.

Figure 16: Storage tank placed on the sloping roof [26]

The flat plate solar collector consists mainly of tubing. There are several ways to implement such a system, two examples are shown below (Figure 17).

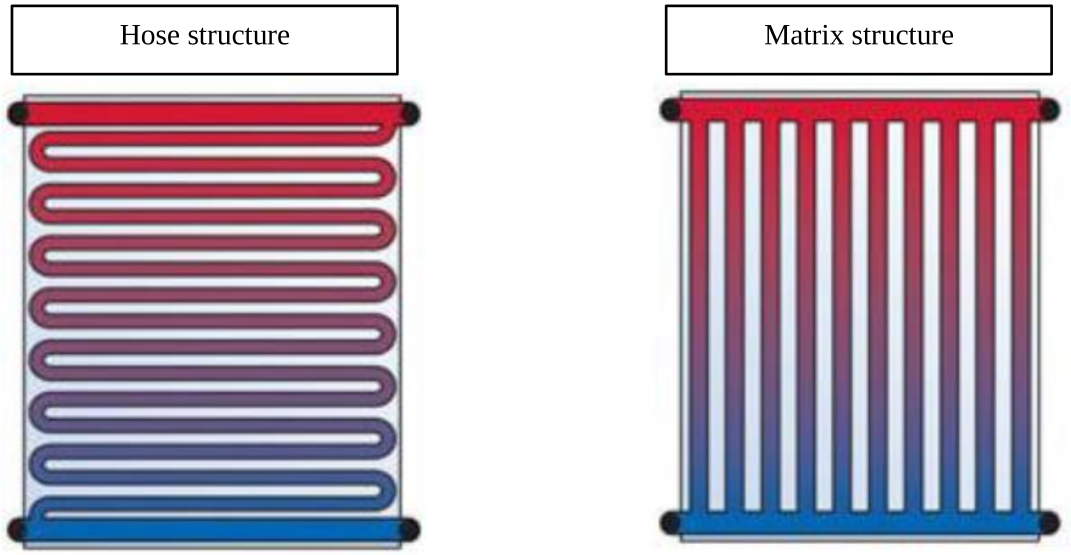

Figure 17: Different implementation forms of tubing [2]

The hose structure consists of one long tube which is zigzagged inside the collector to cover as much of the space as possible. Since it features only one tube, the mass flow will everywhere be the same. A disadvantage of this structure is that it is not ideal to use with natural circulation.

The matrix structure however consist of multiple tubes parallel to each other. The mass flow in the tubes can differ from each other. Especially when making use of natural circulation. Say for example that one tube is totally shaded. The mass flow in this tube will then come to a stop while the liquid might keep running through the other tubes. This will result in a temperature difference in the top between the fluid coming from the different tubes.

Both structures have their advantages. In the hose structure, the mass flow will be the same everywhere and no difference in temperature in the fluid is possible. A disadvantage is that a circulation pump is needed.

In the matrix structure, differences in mass flow and temperature can occur, but it is possible to make use of natural circulation so no circulation pump is needed.

2.6.3 The efficiency

The efficiency of a flat plate solar collector is going to depend on the sun's rays. The solar rays fall in on the solar collector and the fluid can start to heat up. But before the solar rays can heat the fluid there are a number of losses [27].

Figure 18 shows a schematic of the possible losses that can occur in the system. Like the solar collector based on the focal point, these losses can be described as: transmission, reflected and absorbed.

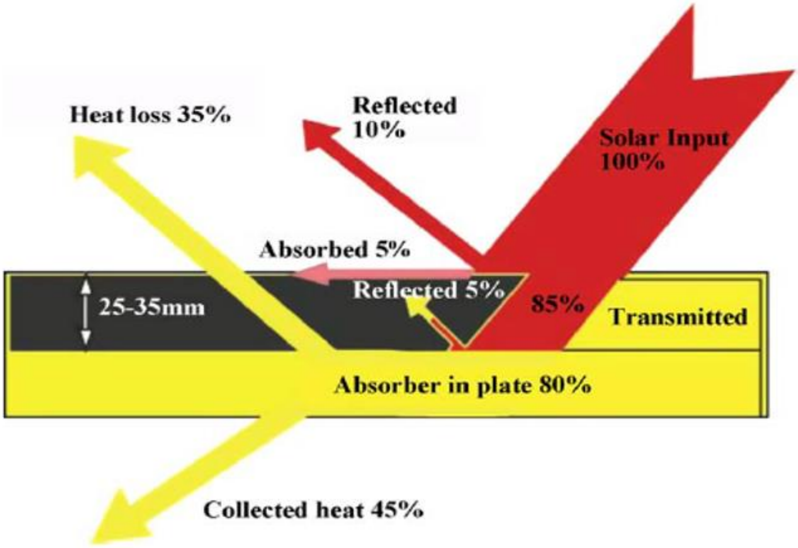

Figure 18: Heat flow through the flat plate solar collector [27]

The incident solar rays first hit the glass plate. Of this energy, 10% is reflected and 5% is absorbed. The remaining 85% then lands on the tubing, 5% of the heat is lost due to reflection on the tubing. Finally, 80% is then absorbed into the tubing. Because of other losses that may occur, the final heat collected is going to be equal to 45%.

The above factors may start to change if the tilt angle is going to change. The tilt angle is the angle between the collectors and the horizontal. Figure 19 gives a clarification of this angle.

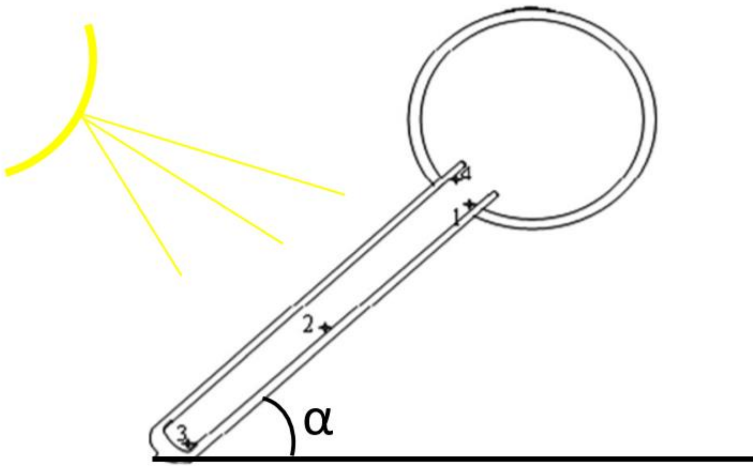

Figure 19: Clarification of the tilt angle [28]

By changing this angle, the sun's rays are going to strike the collectors in a different way. In addition, the factors are also going to change, Figure 20 shows the efficiency for a solar collector placed under a tilt angle of 48.5°. The reflection loss is 34% and the radiation loss is 20%. The final usable energy is 45%. This 45% corresponds to the value from Figure 20.

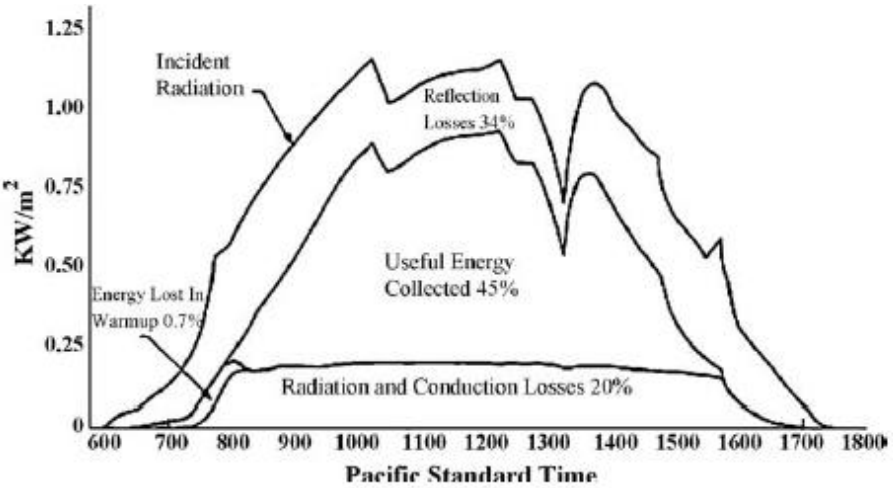

Figure 20: Efficiency of the flat plate solar collector with 48.5° tilt angle [27]

By decreasing this angle, the efficiency raises. Figure 21 shows the efficiency for a tilt angle of 20°. The reflection loss has decreased from 34% to 25%. So by lowering the tilt angle 28.5° the reflection loss is going to decrease by 9%. In addition, the radiation loss also goes down, from 20% to 18%. The other losses also decrease, increasing the usable energy from 45% to 57%.

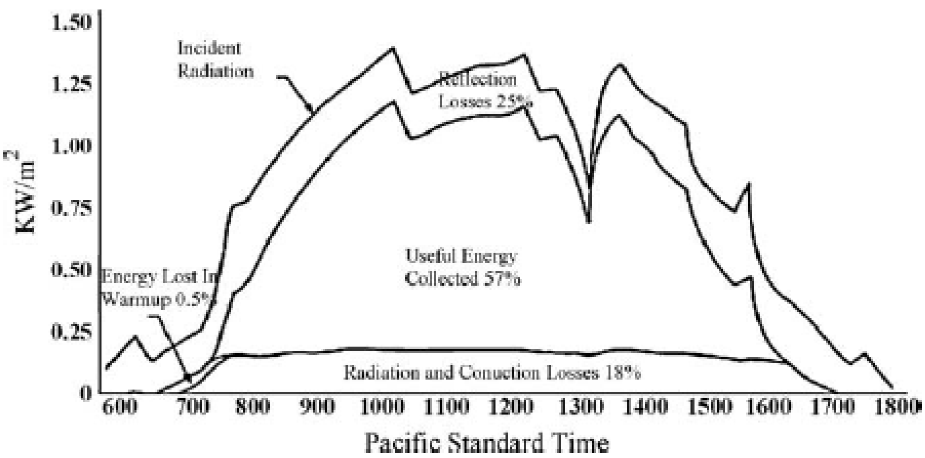

Figure 21: Efficiency of the flat plate solar collector with 20° tilt angle [27]

The efficiency can also be expressed in formulas [29]. Formula 21 shows the heat gain of the solar collector. This heat gain is the multiplication of the solar radiation and the surface area of the collector, considering the loss factors.

$$Q_i = I * \tau\alpha * A \tag{21}$$

Where:

1. Q_i : The heat gain of the solar collector,
2. I : The solar radiation,
3. τ : The transmission factor,
4. α : The absorption factor,
5. A : The surface.

The incoming heat on the collector causes it to heat up. The collector gets a higher temperature than the temperature of the environment. The heat transferred to the environment is written as follows:

$$Q_o = U_L * A * (T_c - T_a) \tag{22}$$

Where:

1. Q_o : The heat transfer to the environment,
2. U_L : The heat transfer coefficient,
3. $(T_c - T_a)$: The temperature difference between the environment and the collector.

The usable heat is the difference between the heat captured and the heat lost to the environment, the usable heat is shown in formula 23

$$Q_u = Q_i - Q_o = I * \tau\alpha * A - U_L * A * (T_c - T_a) \tag{23}$$

Where

1. Q_u : The usable heat,

The usable heat can also be written as the heat that the fluid will absorb and transport through the system:

$$Q_u = m * c_p * (T_o - T_i) \tag{24}$$

Where:

1. m : The mass flow,
2. c_p : The specific heat of water.
3. $(T_o - T_i)$: The temperature difference between the intermediate liquid and the collector

Formula 25 shows the heat removal factor, this factor gives the ratio of the useful heat absorbed by the intermediate fluid to the useful gain of heat over the entire surface of the collector.

$$F_R = \frac{m * c_p * (T_o - T_i)}{A * [I * \tau\alpha - U_L * (T_i - T_a)]} \tag{25}$$

Where:

1. F_R : The heat removal factor.

Formula 24 and 25 are now combined so that the usable heat is written in a different way:

$$Q_u = F_R * A * [I * \tau\alpha - U_L * (T_i - T_a)] \tag{26}$$

Analogous to the heat removal factor, the efficiency (Formula 27) is represented as a ratio of the usable heat gain to the total solar irradiance.

$$\eta = \frac{\int Q_u \, dt}{A * \int I \, dt} \tag{27}$$

Where:

1. η : The efficiency.

In formula 27 the efficiency is represented by integrals, if the heat and irradiation through the collector are constant the efficiency can be written as follows.

$$\eta = \frac{Q_u}{AI} \tag{28}$$

Along with formula 26, the heat removal factor is introduced into the efficiency:

$$\eta = \frac{F_R * A * [I * \tau\alpha - U_L * (T_i - T_a)]}{AI} \tag{29}$$

Finally by simplifying the formula, the efficiency of a flat plate solar collector is shown in formula 30.

$$\eta = F_R\tau\alpha - F_R * U_L * \left(\frac{T_i - T_a}{I}\right) \tag{30}$$

The efficiency of the flat plate solar collector can now be plotted on a graph (Figure 22) where the efficient is placed on the y-axis and the ratio of the difference in temperature to solar radiation is on the x-axis. The directional coefficient is equal to the heat removal factor times the heat transfer coefficient: $-F_R * U_L$.

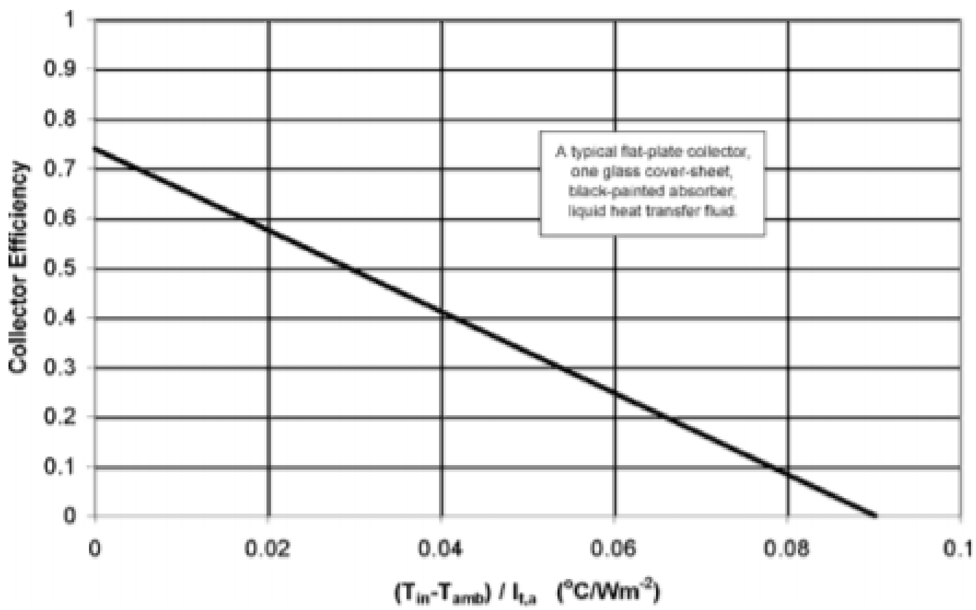

Figure 22: Efficiency of the flat plate solar collector [29]

From this graph, two important points can be derived. On the one hand, the point of intersection with the y-axis and on the other hand, the point of intersection with the x-axis.

At the point of intersection with the y-axis, the maximum efficiency is reached. At that point, the factor $(T_{in} - T_{amb})$ /I is equal to zero. This occurs when the temperature at the inlet is equal to the ambient temperature. At that point, the temperature difference is equal to zero and the entire factor also goes equal to zero.

At the point of intersection with the x-axis, the efficiency has dropped to zero. This point is reached when no more heat is extracted from the collector and the fluid flow comes to a stop. The sun's rays continue to reach the collector, but there is no more flow so the fluid inside the collector continues to heat. This heat is no longer transferred to another medium and the temperature continues to rise. At a certain moment this temperature will be so high that the fluid will start to boil. The temperature will not rise infinitely, it will come to a stop at a certain point. At this point, a stagnation temperature is reached. This stagnation temperature is so high that the absorption surfaces may melt. This causes detrimental effects on the collector such as malfunctions and must be avoided.

2.6.4 The advantages and disadvantages

The biggest advantage of the flat plate solar collector is that it is easy to expand to multiple panels. The pipe system will then be connected to each other in order to obtain more pipe length. In addition, there is no circulation pump needed if a matrix structure is chosen. The disadvantage remains that a circulation pump is needed if the hose structure is chosen.

The advantages of a flat plate solar collector:

- No circulation with the matrix structure,
- Easy to expand to more panels,
- Most known type of solar collector.

The disadvantages of a flat plate solar boiler:

- Circulation pump needed with snake structure.

2.7 Evacuated tube solar collector

2.7.1 The principle

A evacuated tube solar collector consists of a number of tubes connected together in a water storage tank. These tubes are different in structure from the flat plate solar collector. Each evacuated tube consists of two tubes, these two tubes are separated by a vacuum. Figure 23 shows the principle of a vacuum tube. The sun's rays fall in on the outer tube and pass through the vacuum to the inner tube, this causes the intermediate fluid to heat up to boiling point. This will make the intermediate fluid evaporate which makes it rise in the tube. The vapor will condense and give away its heat upon contact with the water in the vessel. The condensate will then flow back to the bottom where it can heat up again. The vacuum in between the two pipes serves as an insulator, so that the heat absorbed cannot be lost to the environment. As a result, the efficiency will be 40% higher than the flat plate solar collector.

The evacuated tube solar collector is always an indirect system since an intermediate fluid and heat exchanger are needed. It also makes use of natural circulation so no circulation pump is needed.

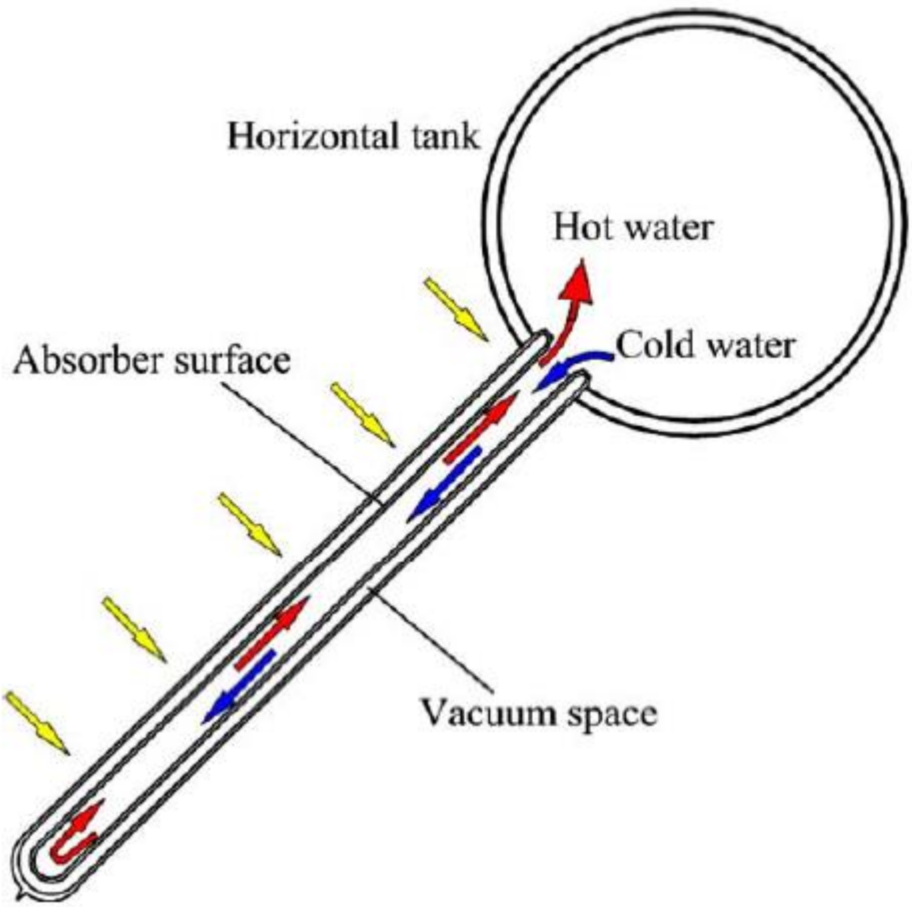

Figure 23: Evacuated tube principle [30]

2.7.2 The theoretical design

As already said, an evacuated tube solar collector consist of multiple vacuum tubes connected to a water storage tank as can be seen on Figure 24 [30]. The tubes have to be angled down to make the natural convection work because the hot vapor has to rise inside the tubes until it reaches the tank. The tubes are usually made from glass and are directly inserted in the water storage tank. This way, the water in the storage tank is in direct contact with the absorber surface of the tube. As intermediate fluid, water is usually used in climates where it does not freeze. This way, the fluid will boil at 100 °C and steam is already created and the natural circulation will start.

The heat exchanger is part of the glass tube itself. This way, the intermediate water never leaves the glass tube and never mixes with water from other tubes or the water tank. This makes it possible to change a single tube when it is broken since the tubes are not connected with each other.

Figure 24: Example evacuated tube solar collector [30]

2.7.3 The efficiency

To determine the thermal efficiency [31] of the evacuated tube solar collector, the heat absorbed by the fluid inside the pipes and the solar irradiation are needed. In this case, the heat absorbed by the fluid inside the tubes is equal to the heat the water will absorb since there is no loss of heat through the vacuum.

The absorbed heat can be found using the following formula:

$$Q_u = m * c_p * (T_o - T_i) \tag{31}$$

Where:

1. Q_u : The absorbed heat by the fluid inside the tubes,
2. m : The mass flow of the fluid inside the tubes,
3. c_p : The specific heat of the fluid inside the tubes,
4. $(T_o - T_i)$: Difference in temperature between hot and cold side inside the tubes.

The incoming heat can be found using the solar radiation and the total area of the tubes perpendicular on the incident solar rays.

$$Q_i = I * A_t \tag{32}$$

Where:

1. Q_i : Total incoming heat,
2. I : Solar radiation,
3. A_t : Total area perpendicular to solar rays.

The thermal efficiency can now be found using the following formula:

$$\eta = \frac{Q_u}{Q_i} \tag{33}$$

Formula’s 31 and 32 can be filled in formula 33 to give us formula 34.

$$\eta = \frac{m * c_p * (T_o - T_i)}{I * A_t} \tag{34}$$

2.7.4 The advantages and disadvantages

The main advantage of this solar collector is that the efficiency is much higher, this is due to the vacuum that serves as an insulation. In ideal conditions, the temperature inside the tube can reach up to 270 °C. In addition to the vacuum, the round tubes allow the sun's rays to enter from any angle. This ensures that the location requires fewer specifications. This type also has disadvantages, one of which is that the design is expensive. Because a vacuum must prevail, it will require maintenance to keep the vacuum as good as possible. Due to the age of the tubing, the condition of the vacuum may vary from when it was purchased.

The advantages of a evacuated tube solar collector:

- High temperatures of up to 270 °C,
- Optimal absorption of solar rays,
- Easy to extend to more panels,
- No circulation pump needed,
- Round tube has less location specifications.

The disadvantages of a evacuated tube solar collector:

- Difficult design due to vacuum,
- Expensive design,
- Maintenance needed.

2.8 The batch collector

2.8.1 The principle

The final design that will be discussed is the batch collector. The principle is similar to the solar collector based on the focal point in the sense that also a reflective material is used to redirect the incoming solar rays. The difference is that now a vessel is placed in the focal point instead of a single tube. Because a vessel is way larger in diameter than the tubes used in the solar collector based on the focal point, the focal point does not have to be as precise. It is enough to reflect the incoming solar rays onto the vessel (Figure 25).

This is a direct system so it does not use an intermediate fluid and heat exchanger. The water to be heated is directly put inside the vessel. It also makes use of natural circulation. When the water in the tank heats up, the hot water rises to the top over the cold water. This way, the hot water can be tapped from the top of the tank while simultaneously refilling cold water from the bottom and no circulation pump is needed.

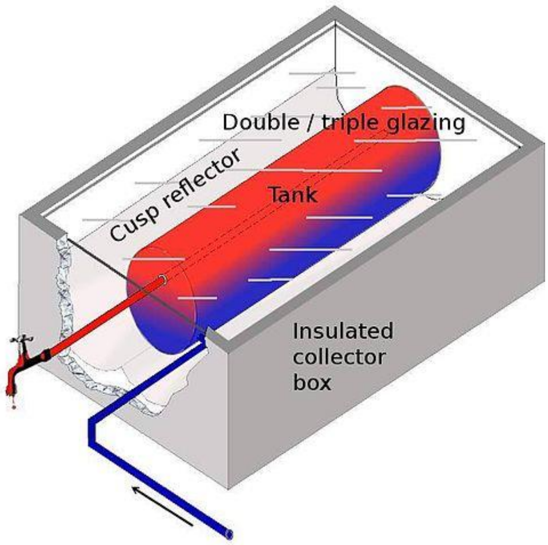

Figure 25: Batch collector principle [32]

2.8.2 The theoretical design

As shown in Figure 26, a batch collector consists of a large vessel placed behind a glass screen. The sun's rays fall in through the glass onto the vessel, causing the vessel and the water in the vessel to heat up. Around the vessel there is a reflective foil. This foil will make sure all solar rays are reflected onto the vessel by making use of the same principle as the solar collector based on the focal point. As earlier said, cold water is refilled at the bottom and hot water will rise and accumulate at the top of the vessel. The vessel is placed in a box for three reasons. The first one is to make the area which solar rays can fall in larger. This way, more solar rays hit the vessel. The second reason is for insulation. Because the vessel itself heats up due to incoming solar rays, it cannot be insulated. This is why the vessel is placed inside an insulated box to reduce the heat loss to the environment. The last reason is to protect the vessel and reflective foil from weather condition and other external influences.

Figure 26: Example batch collector [33]

2.8.3 The efficiency

The efficiency of a batch collector can be calculated in the same way as the efficiency of other solar collectors. This calculation starts with calculating the useful heat absorption which will be divided by the total incoming energy from the sun [34].

The useful heat absorption can be found using the following formula:

$$q_u = Fr * (W_\alpha - D_o) * L_\alpha \left[S - \frac{U_1}{C} * (T_{wi} - T_a) \right] \quad (35)$$

Where:

1. q_u : The useful heat gain,
2. Fr : The heat removal factor (ratio between actual and maximal heat transfer),
3. W_α : System aperture width,
4. D_o : Outside diameter of storage tank,
5. L_α : System aperture length,
6. S : Solar radiation,
7. U_1 : Overall heat loss coefficient,
8. C : Concentration ratio,
9. T_{wi} : Water inlet temperature,
10. T_a : Ambient temperature.

The total energy incoming energy can be found using the following formula:

$$q_t = I_b * R_b * W_\alpha * L_\alpha \quad (36)$$

Where:

1. q_t : The total incoming energy,
2. I_b : Incoming solar radiation,
3. R_b : Tilt factor solar radiation.

With the total incoming energy and the useful heat gain, the thermal efficiency can be determined.

$$\eta = \frac{q_u}{q_t} \tag{37}$$

Where:

1. η : Thermal efficiency.

To get a better insight on the functioning of the batch collector, the experimental temperature variation during one day is discussed. To get this data, the parameters from Table 3 are used.

Table 3: Used design parameters

Parameter	Value
System aperture width (W_α)	0,585 m
System aperture area (A_α)	1,1466 m²
Absorber surface area (A_r)	1,196 m²
Concentration ratio (C)	0,9586
System depth (D_s)	0,457 m
Storage tank volume (V_t)	0,1 m³

With the design parameters from Table 3, the next temperature variation can be found.

Figure 27 shows the temperature variation with a maximum water temperature at 3 p.m. of around 60 degrees. After this, it starts to cool down in the afternoon and during the night until 6 a.m. in the morning. At this point, the water has a temperature of around 23 degrees.

The temperature variation shows us that the water consumption should be minimized during the morning hours since the water is still rising in temperature then. Between 12 p.m. and 18 p.m. the highest efficiency is reached of around 35%.

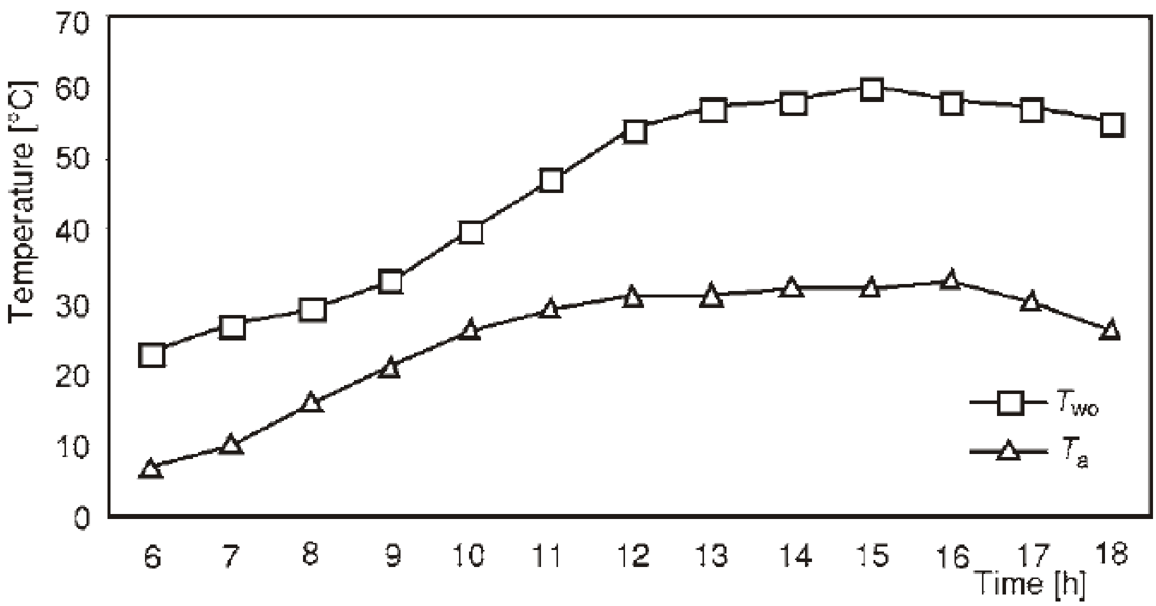

Figure 27: Temperature variation during the day [34]

2.8.4 The advantages and disadvantages

Because the batch collector doesn't need a circulation pump, heat exchanger or intermediate fluid, this design can be 50% cheaper. Also, the water usage during the morning should be minimized to reach a higher temperature in the afternoon. Last, the water tank will cool down easily during the night since the tank cannot be insulated.

The advantages of a batch collector:

- Simple design,
- 50% cheaper than the evacuated tube solar collector.

The disadvantages of a batch collector:

- The tank will cool down during the night due to no insulation,
- The flow rate depends on the volume of the vessel,
- Not easily expandable to multiple panels,
- Limited water usage in the morning.

2.9 Electric heating element

A big problem with solar collectors is the disparity in hot water production. Most of hot water is produced in the afternoon while the production in morning and forenoon is minimal. A solution for this problem is the addition of an electric heating element in the water storage tank [31]. This addition is possible for every design of solar collector that makes use of a hot water storage tank, but will only be discussed for the evacuated tube solar collector.

Figure 28 shows us the evolution of the solar radiation and the ambient temperature during one day as well as the wind velocity. The solar radiation starts in the morning around 100 W/m² and begins to rise during the forenoon. The highest values are reached in the afternoon with a peak of 1000 W/m² at around 14:30. Most of hot water will be produced between 12:00 and 16:00 while in the morning and forenoon, the production will be little.

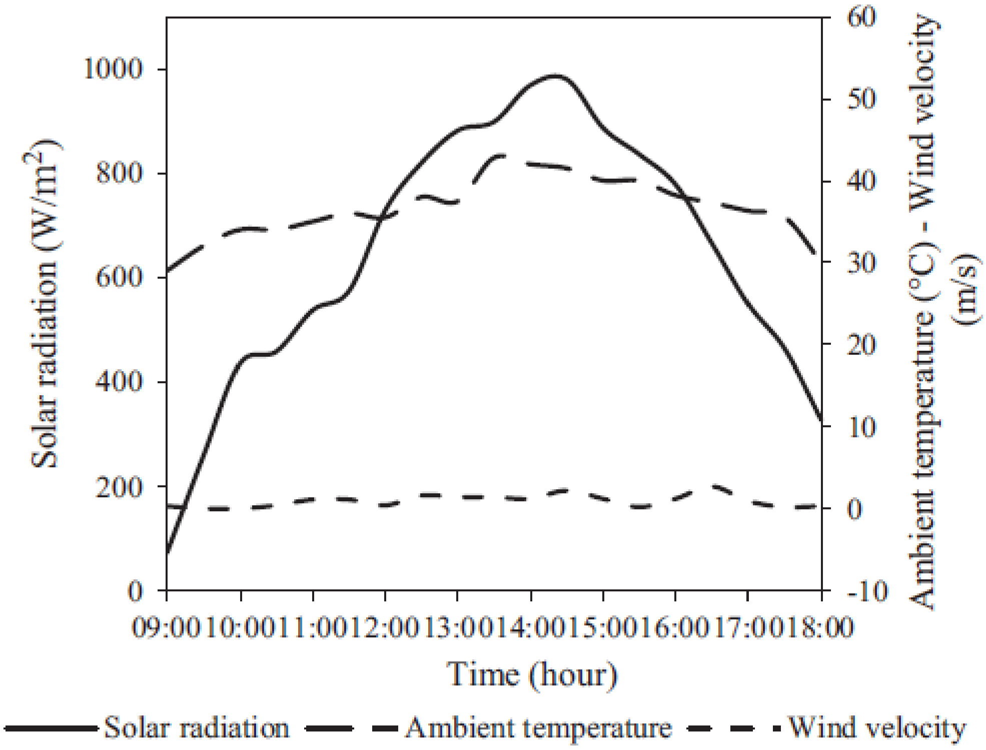

Figure 28: Solar radiation, ambient temperature and wind velocity during one day [31]

Figure 29 shows the input of the electric heating element during one day. Figure 30 shows the input ($T_{c,i}$) and output temperature ($T_{c,o}$) of the fluid inside the collector and the water storage tank temperature (T_t).

The heat element is active in the morning from 9:00 to 10:00 to get the water in the storage tank to the desired temperature. After 10:00, the heat element is only used to compensate heat losses to keep the water in the storage tank at the desired temperature. From 14:00 on, the evacuated tubes take over the heating of the water storage tank so the heat element is not needed anymore.

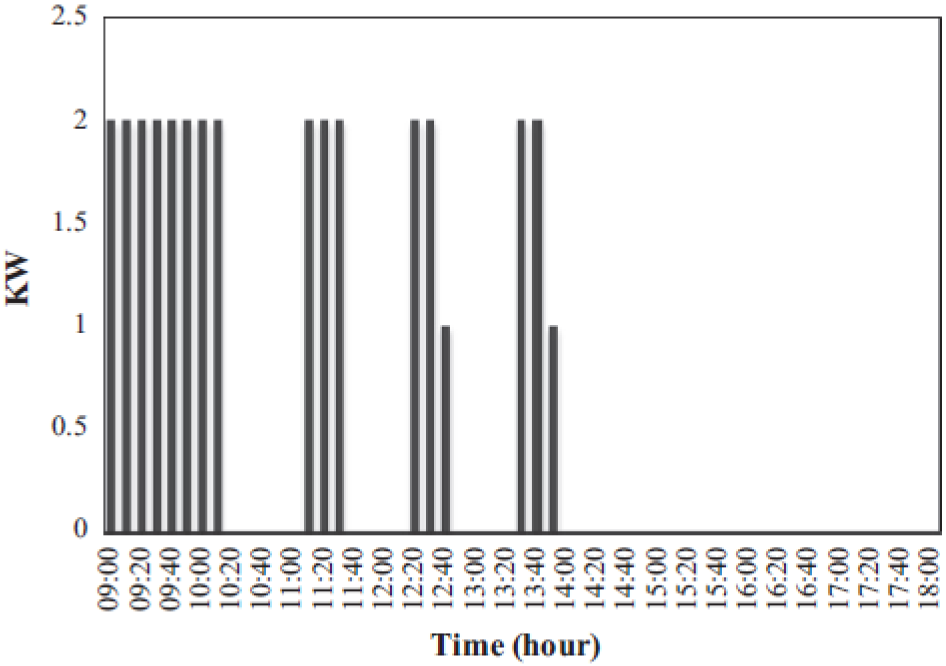

Figure 29: Input electric heat element [31]

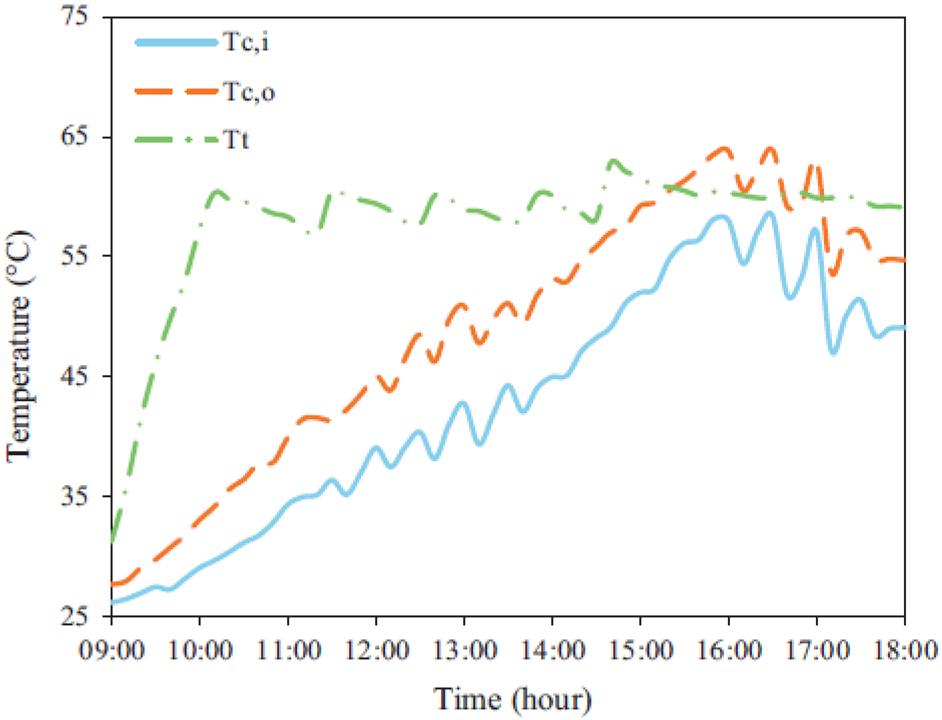

Figure 30: Inlet and outlet fluid temperature and storage tank temperature [31]

The addition of an electric heating element makes sure the available hot water stays around the desired temperature. It is useful to compensate the lower solar radiation during the morning hours, but it can also be used during cloudy days with lower solar radiation where the water would never hit the desired temperature without the electric heating element.

Another solution to ensure hot water during the whole day is making use of an extra storage tank. The water in the collector tank will heat up during the day and in the evening when there is no more solar radiation, the water can be transferred from the collector tank to the extra storage tank. The hot water in the extra tank then can be used during the next day. The extra tank should be insulated, but it will always drop a few degrees during the night. To further reduce the temperature loss of the water, the tank can be placed inside. The temperature will not drop as much during the night inside as outside so the temperature loss will be smaller.

3. SWOT analysis

The purpose of this master thesis is to design a setup to boil large amounts of water in Kenya. This installation must not only be functional, but it must also be easily reproducible by the local population so that it can be implemented in different places later on.

Therefore, the limiting and determining factors will be different the same project would be done in Belgium. The cost price and maintenance are important factors, as is the difficulty of production.

In order to choose the right concept, a SWOT analysis will be performed on the earlier discussed concepts.

3.1 SWOT Analysis: Solar collector based on the focal point

Table 4: SWOT-Analysis: Solar collector based on the focal distance

Strenghts:	Weaknesses:
- Temperature around boiling point, - Fast heat production, - Easy design.	- Takes up a lot of space, - Chance of steam production when using water => intermediate fluid needed, - Heat exchanger needed, - Mirrors must be kept clean.
Opportunities:	**Threats:**
- Buffer tank for hot water storage.	- Precise production of the mirrors so that a focal point is formed; - Solid arrangement of the tube so that it remains in the focal point.

By placing the tube in the focal point of a parabolic mirror, the temperatures of the fluid rise very sharply. This makes it necessary to use a heat liquid so that no steam is created in the pipe. Because of these very high temperatures, a high hot water production can be realized. This in combination with a buffer tank to store this hot water can ensure that hot water is continuously available.

The shape of the mirror is also very important for the proper functioning of the installation. This will make the installation difficult to reproduce by the local population.

Some form of maintenance will also be required to keep the installation functional. It is important that the mirrors remain clean so that the sun's rays are properly reflected. In dusty areas these mirrors will need to be cleaned more often. In addition to cleaning the mirrors, it should be checked whether the pipe is still in the focal point of the mirrors and if not, it should be adjusted.

3.2 SWOT Analysis: Spherical solar collector

Table 5: SWOT-Analysis: Spherical solar collector

Strengths:	Weaknesses:
- Simple construction, - High mass flow, - No heat exchanger needed, - Inexpensive.	- Low temperature gain (20-30 °C), - Circulation pump needed.
Opportunities:	**Threats:**
- Can be reproduced due to simple construction; - Multiple modules to increase temperature gain/mass flow.	- Efficiency dependent on the angle of the sun; - Dome has to be kept clean to improve heat production.

Due to its simple principle and construction, this design can easily be reproduced in Africa. The installation can also easily be expanded to multiple modules to increase the temperature gain/mass flow dependent on the configuration (series or parallel).

This type of solar collector requires also some form of maintenance. The dome of the collector has to be kept clean to improve the efficiency. A circulation pump is also required. This requests also a form of maintenance to prevent failure of the pump.

The main problem with this type of solar collector is that the temperature gain is relatively low. It is commonly used to heat pools where the collector is directly placed after the filter system. This way, no extra circulation pump is needed. For this application, a temperature gain of around 20 or 30 degrees is sufficient to heat the pool by a few degrees during sunny days. However, for cooking purposes, this low temperature gain simply is not enough.

3.3 SWOT Analysis: Flat plate solar collector

Table 6: SWOT-Analysis: Flat plate solar collector

Strenghts:	Weaknesses:
- Simple construction, - Most known type of solar boiler, - Large heat output, - Can be done without heat exchanger.	- Buffer tank for hot water storage required, - Slow heat production => ± 7 hours for 70 °C.
Opportunities:	**Threats:**
- Can without circulation pump, - Can be reproduced,	- Panel must be at the right angle, depending on the trajectory of the sun; - Many connections of pipes => depending on structure.

This type of solar collector is the most known type. It is also relatively simple in construction which makes it possible for local people to reproduce the installation. In addition, this type of solar collector is also flexible, for example, it can be chosen for a hose or a matrix structure, both of which have their advantages and disadvantages. Also, it is not necessary to use a heat fluid depending on the conditions of use.

As with the focal solar collector, dust has a negative impact on the operation of the system. As a result, some form of maintenance will also be necessary here.

A buffer tank will also be required here. This will store hot water during warm moments in the day so that it can be used during colder moments. In this way the hot water will be continuously available.

3.4 SWOT Analysis: Evacuated tube solar collector

Table 7: SWOT-Analysis: Evacuated tube solar collector

Strengths:	Weaknesses:
- High heat production, - No heat circulation pump needed, - High efficiency.	- Expensive and difficult construction; - Intermediate fluid and heat exchanger needed; - Difficult to reproduce.
Opportunities:	**Threats:**
- Number of tubes can easily be chosen.	- Tubes have to be kept clean to improve heat production; - Vacuum has to be replaced over time.

Because of the vacuum around the tubes, close to none heat is lost to the environment due to transmission losses. This causes the efficiency of this type to be the highest from all types discussed above. This also causes the heat gain to be high.

Inside the tubes, natural convection is used to get the heat to the heat exchanger in the water tank. This means no circulation pump is needed.

As for maintenance, the tubes have to be kept clean like every type of solar collector. In addition to this cleaning, the vacuum has to be replaced over time to not lose in on the efficiency.

The biggest problems with this type of solar collector are the high cost and the difficult construction. The high cost itself makes it difficult to reproduce the installation by the local population. But the difficult production of the vacuum tubes makes it not feasible to build the installation in the first place with the limited materials in Kenya.

3.5 SWOT Analysis: Batch collector

Table 8: SWOT-Analysis: Batch collector

Strengths:	Weaknesses:
- Simple construction, - 50% cheaper, - No heat fluid required, - No circulation pump required.	- Slow production => ± 6 hours depending on size tank, - Large setup.
Opportunities:	**Threats:**
- Buffer tank for hot water storage, - Easily reproducible.	- Tank must remain filled for proper operation.

Due to the lack of heat fluid and a circulation pump, this type of solar collector is very simple and inexpensive to construct. As a result, it is easily reproducible by locals.

For proper operation, the tank must be continuously refilled. Thus, this type requires a little more maintenance than the previous types discussed.

The major problem with this solar collector is that it has a very slow heat production. In order to provide a large heat production, it will therefore be necessary to build several collectors. This is possible in combination with a buffer tank, which will quickly make this a very large set-up.

3.6 Conclusion

From the analysis above, it is decided to use the flat plate solar collector. It uses a simple principle and has a relatively simple construction. This should make it easier to reproduce by the local population. It is also a flexible design so it can be customized to fit different situations with minor adjustments. The flat plate solar collector can also be easily extended to multiple panels. In this way, the desired temperature can always be met. When multiple panels are installed, the final temperature will be higher. A disadvantage is that some form of maintenance will always be necessary in the form of keeping the panels clean. This is needed because dust has a negative effect on the efficiency of the installation. This maintenance will always be needed, regardless of which type of solar collector is chosen.

It is also decided to design the installation based on natural circulation. This way, there is no extra cost for a circulation pump and the power it needs. This also reduces the maintenance and increases the reliability because there is no pump that can fail and electrical blackouts don't affect the installation.

Because the installation is going to use natural circulation, the matrix structure is preferred for the tubing inside the collector since natural circulation works better with the matrix structure. With a hose structure, the pressure loss would be too high, preventing natural circulation.

The installation is also going to work indirect with a glycol solution as intermediate fluid. This because the water in Mombasa has a lot of dissolved salts in it. The use of this water inside the collector would result in a buildup of lime inside the piping of the collector which reduces the efficiency and the lifespan of the installation.

Because the cooking starts already at 7 a.m., a system is needed to ensure hot water during the whole day. For this, an extra storage tank is chosen. The other option is to install an electric heating element in the collector tank. This would come with an extra purchase cost as well as a working cost. The usage of an extra storage tank also doesn't impact the reliability as much as the electric heating element since it does not use any electrical components that might malfunction. Also, when using an electric heating element this will require another power source which will make maintenance more difficult.

4. The concept

From the comparative study conducted, it is decided to use the flat plate solar collector with the matrix structure and a glycol solution as intermediate fluid. The installation will also make use of natural circulation. Figure 31 shows a schematic overview of the setup.

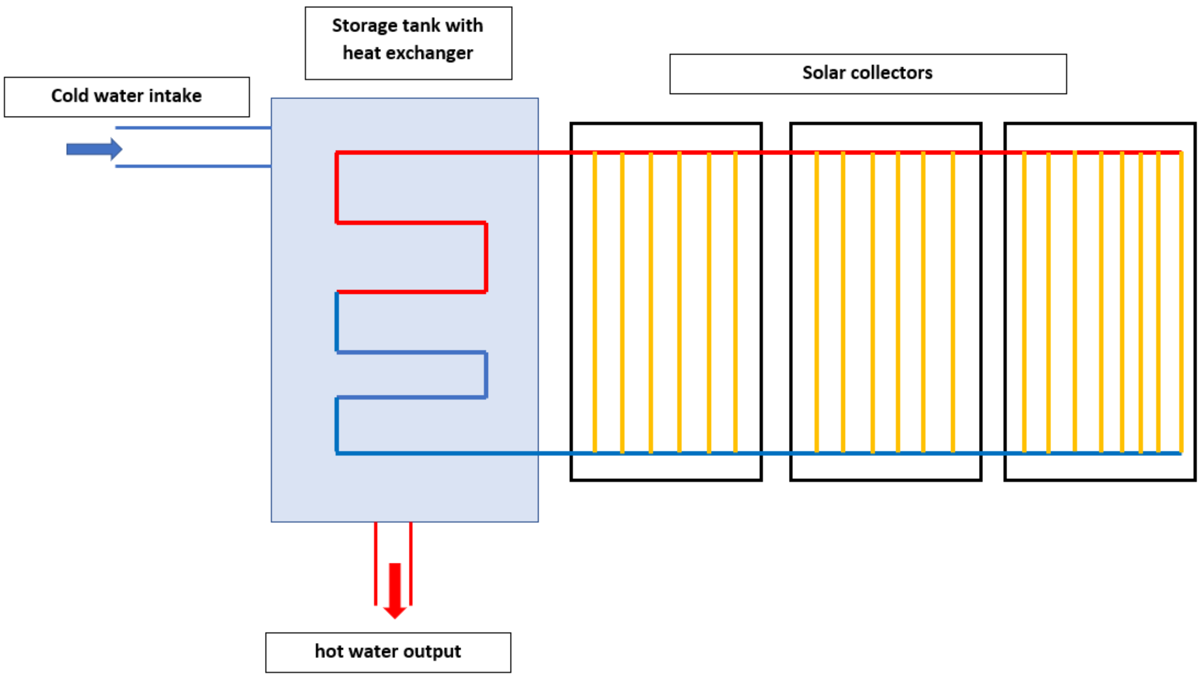

Figure 31: Concept of the flat plate solar collector

The installation consists of multiple panels which will be connected in parallel. Through these panels, the glycol solution will flow. This fluid will be heated by the incident solar rays on the panels. The intermediate fluid will then carry the gained heat inside the water storage tank, and transfer it to water through a heat exchanger. This will cause the intermediate fluid to be cooled down when it enters the panels again to collect heat. This way, the water will never leave the storage tank during the heating process. The storage tank is equipped with two water connections. One for tapping the hot water out of the tank and one for refilling cold water in the tank.

To make the natural circulation work, the storage tank has to be placed higher than the panels. The panels themselves also have to be installed at an angle to start the natural circulation process in the mornings. This will be clarified during the calculations of natural convection.

4.1 Calculations for dimensioning

To get a rough idea of the size of the installation, a calculation of the absorbed energy by the water in the storage tank is done. The TUM has an average water consumption of 250 liters for cooking. For this calculation, a storage tank of 300 liters is assumed to have some reserve hot water for high consumption days. This tank will be filled with cold water of around 20 °C. The ultimate goal is to obtain on output temperature of around 70 °C. This means a temperature gain of 50 °C. The heat needed can be calculated with the following formula:

$$Q = m * C_P * \Delta T \tag{38}$$

Where:

1. Q: Required amount of heat (kJ),
2. m: Mass of water (ρ ∗ V),
3. C_P: Specific heat of water = 4.19 $\frac{kJ}{kgK}$,
4. ΔT: Temperature difference.

By replacing the mass with the density (ρ) times the volume (V) of the water, the formula for the required heat can be further elaborated.

$$Q = V * \rho * C_P * \Delta T \tag{39}$$

$$Q = 0.300\, m^3 * 998.29 \frac{kg}{m^3} * 4.19 \frac{kJ}{kgK} * (70 - 20)K = 62\,742.53\, kJ \tag{40}$$

The heat required to heat the storage tank from 20 °C to 70 °C is equal to 62742.53kJ or 17.43 kWh.

4.1.1 Formulas for natural convection

The use of natural convection brings a number of advantages. For example, the cost of the installation will decrease since there is no need to use a circulation pump. Another advantage is that the flow rate depends on solar radiation. This speed will be lower when there is less sunshine, so the fluid will stay longer in the collector. Because of this the output temperature of the collector will be more constant than when we use a constant flow. In addition, if there is no solar irradiation, there will be no flow so the system will not extract heat from the hot water tank.

The use of natural convection also has some design limitations. Namely, this natural convection can only realize a limited pressure difference. The pressure loss through the collector and through the pipes should therefore be limited. When the pressure loss becomes too high, the intermediate fluid will flow slower which increases the risk of boiling in the collector. An additional limitation is that the heat exchanger must be located higher than the collector in order to realize a pressure difference. This will become clear from the calculations [35], [36], [37].

For the calculations we use the schematic representation below (Figure 32).

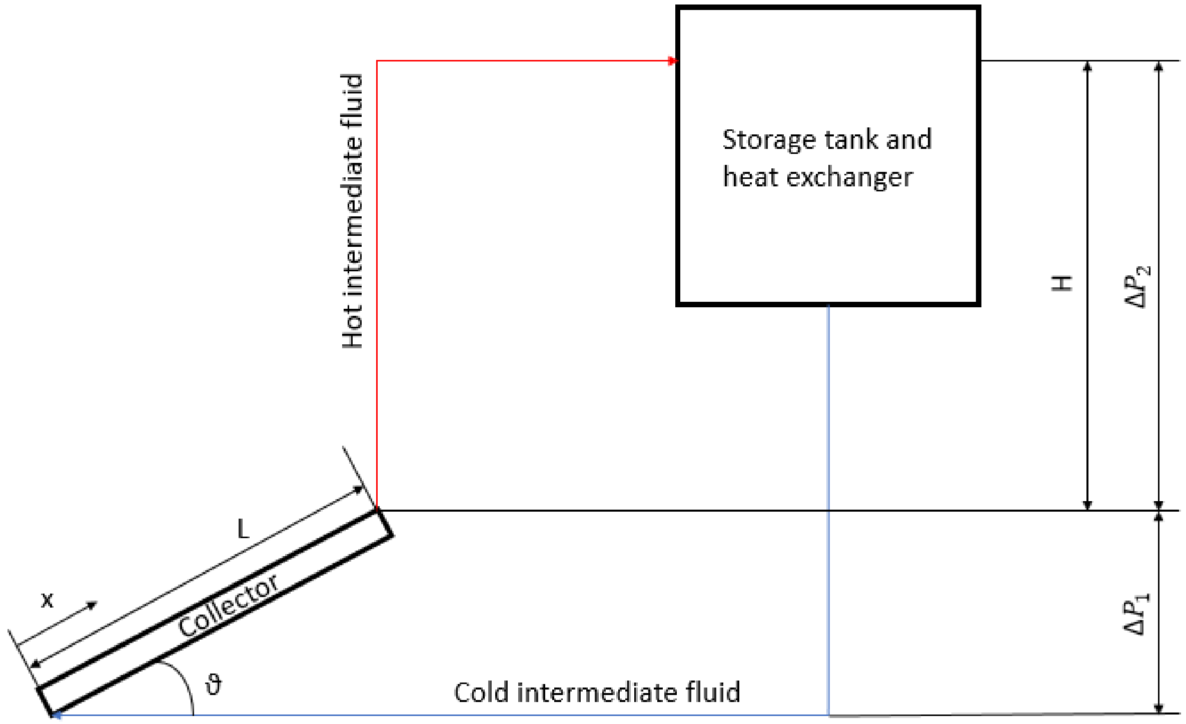

Figure 32: Schematic representation to explain natural convection.

Figure 32 shows the schematic representation of a solar collector installation where natural convection can occur. Due to incident solar rays, the temperature of the intermediate fluid through the collector will rise. This temperature difference will result in a difference in density of the fluid before and after the collector. This temperature difference will result in a pressure which will make the intermediate fluid circulate.

The pressure difference realized by the difference in density consists of two parts, which can be determined separately.

To determine the pressure difference through the collector (ΔP_1) it must be taken into account that the temperature of the intermediate fluid depends on its position in the collector. This temperature is linear in function of the distance in the collector.

$$\Delta P = \rho * g * H \tag{41}$$

Archimedes' law (Formula 41) is used to determine the pressure difference. Here the density difference is a function of the distance through the collector. The height is also written as a function of the distance through the collector (Formula 42).

$$\Delta P_1 = g * sin(\vartheta) * \int_0^L (\rho_c - \rho_x) dx \tag{42}$$

Where:

1. ρ_c : The density of the cold intermediate fluid on the inlet side,
2. ρ_x : The density of the intermediate fluid at distance x in the collector,
3. L : The length of the collector.

In practice, transporting the hot intermediate fluid will cause a small drop in temperature. However, this temperature drop is not taken into account. This will not give a major error since this temperature drop is insignificant compared to the temperature difference between the hot and cold side of the collector. The pressure difference (ΔP_2) is also determined using Archimedes' law (Formula 43).

$$\Delta P_2 = (\rho_c - \rho_h) * g * H \tag{43}$$

Where:

1. ρ_c : The density of the cold intermediate fluid in the cold pipe,
2. ρ_h : The density of the hot intermediate fluid in the hot pipe,
3. H : The height difference between the heat exchanger and the top of the collector.

The total pressure difference is now given by the sum of both pressure differences.

$$\Delta P_t = g * sin(\vartheta) * \int_0^L (\rho_c - \rho_x)dx + (\rho_c - \rho_h) * g * H \tag{44}$$

Where:

1. ΔP_t : The total pressure difference realized by natural convection.

In Formula 44, the pressure due to the natural convection is given in function of the difference in density of the intermediate fluid. For the further calculations, this pressure needs to be expressed in function of the temperature difference between the hot and cold intermediate fluid. This means a relation between the density and the temperature of a 30% glycol solution has to be found.

When the density of the 30% glycol solution is plotted against the temperature, following graph (Figure 33) is created [13].

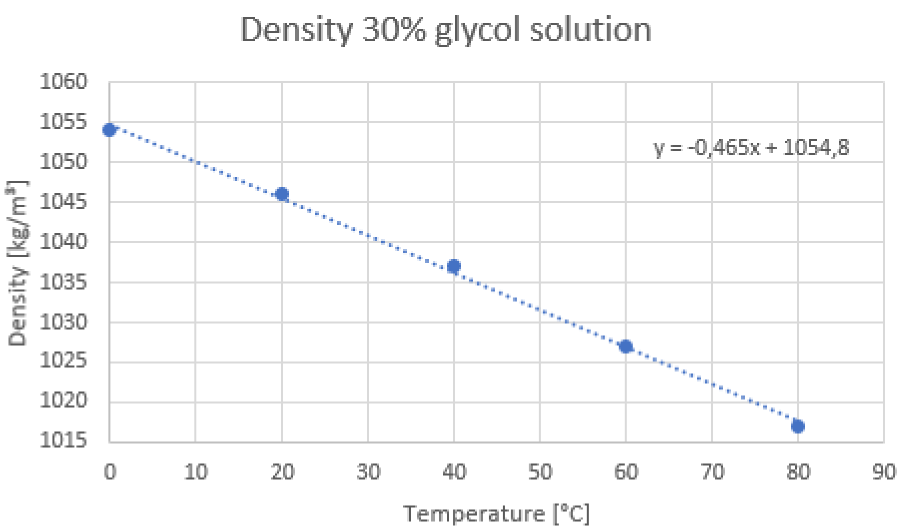

Figure 33: Density in function of the temperature, 30% glycol solution

The density in function of the temperature can be approached by a linear function. This will result in following relation:

$$\rho_{(t)} = -\beta * T + \rho_{0°C} \tag{45}$$

Where:

1. $\rho_{(t)}$: The density of the intermediate fluid at the given temperature,
2. β: The expansion coefficient of the intermediate fluid,
3. T: The temperature op the intermediate fluid,
4. $\rho_{0°C}$: The density of the intermediate fluid at 0 °C.

When Formula 45 is implemented in Formula 44, Formula 46 is created. This formula gives the pressure due to natural convection in function of the temperatures of the intermediate fluid.

$$\Delta P_t = g * \beta * \left[sin(\vartheta) * \int_0^L (T - T_c)dx + H * (T_h - T_c)\right] \tag{46}$$

Where:

1. T_c: The temperature of the hot intermediate fluid,
2. T_h: The temperature of the cold intermediate fluid.

The rise in temperature inside the collector is assumed linear in function of the distance inside the collector:

$$T - T_c = (T_h - T_c) * \frac{x}{L} \tag{47}$$

So:

$$\int_0^L (T - T_c)\, dx = (T_h - T_c) * \frac{L}{2} \tag{48}$$

Formula 48 can be filled in Formula 46 to give the total pressure due to natural convection (Formula 49).

$$\Delta P_t = g * \beta * (T_w - T_k) * \left(\frac{L}{2} * sin(\vartheta) + H\right) \tag{49}$$

This total pressure will in stable conditions be equal to the pressure loss through the collector and the piping from and to the collector.

$$\Delta P_{loss} = \Delta P_c + \Delta P_p \tag{50}$$

Where:

1. ΔP_{loss}: The total pressure loss of the system,
2. ΔP_c: The pressure loss through the collector,
3. ΔP_p: The pressure loss through the piping.

The pressure loss through a pipe can be calculated with Formulas 51, 52, 53, 54 [37]:

$$\Delta P = f * \frac{L}{D} * \frac{\rho}{2} * v^2 \tag{51}$$

$$f = \frac{64}{Re}\ (laminar\ flow) \tag{52}$$

$$Re = \frac{\rho * v * d}{\mu} \tag{53}$$

So:

$$\Delta P = 32 * \frac{L * \mu}{D^2} * v \tag{54}$$

Where:

1. L: The length of the pipe,
2. μ: The dynamic viscosity of the intermediate fluid,
3. D: The diameter of the pipe,
4. v: The speed of the intermediate fluid through the pipe.

The speed of the intermediate fluid can be written in function of the mass flow of the fluid:

$$v = \frac{\dot{m}}{\pi * \frac{D^2}{4} * \rho} \tag{55}$$

Substitution of Formula 55 in Formula 54 gives Formula 56:

$$\Delta P = 32 * \frac{L * \mu}{D^2} * \frac{\dot{m}}{\pi * \frac{D^2}{4} * \rho} = 128 * \frac{L * \mu * \dot{m}}{\pi * D^4 * \rho} \tag{56}$$

Where:

1. $\dot{m}$: The mass flow of the intermediate fluid,
2. ρ: The density of the intermediate fluid.

The system consists of multiple tubes so the total pressure loss can be written as a combination of Formula 56 for each tube. The equation of the total pressure loss can always be rewritten to a constant multiplied by the mass flow, since all parameters are assumed constant except the mass flow.

This total pressure loss has to be equal to the pressure realized by the natural convection when the system is in stable conditions. When the total pressure loss is equated to the pressure from Formula 49, Formula 57 is gotten. This formula gives a first relation between the mass flow and the temperature difference of the intermediate fluid.

$$\kappa * \dot{m} \ = \ g * \ \beta * \rho_{0°C} * (T_w - T_k) * \left(\frac{L}{2} * \sin(\vartheta) + H\right) \tag{57}$$

Where:

1. κ: The factor between the pressure loss and the mass flow.

Another relation between the mass flow and the temperature difference can be found using the absorbed energy by the intermediate fluid. For this purpose, the energy coming from the sun is calculated with the following formula:

$$\dot{Q} = A_c * \alpha_c * I \tag{58}$$

Where:

1. $\dot{Q}$: The power from the sun absorbed by the intermediate fluid,
2. A_c: The area of the collectors,
3. α_c: The coefficient of absorption,
4. I: The energy from solar radiation.

This absorbed heat will cause the intermediate fluid to rise in temperature. This temperature gain can be found with the following formula:

$$\dot{Q} = \dot{m} * c_p * (T_h - T_c) \tag{59}$$

Where:

1. $\dot{m}$: The mass flow of the intermediate fluid,
2. c_p: The specific heat of the intermediate fluid,
3. $T_h - T_c$: The rise in temperature of the intermediate fluid.

Formula 59 gives us a second equation with the mass flow and the temperature as variables. This equation in combination with Formula 57, gives us two equations with two variables. This means a value can be found for the mass flow and the temperature gain in function of the incident solar energy. This method will also be used in the simulation later on.

4.1.2 Temperature loss during the night

In Mombasa, there is an average of 12 hours of sunshine per day. This varies little throughout the year because Mombasa is located very close to the equator. In the morning at 7 a.m., the sun rises. From this moment, the solar collector can start to collect heat which will increase the temperature in the storage tank. This also means that the sun will set at 7 p.m. in the evening. Due to the absence of the solar rays and the dropping environmental temperature, the temperature in the water storage tank may drop. In order to minimize the temperature drop of the water in the storage tank, the hot water will be transferred to a separate insulated storage tank. This tank will be located inside the kitchen. This way, the hot water is quickly available for cooking and the drop in temperature during the night will be smaller, since it does not cool down as much inside as outside. Throughout the year, the nightly temperature is fairly constant at ± 25 °C. The storage tank in the kitchen is provided with insulation so that the temperature drop remains limited. The schematic cross section of the tank is given in Figure 34. In this section the loss in temperature of the water is determined, using various formulas.

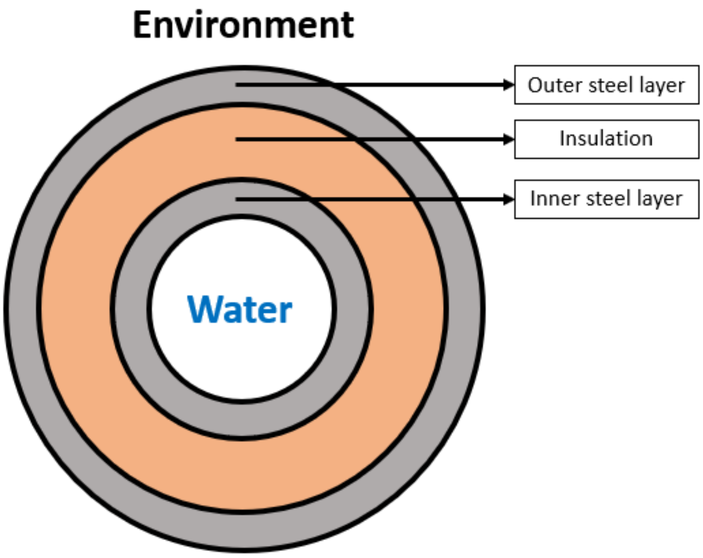

Figure 34: Schematic cross section insulated storage tank

In general, heat can leave an object in three different ways [38]. The first way is conduction. This happens when two objects with a different temperature come in contact with each other. The object with the higher temperature also has the higher kinetic energy. This object will give away energy to the object with the lower temperature. This will cause the object with the higher temperature to cool down, while the other object heats up. This conduction will keep happening until both objects are on the same temperature.

The second way is convection. This is a heat transfer between an object and a gas or fluid stream. When a stream flows around an object with a higher temperature, the stream will extract heat from the object, causing the object to cool down and the stream to heat up.

The last way is radiation. This kind of heat transfer happens between objects which are not in contact with each other. The object with the highest temperature will transfer its heat to the colder object by transmitting electromagnetic radiation. This will also cause the hot object to cool down and the cold object to heat up. This kind of heat transfer will not occur in this situation, and thus will not be used in the calculations.

This calculation considers a cylindric storage tank of steel. On the outside of this tank, a layer of insulation is applied. On top of the insulation, another steel layer is applied to hold the insulation in place and protect the insulation. To find the total heat transfer, multiple resistances have to be calculated. Three resistances against conduction have to be calculated, one for the inner steel layer, again for the insulation and one more for the outer steel layer. Resistance against convection has to be calculated twice. Once between the water in the tank and the inner steel layer and once again between the outer steel layer of the tank and the outside air.

Formula 60 gives the resistance against conduction through cylindrical objects. This value shows how easy or difficult heat is conducted through an object.

$$R = \frac{ln\left(\frac{r_o}{r_i}\right)}{k * 2\pi * L} \tag{60}$$

Where:

1. R: The resistance against heat conduction,
2. r_o: The outside radius,
3. r_i: The inside radius,
4. k: The thermic conductivity,
5. L: The length of the storage tank.

Formula 61 gives the resistance against convection. This resistance shows how easy or difficult heat is transferred through convection.

$$R = \frac{1}{h * A} \tag{61}$$

Where:

1. R: The resistance against convection,
2. h: The convection coefficient,
3. A: The area of the tank.

The total resistance against heat transfer can be found as the sum of the different resistances as seen in Figure 35. This total resistance consists of the three resistances against conduction and two resistances against convection. This total resistance can be found with Formulas 62 and 63.

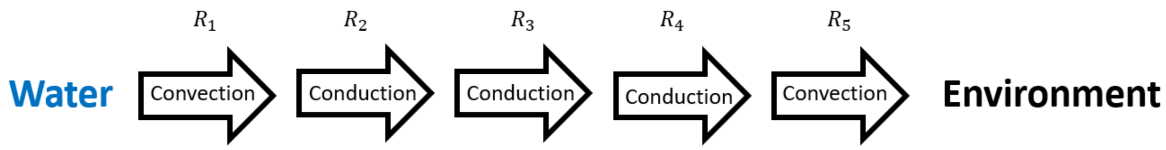

Figure 35: Schematic representation of individual resistances

$$R_{total} = R_1 + R_2 + R_3 + R_4 + R_5 \tag{62}$$

$$R_{total} = \left(\frac{1}{h * A}\right)_1 + \left(\frac{ln\left(\frac{r_o}{r_i}\right)}{k * 2\pi * L}\right)_2 + \left(\frac{ln\left(\frac{r_o}{r_i}\right)}{k * 2\pi * L}\right)_3 + \left(\frac{ln\left(\frac{r_o}{r_i}\right)}{k * 2\pi * L}\right)_4 + \left(\frac{1}{h * A}\right)_5 \tag{63}$$

The total resistance can be entered into formula 64. This formula gives a certain heat flow in function of the resistance and the difference in temperature. This heat flow is the loss of heat through the total system.

$$\dot{Q} = \frac{(t_i - t_o)}{R_{total}} \tag{64}$$

Where:

1. $\dot{Q}$: The total heat flow through the system,
2. $(t_i - t_o)$: The temperature difference between water and environment,
3. R_{total}: The total thermal resistance of the system.

The final step is calculating the temperature loss of the water in the storage tank. This can be done with formula 65:

$$\Delta T = \frac{\dot{Q} * t}{m * C_P} \tag{65}$$

Where:

1. $\dot{Q}$: The total heat flow through the system,
2. t: The time this heat flow is active (the number of hours without sun),
3. m: The mass of water in the vessel,
4. c_P: The specific heat capacity of the water.

This reasoning will be used in the simulation to calculate the temperature loss during the night. This will also be implemented during the day, since there will also be a temperature loss during the day.

4.2 3D design

The literature study revealed that the flat plate solar collector fits the situation the best. To get a better picture of the construction, the installation is drawn in a 3D software. Figure 36 shows a representation of the complete setup of the installation. It can be seen that the water storage tank is placed higher than the collectors. As the calculations have shown, this is needed to be able to use natural convection. The collectors in this drawing are placed under an angle of 30°.

For the casing of the collectors themselves, wood is used. This has a number of advantages in opposition of making use of steel. Some of these advantages are:

- Cheaper,
- Easier production,
- Better insulating properties,
- Lighter weight,
- …

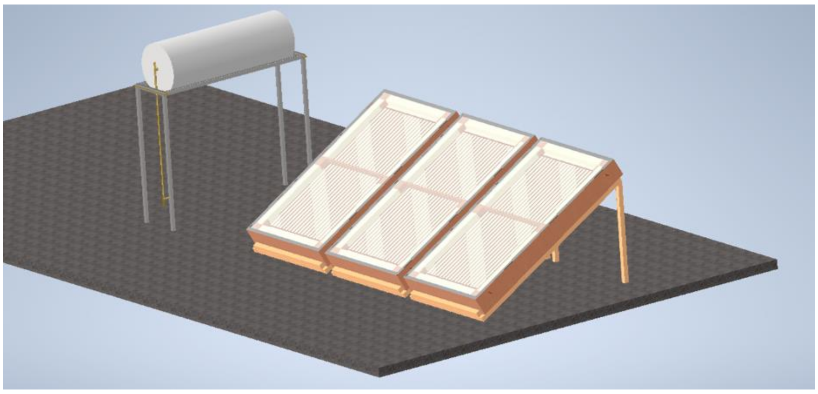

Figure 36: 3D setup of the solar collector

On Figure 37, the matrix structure inside the collectors is clearly shown. The horizontal tubes from the different collectors are connected to each other, so that the collectors are placed parallel to each other. This will increase the mass flow of the intermediate fluid. When the collectors are placed in series, this would increase the temperature and not the mass flow. In theory, this has the same effect on the temperature of the water in the storage tank, but in practice, the temperature of the intermediate fluid is limited to around 100 °C. With higher temperatures, the intermediate fluid will start to boil and create gas inside the collectors. This is why it is opted to place the collectors parallel to each other.

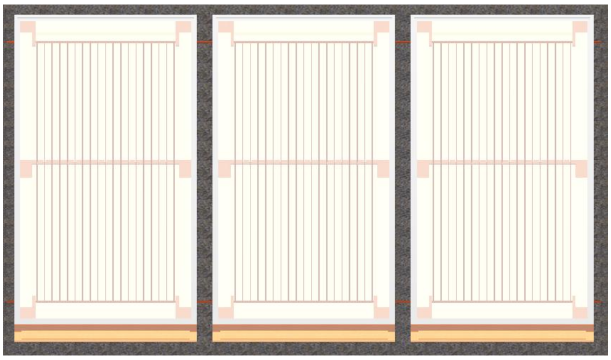

Figure 37: Matrix structure inside the collector

Figure 38 shows the back of the collectors. They are placed on a wooden construction to get them under an angle. This wooden construction is still subject to change, depending on the actual situation and the angle of the roof the installation in going to be placed on.

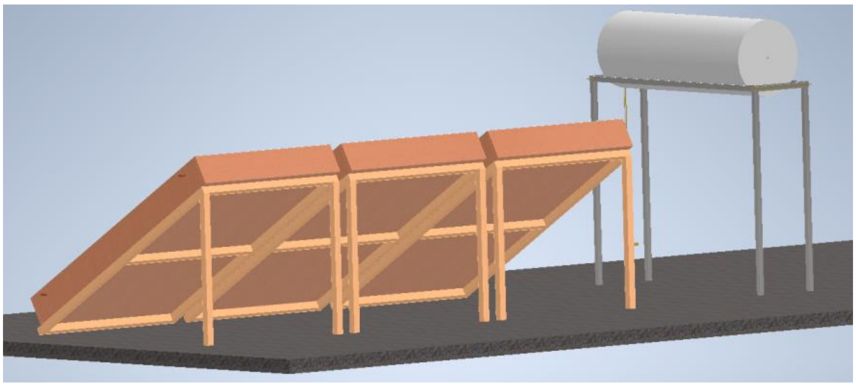

Figure 38: Backside of the collectors

4.2.1 Bill of materials

Using the 3D design, a bill of material can be conducted. This bill of materials is split into 2 different parts. First, the materials needed to construct one collector are listed. The materials on this list will be needed multiple times. In this situation, three collectors are build, so the materials on the first list are needed trice. The second list contains the materials which are only needed once for the installation, independent on the amount of collectors. This contains for example the storage tank and the piping from and to the tank. The dimensions for the copper pipes were determined by formula 54, these values were adjusted until a qualitative result is obtained for the mass flow rate. With an excessively large mass flow, the water would not be able to heat up long enough.

Table 9: Bill of solid materials for one solar collector

Material	per unit (mm)	Amount	Total (mm)
Wooden plate 1200x20 mm	2100	1	2104
Wooden planks 190x20 mm	2060	2	4126
Wooden planks 190x20 mm	1200	2	2406
Wooden planks 100x100 mm	180	6	1094
Wooden planks 180x20 mm	180	4	730
Wooden planks 180x20 mm	1160	1	1164
Copper tube inner diameter 6 mm	1755	19	33385
Copper tube inner diameter 12 mm	1470	2	2946
Rubber seal 15x1 mm	6500	1	6500
Insulation 1000x15	3000		3000
Glass window in frame	1200x2100		
Wood screws	50 mm long	75	
Wooden beams 50x50mm	2100	2	4206
Wooden beams 50x50mm	1100	4	4410
Wooden beams 50x50mm	1050	2	2106

Table 9 shows an overview of the solid materials needed to build one collector. This consist mainly of wooden planks and beams to build the encasing of the collector. This also includes the copper tubing for inside, the insulation and the glass window. The rubber seal is to make the connection between the glass window and the encasing water tight.

Table 10 lists the fluid materials needed for one collector. These mainly consists of paints and varnish. These are needed to coat the wooden encasing to make it resistant to all weather conditions like downfall and UV light. The table also includes wood glue for the construction of the encasing of the collector.

Table 10: Bill of fluid materials for one solar collector

Material	Area (m^2)	Per layer (liters)	# layers	Total (liters)
Stain blocking primer	6	0,500	1	0,500
Latex outdoor primer	6	0,500	3	1,500
Exterior latex paint	6	0,500	3	1,500
Wood glue				1

The last table (Table 11), now shows the materials needed only once for the installation. This includes the water storage tanks and the steel profiles to hold it up. These steel profiles are still subject to change, depending on the outlines of the site. The table also includes the plumbing. The actual numbers of these components will also become clear with the inspection of the site.

Table 11: Bill of materials needed once for the installation

Material	per unit (mm)	Amount	Total (mm)
Insulated water tank 250 liters		2	
Steel profile 40x40x2mm	1700	2	3406
Steel profile 40x40x2mm	480	2	966
Steel profile 40x40x2mm	1400	4	5610
Water pipe connectors and fittings		?	
Valves		?	
Insulated water pipe		?	

5. Simulations

To get a better idea of the size and the production of the installation, multiple simulations are conducted. For these simulations, the solar irradiation is used to find the heat production. Besides the solar irradiation, multiple parameters and characteristics are needed from the installation. With these parameters and data, the outcome can be calculated using the thought process of section 4.1. The following simulations are performed using Python.

5.1 One data point

The first few simulations are done using the solar irradiation found from Nigeria [35]. Later on, data from Mombasa itself was used. For this, an average day was chosen to get an estimate of the average heat production of the installation in Mombasa.

5.1.1 Data collection

The written Python code creates a number of graphs. Most important of these are the temperature throughout the day. This simulation starts from 7 a.m. when the sun rises until 7 p.m. when the sun sets. The first simulations which used weather data from Nigeria for the solar irradiance, are not further discussed in this thesis. All graphs displayed in this thesis are using the solar irradiance of Mombasa.

Table 12 shows both weather data. In general Nigeria has a higher solar irradiance than Mombasa. Both climates can be compared, but the weather data from Nigeria is from a sunny day while the weather data from Mombasa is from an average day. To obtain a qualitative result, an average day is chosen for the further simulations. If a better day occurs in Mombasa the solar irradiance will also be higher.

Table 12: Solar radiation for Mombasa and Nigeria [35]

Hour of the day	Solar radiation (W/m^2) Mombasa	Solar radiation (W/m^2) Nigeria
7.00 AM	36	421
8.00 AM	135	571
9.00 AM	216	457
10.00 AM	338	662
11.00 AM	526	712
12.00 PM	513	894
1.00 PM	625	993
2.00 PM	582	938
3.00 PM	551	783
4.00 PM	580	645
5.00 PM	364	682
6.00 PM	119	564
7.00 PM	20	432

5.1.2 Temperature variation exclusive night

The number of collectors will play a role in the temperature increase graphs. If several collectors are used, the surface area (formula 58) will increase, which means that the absorbed power will also increase.

Figure 39 shows the temperature variation for 1 collector throughout the day. The red line shows the temperature progression of the glycol solution at the exit of the collectors. Its collected heat is released into the water storage tank by a heat exchanger. The temperature progression in the tank is shown by the blue line. When using 1 solar collector, the temperature in the water storage tank rises to 39 °C at the end of the day. The desired temperature was set at ±70 °C. This temperature has not yet been reached, so additional collectors have to be placed.

The stepped variation of temperature of the intermediate fluid is a result of the use of hourly data for the solar irradiation. This means that the solar irradiation is presumed constant during each hour of the day. This way, steps in the solar radiation will occur, which will also result in steps in the temperature gain.

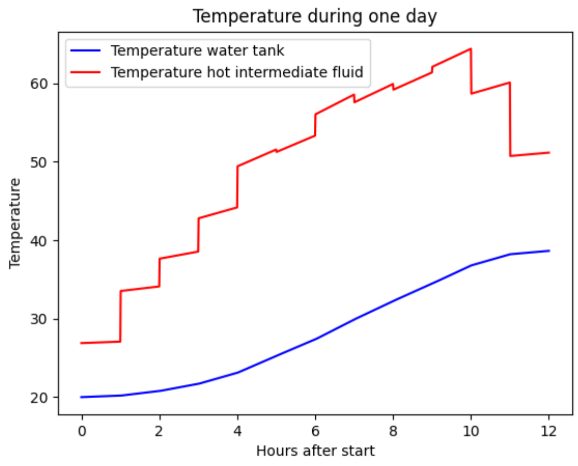

Figure 39: Temperature evolution through the day for 1 collector

When using 3 collectors (Figure 40), the temperature progression starts to increase faster than in Figure 39. The temperature in the storage tank at the end of the day has increased to 75 °C. This is an increase of 36 °C compared to using 1 collector. The design temperature of 70 °C is now reached. However, this value of 75 °C is a theoretical value. For this simulation, multiple assumptions had to be made. The actual temperatures could still vary from this theoretical value.

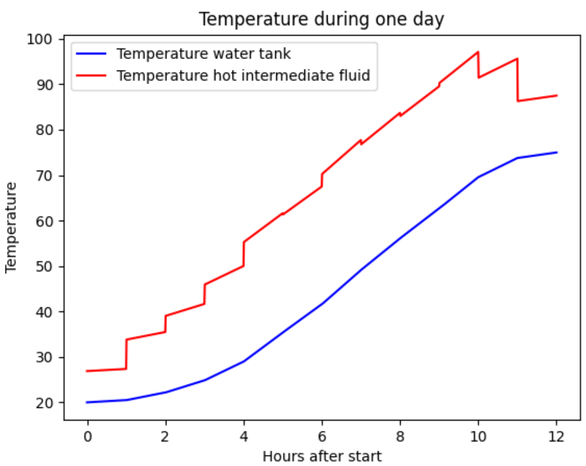

Figure 40: Temperature evolution through the day for 3 collectors

5.1.3 Temperature variation inclusive night

The graph below says even more about the temperature variation of the water in the storage tank since it also features the night. During the night, a temperature loss will occur due to the lack of solar irradiation. The formulas for this temperature loss were discussed in section 4.1.2. These formulas can now be applied in the existing simulations. The starting time of the simulation is still 7 a.m. in the morning, but it does not stop until 7 a.m. the next morning. At 7 p.m., the sun sets so no more heat is absorbed by the intermediate fluid in the collector. This can be seen on Figure 41 as the point where the intermediate fluid and the water in the storage tank have the same temperature. This will stay this way for the whole night.

Figure 41 shows the temperature evolution for 1 day. The maximal temperature in the storage tank is around 39 °C. This is the same value found with the earlier performed simulation. A more interesting value from this graph is the temperature of the water in the storage tank after the night. This temperature is around 38 °C. This means the temperature of the water in the storage tank decreases by around 1 °C during the night when using only one collector.

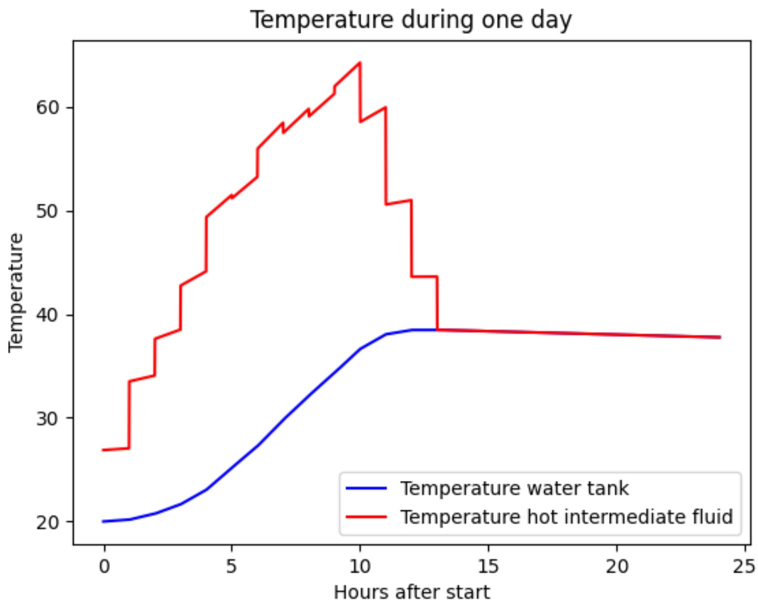

Figure 41: Temperature evolution for a whole day with 1 collector

If three collectors are used again, the temperature of the water in the storage tank will increase. But because the water temperature will increase, the temperature loss during the night will also increase. Figure 42 shows the temperature gain throughout the day when 3 collectors are used. The maximum temperature of the water tank is 75 °C. The temperature loss during the night is 3 °C when using 3 collectors. This means that the temperature will be 72 °C in the next morning.

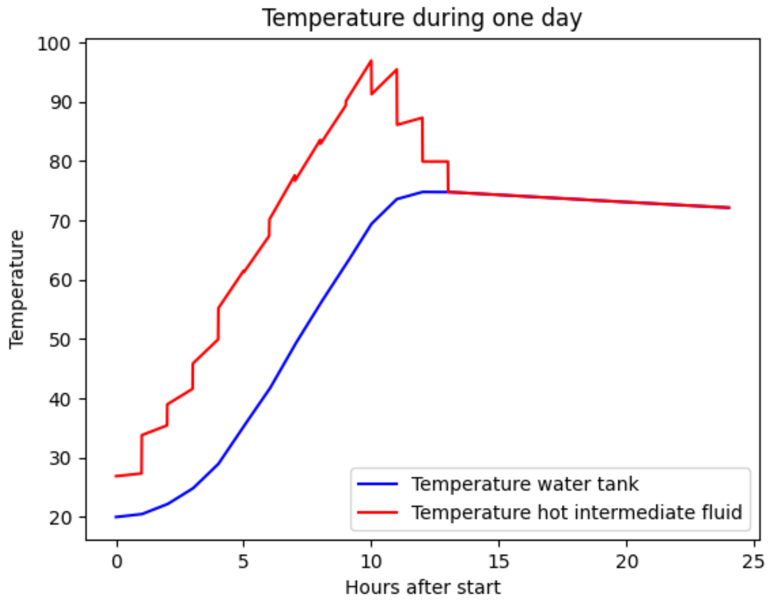

Figure 42: Temperature evolution for a whole day with 3 collectors

5.1.4 Conclusion

In order to draw a conclusion from the different graphs above, a summarizing table was made with the most relevant values (Table 13).

The first included value is the maximum temperature of the intermediate fluid for the different situations. This value is the same when the same amount of collectors is used. When 1 collector is used, the intermediate fluid reaches a maximum of 66 °C. When 3 collectors are used on the other hand, a temperature of 96 °C is reached. These collectors are placed parallel to each other. As told earlier, this will increase the mass flow of the intermediate fluid and not the temperature gain. From Table 13, it might seem like the temperature gain is increased from 66 °C to 96 °C. However, only the temperature gain of the water in the storage tank increased and not the temperature gain of the intermediate fluid.

The second important value is the temperature of the water in the storage tank at the end of the simulation. This can be simulated with and without the night. When the two values are compared, the temperature loss during the night can be found. This temperature loss is relatively small when 1 collector is used. This is a result of the relatively small difference in temperature between the water in the storage tank and the ambient temperature. The average temperature during the night drops to around 25 °C. This means a temperature difference of around 14 °C. When 3 collectors are used, this temperature difference is around 50 °C. This bigger difference will result in a bigger temperature loss during the night of around 3 °C.

Table 13: Results for the one data point collection

	1 Collector		3 Collectors	
	Inclusive night	Exclusive night	Inclusive night	Exclusive night
Max. temperature collector	66 °C	66 °C	96 °C	96 °C
Last temperature hot water tank	38 °C	39 °C	72 °C	75 °C
Temperature loss during night	1 °C	/	3 °C	/

5.2 Multiple data points

The previous simulations were performed using data collected over one day. In practice, this day can be a bad day or a good day. In order to obtain a better result, the following paragraph uses data from several days. This way, an average production can be determined. This gives a more reliable result than using one data point.

5.2.1 Data collection

The data collection for several days is examined over 15 days. Not only the solar radiation of Mombasa is taken into account, but also the solar radiation of Bilzen. Bilzen is the home town of the students who are doing this master's thesis. A comparison can then be made between the climate of Bilzen and the climate of Mombasa.

The data for both cities are taken from the ‘TU tiempo’ website. This website displays the solar radiation for each day for each hour [39], [40]. The results of this data are shown in Table 14 and Table 15. These results can then be entered into the simulations to produce graphs for the temperature output.

Table 14: Solar radiation in Mombasa for multiple days

Hour	6/03	7/03	8/03	9/03	10/03	11/03	12/03	13/03	14/03	15/03	16/03	17/03	18/03	19/03	20/03
7.00 AM	30	86	23	23	49	26	90	72	29	26	41	56	59	35	52
8.00 AM	111	302	85	86	166	137	317	238	123	94	136	166	184	121	142
9.00 AM	177	487	141	142	254	228	509	355	231	160	205	219	260	198	162
10.00 AM	216	572	187	188	305	294	713	526	550	514	388	376	375	384	268
11.00 AM	427	860	220	220	387	336	863	674	799	787	517	529	475	566	373
12.00 PM	511	944	237	238	462	351	944	777	930	929	616	649	547	709	461
1.00 PM	601	951	275	238	647	464	949	828	931	921	669	717	580	785	515
2.00 PM	504	889	245	222	560	522	886	807	867	847	666	720	569	783	525
3.00 PM	424	762	210	191	555	513	760	714	741	713	602	651	510	702	484
4.00 PM	523	146	146	146	580	328	580	561	512	477	452	520	437	534	427
5.00 PM	326	91	91	152	360	155	358	352	237	216	273	330	291	326	287
6.00 PM	118	77	29	56	113	30	109	107	27	26	79	98	88	92	86
7.00 PM	0	0	0	0	0	0	0	0	0	0	0	0	0	0	0

From the above table, it can be concluded that March 8 and 9 are colder days because the solar radiation here is a lot lower than the rest. This observation can also be made for the better days. For example, the days 7, 12 and 13 March are better days with significantly higher irradiance than the rest of the days.

If March 8 or 9 were used for the simulations in Section 5.1 then the temperature output will be much lower. Later in the graphs it will become clear how much lower this temperature will be. From these data it can already be concluded that it is better to take as many data points as possible in order to obtain the best possible result.

Table 15: Solar radiation in Bilzen for multiple days

Hour	6/03	7/03	8/03	9/03	10/03	11/03	12/03	13/03	14/03	15/03	16/03	17/03	18/03	19/03	20/03
7.00 AM	0	0	0	0	0	0	0	0	0	0	0	0	0	0	0
8.00 AM	81	87	23	47	29	28	41	38	35	42	135	135	114	159	5
9.00 AM	229	235	61	62	75	65	80	94	72	101	265	253	222	305	166
10.00 AM	353	359	365	93	121	96	97	152	100	164	356	327	310	425	311
11.00 AM	446	452	458	123	140	122	120	228	125	189	399	344	374	506	430
12.00 PM	502	508	513	135	144	141	134	295	141	196	387	303	409	543	508
1.00 PM	516	522	527	133	135	148	137	339	147	186	325	210	414	529	534
2.00 PM	488	493	460	289	127	139	234	271	137	163	359	199	363	519	504
3.00 PM	419	424	123	340	110	118	274	184	117	129	350	174	287	464	478
4.00 PM	315	317	81	299	84	89	253	96	89	90	294	135	198	369	417
5.00 PM	181	181	48	173	50	68	143	58	55	56	198	86	109	240	326
6.00 PM	28	32	10	37	12	21	35	17	17	18	68	30	32	89	211
7.00 PM	0	0	0	0	0	0	0	0	0	0	0	0	0	0	80

The above table shows the results of the solar irradiation in Bilzen. For both results the total radiation for each day can be determined. Then an average can be taken over these different days. For the results in Mombasa this average radiation per day is equal to 4639 W/m², for Bilzen it is equal to 2373 W/m². It is important to note that the average radiation for Bilzen is 48.8% lower than in Mombasa. Later on from the graphs, it can be determined if this percentage will also appear in the temperature output.

5.2.2 Results

Using the above dates, the simulations can be adjusted to several days. Only the temperature of the water storage tank will be considered. The temperature of the intermediate fluid does not give any additional relevant information. Figure 43 shows the result of the temperatures for several days. Here a distinction has been made between Mombasa and Bilzen. The red color shows the temperature result of Mombasa and the blue color shows the one of Bilzen.

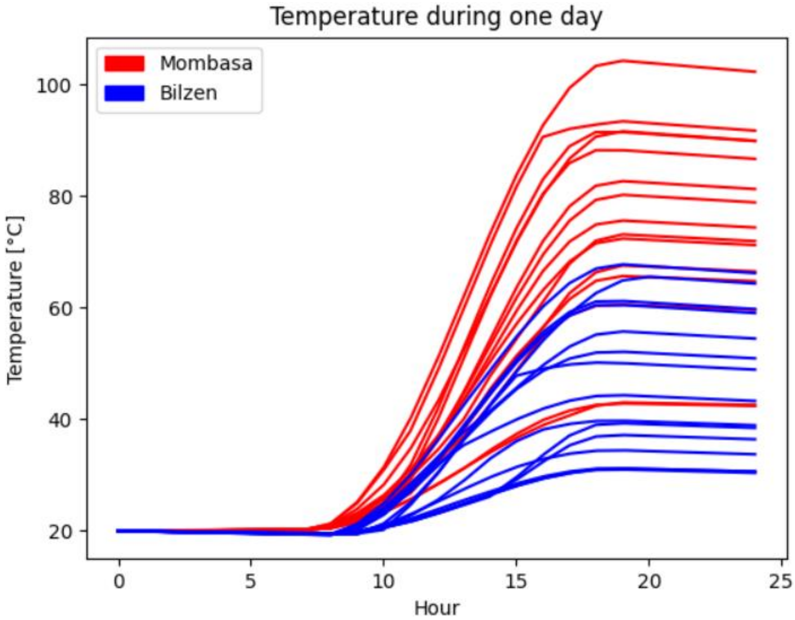

Figure 43: Temperature variation during one day for multiple days(06/03/2021-20/03/2021)

From the figure above, it can be concluded that there will be a higher temperature output with the climate of Mombasa than with the climate of Bilzen. There are two days in Mombasa where the output is much lower. These are respectively the days 8 and 9 March which were already considered as worse days from Table 14. During the period of data collection, the results of the best days in Bilzen lay around the results of the worst days in Mombasa. This means that the solar collector will be less effective in Bilzen than in Mombasa. The same temperatures as in Mombasa can be reached in Bilzen when the system makes use of more collectors for the same amount of water.

Because the temperatures are difficult to read from the figure, these results are again shown in a table. Table 16 shows the temperatures for both climates. These temperatures are listed from lowest to highest for both locations.

Table 16: Maximum temperature water tank for multiple days

Maximum temperature water tank		
Date	**Mombasa**	**Bilzen**
6/03/2021	67.57 °C	60.49 °C
7/03/2021	93.47 °C	61.26 °C
8/03/2021	42.98 °C	50.18 °C
9/03/2021	42.69 °C	39.33 °C
10/03/2021	73.19 °C	31.02 °C
11/03/2021	60.53 °C	31.21 °C
12/03/2021	104.23 °C	37.22 °C
13/03/2021	91.65 °C	39.71 °C
14/03/2021	91.43 °C	31.18 °C
15/03/2021	88.25 °C	34.44 °C
16/03/2021	75.67 °C	55.79 °C
17/03/2021	80.23 °C	44.32 °C
18/03/2021	72.38 °C	52.13 °C
19/03/2021	82.71 °C	67.79 °C
20/03/2021	65.71 °C	65.65 °C

The results form Mombasa are spread between 42 °C and 104 °C. If 104 °C occurs, the water in the water tank will start to boil. The steam that is released will then cause blockages that could stop the system from working. For this measuring point we have to make sure that this will not occur. In practice, this is achieved by installing a pressure release valve in the storage water tank. This valve will open when the pressure rises above 10 MPa to let the steam out. The results from Bilzen vary from 31 °C to 68 °C. These results that could be expected due to the colder climate. For these days the average temperature output can now be determined. These are shown in Table 17. The average temperature output of Mombasa is equal to 75.15 °C. This already gives a difference with the 46.78 °C of Bilzen, in percentage terms this is 38% lower. If this percentage is compared with the 48% of solar radiation then it cannot be said that there is a 1 to 1 relationship but these results will be proportional. If there is less solar irradiation then the temperature of the vessel with water will be lower.

The average output of the barrel with water is higher than 70°C, this 70°C was one of the targets. From this it can be concluded that this objective is achieved even though there are a few bad days in a week in terms of the solar irradiation.

The average output of the barrel with water is higher than 70 °C, which was the main target. The simulation shows a promising result in terms of reaching this target. Even with the days with low solar irradiation, the target is reached on average.

Table 17: Average temperature water tank for multiple days

Average temperature water tank	
Mombasa	**Bilzen**
75.15 °C	46.78 °C

5.2.3 Conclusion

The results of the temperatures in the vessel with water are different for different days. These differences are far apart so it can be concluded that the solar radiation has a great effect on the output in temperature. On the best day a temperature of 104°C is reached, this temperature is even too good because it can cause high pressures due to steam creation. Since this is only one data point, this will not occur too often.

It will always be better to take several days for the simulations. If the data is used from March 8 or 9 then incorrect conclusions would be made here based on the results. By using multiple dates, it quickly becomes clear that these are bad days due to cloud cover.

From Table 17, one can conclude that the average output for Mombasa meets the predetermined targets. However, these are simulations and later it will be clear if the actual situation will also meet this target. Furthermore, it can be said that the March 7, 12 and 13 were the best days for Mombasa and they also give the best results. Respectively, these results are equal to 93.47 °C, 104.23 °C and 91.65 °C.

6. Comparison between buying or building from scratch

In this section, a comparison will be made between making the installation from scratch or buying the solar collectors. If the solar collectors are purchased, the pipeline itself will be laid to the desired position.

For an optimal comparison, several aspects which play a role in the effectiveness of the installation are compared. These aspects include price, lifespan and simulation results. In addition, a few company visits were carried out to get an idea of the current state of the use of solar energy in Kenya.

6.1 Visit Rainbow4Kids Ukunda

During the 2016-2017 academic year, a master's thesis was conducted in a secondary school called Rainbow4Kids (Figure 44) located in Ukunda. This school is located approximately 36 km away from Mombasa. Within this master thesis, the kitchen of the small school was optimized and a solar collector was installed to reduce energy costs, and this way, reduce the impact on the environment. The ergonomics of the kitchen where improved by installing a lever system for lifting the large cooking pots. This way, the cook does not have to lift the heavy cooking pots him/herself. To improve the energy consumption, the stoves are constructed in a way that as much heat from the fire reaches the cooking pots to reduce energy costs.

To reduce the energy cost even further, a solar collector was constructed to preheat the water used for cooking. This solar collector would be a great example, since it features a similar climate and similar conditions as the solar heater designed in this thesis.

Figure 44: Rainbow4Kids primary school

Once we arrived at the little school, a tour was given to look at the current situation. The first part of the tour was inside the kitchen. The lever system and the kitchen where still operational and in great condition. The lever system is shown on Figure 45. On Figure 46, the water tap where the hot water was provided in the kitchen is shown. It came as a surprise that the solar collector is not functional anymore. The use of the preheated water was stopped due to impurities, already after one and a half month. These impurities made the water not suitable for cooking anymore. This was probably a result of the poor water quality in Kenya. The use of this water might have caused an accumulation of lime and other impurities, making the water not suitable for cooking.

Figure 45: The lever system in the kitchen

Figure 46: The hot-water tap

Several months after the use of the system was stopped, a heavy storm caused the water storage tank to collapse. This vessel was placed at a height on a steel structure (Figure 47). Due to this height, a water pressure was available at the tap in the kitchen. From the moment the tank fell down, it was decided to take down the installation due to safety reasons. There are small children walking in the school and this could cause danger. The installation was dismantled and the parts might have been sold. The only parts of the installation that can still be found at the school are the water tap from Figure 46 and the glass cover panels, as seen in Figure 48.

Figure 47: Steel construction for the water storage tank [2]

Figure 48: Leftover glass panels from the installation

For this installation, it was decided to build the solar collector from scratch from local materials. This way, the installation can be easier implemented in other locations since only local materials are used. But due to some unforeseen problems, the use of the installation had to be stopped.

This was an example of an installation build from scratch. This will be compared on several factors with installations that can be bought in Kenya in the next few paragraphs.

6.2 Visit solar technology companies

The first company visit was an energy center called 'MOE Mtwapa energy center'. This center has several implementations of how durable energy can be used, including solar collectors. This energy center also functions as example for establishing other energy centers [41].

Figure 49 shows an example of the solar collector installed at the site. The solar collector is of the brand 'Megasun' and can store 200 Liters of water in the tank at the top of the collectors. The piping inside the collector is done using a matrix structure and the installation makes use of natural convection instead of a circulation pump. The working principle and construction are highly comparable with the installation designed in this thesis.

The energy center does not sell their devices, this is only to show that there is a sustainable use of renewable energy sources. Nevertheless, this brand is sold by other companies. One of these companies is 'Chloride Exide' [42], the price of this solar collector, together with other brands, will be discussed in section 6.3.

Figure 49: Solar collector installed at the MOE Mtwapa energy center

'Sollatek' [43] was the second company visited. This is a company that specializes in applications where solar radiation plays a major role. They also specialize in power components for electricity consumption.

Figure 50 shows their implementation of the same type of solar collector. The construction is highly comparable with the construction of the Megasun solar collector. It also features a 200 liter water storage tank, the matrix structure inside the collector and it uses natural convection.

Figure 50: Solar collector installed at Sollatek

6.3 Price

Price is going to be one of the most important aspects for the decision. This installation will be built in a developing country so there is not an extensive budget available.

Using the materials list from the master thesis from the previous thesis in Rainbow4Kids, the cost of building the installation and purchasing the installation can be compared. Table 18 shows the cost of the materials for the solar collector building it from scratch. In this process, durable materials such as aluminum, glass and copper were chosen. This ensures that the costs will be higher than when using cheaper materials such as wood.

Table 18: Cost list solar collector installation make it yourself

Material	Cost price (Shilling)	Cost price (Euro)
Glass panel	85000	654
Copper tube 1/4"	59925	461
Copper tube 1/2"	17650	136
Paint	64330	495
Isolation	33002	253
Circulation pumps	22311	171
Steel plate	16800	129
Wood	13000	100
Welding equipment	19000	146
Screws	2000	15
Tubes	24073	185
Silicone	3770	29
Electrical components	42700	329
Profiles	7610	58
Total price	411 173	3 163

The total price for building the installation comes to 411 173 shillings, which is equivalent to 3 163 euros. This price includes only the cost of the solar collectors, the price for the storage tank and the associated accessories are not yet included. At first sight, this is a high price for the entire installation. In the table you can see that the glass panels and the copper pipes provide a large cost. These are materials that are needed because the collectors need to be protected from the weather and the copper pipes are needed for the optimal absorption of the sun's rays.

When deciding to purchase the collectors there are a number of choices of companies. For an optimal analysis, three companies were chosen, each offering a 300 liter solar collector with a matrix structure. The daily needed amount of water is 250 liters on average, so a solar collector of 200 liters would be too small.

The various companies are presented in Table 19. Prices are shown in shillings and in euros. The prices range from 1700 to 1800 euros depending on the type of company. The cheapest solution is the company Sollatek with a price of 1712.96 euros. This is a difference from the other two companies that give about the same price. In general, Sollatek is 5% cheaper than the most expensive solution, Voltex engineering.

In addition, Sollatek offers a control unit that makes it possible to measure the temperature inside the vessel. This measuring unit costs 17 000 shillings, approximately 130 euros. This unit of measurement is already included in the price. If this price is not included then Sollatek would be 12% cheaper than Voltex. The other companies do not have this service so Sollatek gives the best results for the cheapest price.

Table 19: Cost price from the different companies

Company	Cost price (Shilling)	Cost price (Euro)
Sollatek	222 685	1712.96
Chloride Exide	233 044	1792.64
Voltex engineering	234 436	1803.35

For the comparison between purchasing and making it from scratch, only the company Sollatek is considered because it gives the best results. To make the whole installation from scratch, it is almost twice as expensive as buying it. Due to the poor water quality, the solution to make the installation yourself involves an additional risk. If only the price is considered then the choice to purchase the panels is made. The other parameters for comparison are discussed in the following paragraphs.

The price of the total installation is now compared with each other, but the performance of the different installations might differ. The more expensive solution might reach higher temperatures and thus still be the better solution. To take this in account, the price per unit of energy gained is compared between the solar collector from scratch and the one from Sollatek. This calculation will be done based on the results of the simulations at the end of section 6.4.

6.4 Results simulations

For simulation results, there are some parameters that change when comparing making and buying. For example, the collectors are smaller when the system is purchased, and there are also fewer vertical pipes that collect the sun's rays. A summary of the different parameters that change is presented in Table 20.

Table 20: Difference between parameters making and buying

	Making	Buying
Number of vertical pipes	19	8
Tank size (L)	250	300
Length of the riser (m)	2	1.455
Length of the header (m)	1	0.96
Area (m^2)	2	1.3968
Diameter of the riser (m)	0.006	0.0072
Diameter of the header (m)	0.012	0.0206
Tank height	0.5	0.2

If these parameters are inserted in the simulations than there are two types of results that are obtained. These results are the graphs for the temperature rise for buying and making the system. The temperature rise for making the system is presented in Figure 51. Here the intermediate fluid reaches a maximum value of 92.20 °C at the 10th hour from the start. This hour corresponds to 6 p.m. in the evening. From that time the sun sets and there will be no temperature gain. The temperature of the water tank reaches a maximum of 70.10 °C at the 13th hour of the day. This occurs later than the maximum of the intermediate fluid. At the 13th hour of the day both temperatures will be equal to each other and the system will come to a standstill.

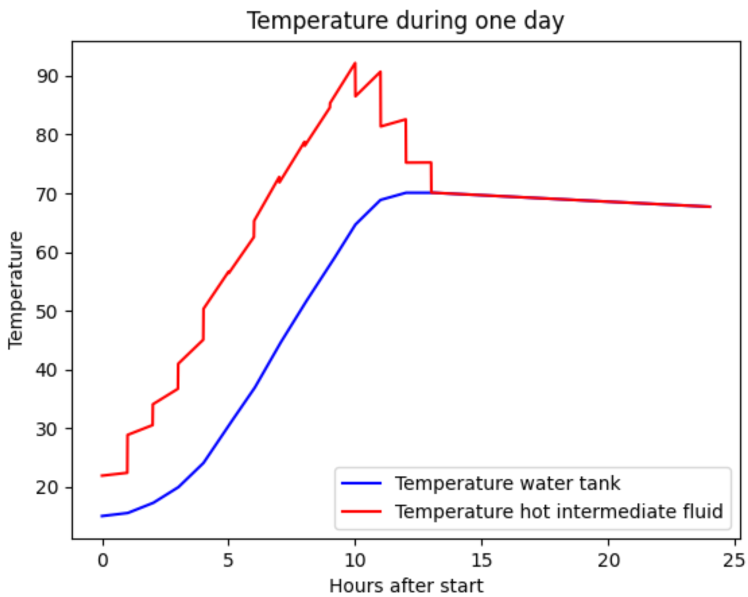

Figure 51: Temperature variation during one day by making the installation

For this installation it is also possible to determine the temperature loss. This loss amounts to 3.49 °C for the whole day. From the point when the collector and the tank have a higher temperature than the environment, a heat transfer can occur from the collector and the tank to the environment. So the temperature loss occurs from that point on.

Now the parameters can be adjusted to the system to purchase. Figure 52 shows the result of the temperature increase during the day. The maximum reached temperature of the intermediate fluid is 74.26 °C. This is 17.67% lower than the previous system. In addition, this maximum is also reached at the 10th hour of the day since the same solar irradiation is used. The water tank has a maximum temperature of 49.17 °C and it is reached at the 12th hour of the day. This value is 29.87% lower than the previous setup. Both decreases in temperature are due to the size of the collectors. When purchasing the collectors the area is smaller, this reduction is 30.16%. If this is compared with the loss of temperature these values correspond. For a 30.16% reduction in surface area there is a 29.87% decrease in maximum reachable temperature.

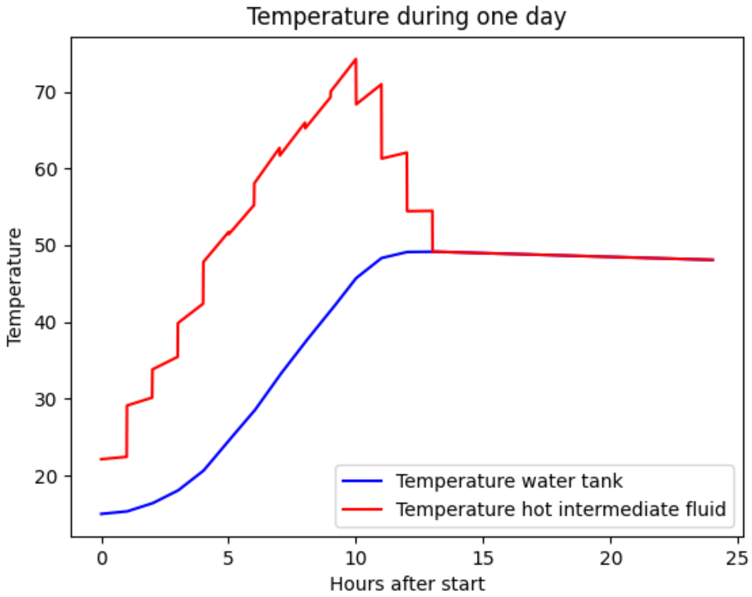

Figure 52: Temperature during one day by buying the installation

For this installation, the temperature loss can also be determined. This amounts to 1.43 °C for the whole day. This is 59.60% lower than the previous installation. This is because the maximum temperature is lower so less heat will flow into the environment.

With these temperatures, the purchase cost per energy unit can be compared. For this matter, the maximum reached water temperature is considered. This is 68.75 °C for the installation built from scratch and 49.17 °C for the installation from Sollatek. Another important difference is the size of the water storage tank. The installation built from scratch features a tank of 250 liters while the one from Sollatek has a volume of 300 liters. The heat absorbed by the water now can be found by multiplying the volume with the temperature gain. The heat coefficient and the specific mass of water are left out because they are the same for both systems. This results in 13775 L°C for the installation built from scratch and 10251 L°C for the one from Sollatek. Taking the purchase cost in account, this results in 0.2296 €/L°C for the installation built from scratch and 0.1671 €/L°C. This means that the installation built from scratch is 37.40% more expensive than the one from Sollatek when energy production is considered.

6.5 Lifespan

The last factor discussed is lifespan, next to the price this is the most important factor for consideration between purchasing and making the system. When the installation is installed, it is also intended that the installation will continue to work. If the lifespan is too short the installation failed its purpose in being durable.

The lifespan is often determined by the type of materials used. If durable materials are used then the lifespan will increase. In addition, the lifespan is often limited by factors that cannot be taken into account. In the case of the situation in the school at Ukunda these factors are the water quality and the weather conditions.

The weather conditions are a factor that can't be affected, for the copper pipes there are a number of solutions to extend the lifespan [44]. These solutions relate to treating the water that will flow through the pipes. First, a water treatment device can be installed. This device will use an ion exchanger or osmosis technology to remove the impurities from the water. These impurities will then not be able to hit the pipes later and in this way there is less chance of clogging.

Secondly, there is a degassing system that can ensure that harmful gases are removed from the water by aerating the water. This method is going to prevent the growth of biofilm. Biofilm [45] is a growth of microorganisms that build up against the inside of pipes and can cause blockages.

Finally, a water softener can be installed. When oxygenated water comes into contact with the copper pipes, pitting corrosion can occur [46]. This corrosion can get worse over time causing leaks. Installing a water softener will drastically reduce this problem. The occurrence of corrosion can be measured by measuring the rate of growth.

The corrosion rate can be determined in two ways, by weight removal and by polarization resistance measurements [47]. Measuring by weight removal gives the best results. In this process, a reference is first established by weighing the pipes. By exposing the water to the copper pipes, the corrosion starts attacking the pipes. The corrosion will slowly dissolve the copper pipes so that less copper will be present. After the exposure, everything is rinsed and cleaned. When the pipes are weighed again it can be determined how much copper was lost due to the corrosion and the corrosion rate is measured.

By conducting various tests in which the copper pipes are exposed to the water for different periods of time, the corrosion rate can be determined. Obviously, more corrosion will occur if the water is exposed to the copper pipes for a longer period of time. Using a study by TNO where the corrosion rate was determined before and after treating the water with an AquaCell water softener [47]. Figure 53 below shows the results of this study.

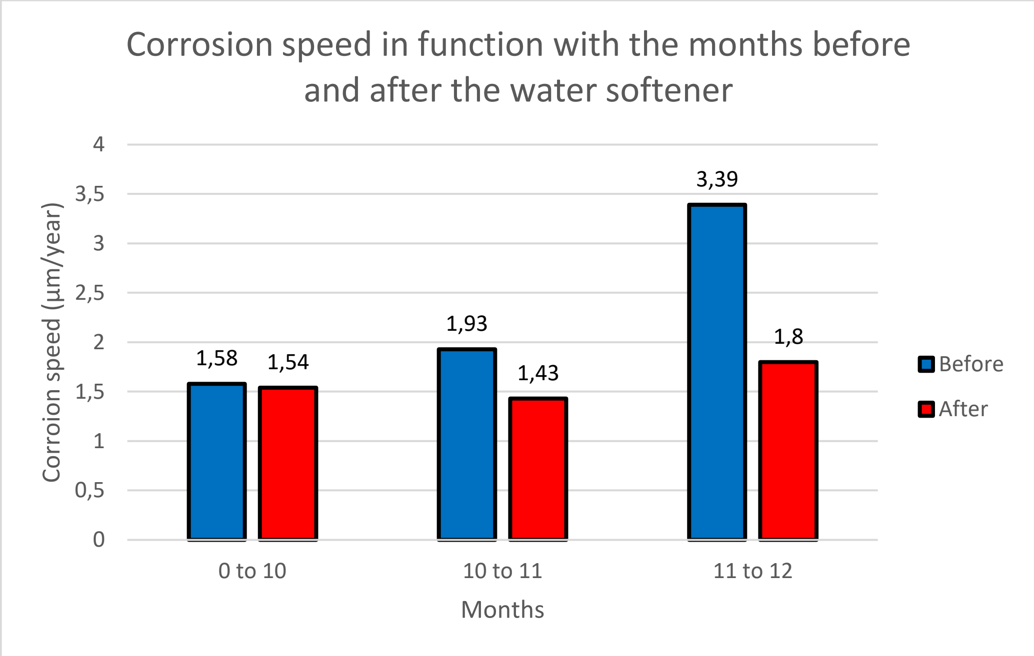

Figure 53: Corrosion speed in function with the months before and after the water softener

At the exposure of 0 to 10 months there is not much difference between the corrosion rates. As of looking at the exposure from 11 to 12 months, there is a big difference between the velocities. For example, the speed after the water softener is 46.90% lower than the speed before the water softener. This is almost half which doubles the life span with the use of a water softener.

Through the use of several methods, the lifespan of copper pipes and the entire system can be dramatically extended. These methods make use of advanced machines which have their price. The purchase of these machines is in this situation where the installation is built in Kenya a difficult aspect because of the price. Per day 300 liters of water is consumed, this comes down to an annual consumption of 109 500 liters or 109.5 m³. An average family of 3 uses 104 m³ of water per year [48]. The price of an average water softener for a family of 3 to 4 people is around 1250 euros [49]. There are also additional costs such as maintenance and cleaning salt. The cost of maintenance is around 150 per year and salt 15 euros per year [50]. If these costs are added up then the price of a water softener is close to the cost of a whole plant. From this it can be concluded that a water softener becomes too expensive in this situation.

The water quality refers to both homemade installation and purchased installation. But the purchased plant was developed for regions with hard water. The pipes are protected from the hardness values of the water in Kenya in two ways [51]. First, the pipes are enameled according to DIN 4753, this method is safe for human health. Second, the pipes are coated with a magnesium anode coating. The electrons of a magnesium coating are strongly negatively charged so that when they come into contact with water they can give a quantity of electrons to the strongly positively charged metal. In this way a cathodic protection is created between the water and the metal [52].

The most economical solution with a good lifespan is to purchase the system because it is not feasible to install a water softener. If a softener can be installed then both solutions are approximately equivalent in terms of life expectancy.

6.6 Conclusion

To make the comparison between purchasing and making it yourself from the above parameters is not an easy task. The concept and simulations were both set up with the idea of making the entire system yourself. This was done so that the installation can be easily distributed to different schools. In this way the knowledge about solar collectors will be further expanded. During the visit to Rainbow4Kids it became clear that building the installation yourself is not always the best solution. Because of the problems that have occurred it would not be wise to build the installation. This is because the problems are to be avoided and because the intention is to make a sustainable system.

While visiting the different companies, it was discovered that research has already been done on solar collectors for hard water. Through this research, these companies are able to deliver a solar collector that has a useful life. In addition, the companies also provide a warranty so that any problems can be solved by the company and the system can continue to work.

Based on the price, a better picture can be formed. It was found that the price for making the whole system is twice as expensive as buying it and 37.40% more expensive when energy production is considered. In addition, the fact that purchasing has a better lifespan makes purchasing the system the best solution.

According to the simulation results, a totally different decision is made. Here it was found that the situation where the collectors were made gives better results than buying the system. This was due to the area of collectors, if a larger area was used then the output will also be larger. These simulations are assumptions so they are not 100% reliable as they may differ from the actual situation.

The lifetime of the system can be extended by installing various machines. The purchase of these machines will result in an additional cost that will make the price of the system even more expensive.

When all these factors are considered, it gives a result that purchasing the system will be better than making it yourself. Only the simulation results show that making the system will be better. But as mentioned earlier these are simulations and they may be different than the actual situation. During the measurement of the situation it will become clear if the simulations will actually match.

For the further course of the project we will then use a purchased installation. From section 6.3 it appears that Sollatek gives the best results so that this company is also approached for the purchase and delivery of the solar collector. Figure 54 below shows the solar collector being purchased. Section 7 shows how the installation of this solar collector will be done

Figure 54: Solar collector from Sollatek [43]

7. Installation

In this section, the installation of the solar collector will be discussed. It will be placed on a sloping roof. This way, the collectors can easily be placed at an angle, which is needed to make natural circulation work. Figure 55 shows the roof where the solar collector will be placed with the suggested location. The exact location on the roof is decided after the shading throughout the day was studied to get the optimal location. The installation of the solar collector will be discussed step by step in chronological order in this section.

Figure 55: The sloping roof for the solar collector

As discussed earlier, this solar collector is purchased from the company Sollatek. Consequently, these materials were delivered to the university. Figure 56 shows the materials packed in a tentative manner. These materials include the frame, the collectors and the storage water tank. Appendix A shows the datasheet of the panel and vessel that are installed on the roof [51].

Figure 56: The delivered packed materials

7.1 The frame

The frame serves as a support where the collectors and the water storage tank will be connected to. The collectors cannot be placed directly on the roof. This frame consists of iron profiles which are assembled with bolts and nuts. The frame is designed in such a way that it can be adjusted for any slope. The roof on which the collectors are placed is already at a tilt angle, so that the frame must be adapted to this angle.

At the top of the frame, the profile is curved. The vessel is placed in this curved part, so that the vessel lies firmly on the roof. Figure 57 shows the curved pieces clearly.

Figure 57: The support frame

Both sides of the frame feature an L-shaped profile. The collector plates will be placed in and fastened with bolts to these profiles. After assembling the frame, it can be placed on the roof. By using screws, the frame is fixed to the roof. Figure 58 shows the finished frame, this is still on the ground. Figure 59 shows the frame already installed on the roof.

Figure 58: The finished support frame

Figure 59: The support frame on the slopping roof

7.2 The collectors

After the frame is attached to the roof, the collectors can be placed on the frame. Since the system is designed for 300 liters of water, 2 panels are used which are built in a matrix structure and are coupled in parallel. Figure 60 shows the placement of the first panel.

Figure 60: Installation of the first panel

First, the first panel is placed loose in between the two L-profiles. Before this panel is fastened with bolts onto the frame, the second panel is placed in position. This way, both panels can still be moved to the desired position before being fastened. Figure 61 shows the installation of the second panel.

Figure 61: Installation of the second panel

Now both panels are in place and can be connected. At each corner of the panels, the copper pipes of the matrix structure are brought out for connection. First, caps are placed on the outside ends of the panels so that the intermediate fluid cannot flow out of the system. Figure 62 shows these caps.

Figure 62: Caps on the end of the inner tubing

Now the panels only need to be connected to each other. This is done with a T-connection. This T-connection is placed at the top and at the bottom in between the panels. At the vertical end of this connection, the inlet of the cold intermediate fluid will be placed at the bottom and the outlet of the hot intermediate fluid will be placed at the top. The cold pipe comes from the water storage tank where the intermediate fluid has cooled down again after going through the panels. The hot pipe is led to the water storage tank where the heat can be transferred the water. Figure 63 shows an example of this T-connection.

Figure 63: The T-connection between the inner tubes

7.3 The storage vessel

The water storage tank is placed in the curved pieces of the frame. This tank weighs about 100 kilograms and has to be carried up the roof of 4 meters high. After the tank is on the roof it had to be placed on the frame. Figure 64 shows the barrel before it was placed on the frame. The bolts attached to the barrel allow the barrel to be secured to the frame. These bolts are shown in the red circles in Figure 64. Figure 65 shows the total system where the vessel and collectors are placed.

Figure 64: The water storage tank

Figure 65: Storage vessel placed on the frame

After installing the vessel, the pipes of the intermediate fluid leading to the tank can be placed. These pipes are attached to the T-connection on the panels. After this connection is made, the intermediate fluid is added to the system. The pure glycol is an expensive liquid, so to make sure that this liquid will not be wasted due to a leak, the system is first filled with water. Once it is confirmed there are no leakages, the pure glycol fluid can be poured in. By mixing 20 liters of water with 2 liters of glycol, a glycol solution of 10% is achieved.

Figure 66: Filling the inner tubing with water (A), adding glycol to the water (B)

7.4 The piping

Now that the collectors and the storage tank have been installed, the pipes can be laid so that the entire system can work. There is a subdivision between the cold-water pipes and the hot water pipes. The cold pipe contains the cold water that is pumped to the tank. This cold water flows into the storage tank and will be heated up by the intermediate fluid. The heated water will now leave the tank when water is needed. At the same time, cold water is refilled to the storage tank. The hot water is brought to the kitchen by the hot water pipe which ends with a tap.

7.4.1 The cold-water pipe

The plan was to use a pressure pump to pump the cold water up to the storage tank. This pressure pump works on the basis of pressure. When water is taken from the storage vessel, the pressure will start to drop. This change in pressure will be detected by the pump, which will start to pump the water again. The pump continues to operate until the pressure is again above the threshold. Figure 67 shows a schematic layout of the cold piping system.

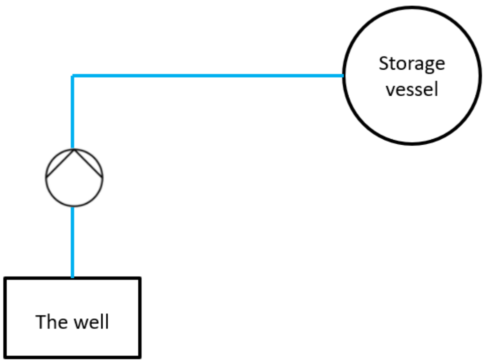

Figure 67: Schematic layout of the cold-water piping system with the pump

After ordering this pump, it became clear that a standard centrifugal pump was delivered. This pump does not work with a pressure but with a float. If the water drops below a certain level the pump starts working. This principle would not be applicable to our system because it was not possible to install a float in the storage tank.

An alternative solution to get pressure in the solar collector tank is using water which is placed higher than the collector. On the highest roof, there is a water storage tank of 10 000 liters that is constantly refilled by an existing pump. After the failed order it was decided to use this storage tank. This tank is at a higher height than the collector tank. By using gravity, this water will automatically flow into the tank under a pressure. In this way, there is no need to use a pump anymore. Figure 68 shows the schematic of this situation.

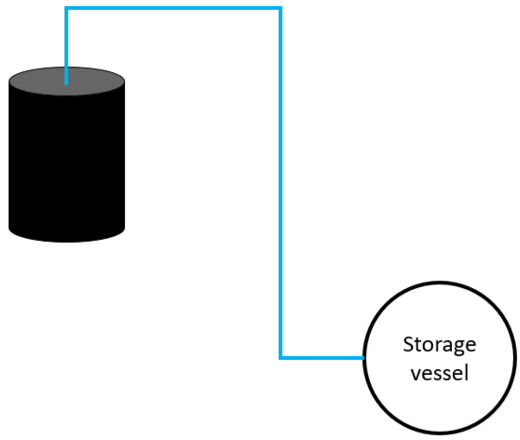

Figure 68: Schematic layout of the cold piping system with the storage tank

Figure 69 shows the cold-water pipe starting from the existing piping of the water tank in the roof. This pipe then goes outside the building (Figure 70) and has a higher position than the collector. This pipe is then routed to the ground (Figure 71).

Figure 69: Cold-water pipe starting from the storage vessel

Figure 70: Cold-water pipe going outside

Figure 71: Cold-water pipe lead to the ground

This pipe is then further routed to the collector tank. Figure 72A and Figure 72B show these pipelines.

Figure 72: Cold-water pipe under the small roof (A), connected to the storage vessel (B)

7.4.2 The hot-water pipe

After installing the cold-water pipe, the hot-water pipe can also be installed. This pipe will eventually end up in the kitchen where the hot water can be used for cooking. Figure 73 shows the hot pipe being laid over the roof. On this figure there is also a small tap on the bottom left. This tap can be used to shut off the hot pipe for maintenance or other practical purposes.

Figure 73: Start of the hot water piping

The hot water line continues to the kitchen. This pipe is shown in Figure 74 in the red circle. This also does not require a pump since the pressure from the water tank on the roof is sufficient. The hot water will flow due to this pressure. However, it will take a while for the hot water to reach the tap due to the amount of water already in the pipe.

Figure 74: Further progression of the hot water pipe

This pipe enters the kitchen through the small window in the right building where the hot pipe comes to its end. The tap at the end of the pipe is shown in Figure 75.

Figure 75: Hot water tap

7.5 The temperature sensor

To ensure that data of the temperature development throughout the day can be collected in a convenient way, a sensor is placed in the collector tank. This sensor will measure the temperature of the water in the tank throughout the day. This temperature will then be shown on a display. Figure 76 shows the temperature sensor on top of the roof. Next to this sensor there is a pressure relief valve. This valve will only open if the tank has a pressure higher than 1MPa inside. In this way a safety has been put in place so that the vessel never has an overpressure that can cause dangerous situations.

Figure 76: Temperature sensor and pressure relief valve

Figure 77 gives a better view of the pressure relief valve where the details of the valve are noted.

Figure 77: Details pressure release valve

The sensor is then guided inside to show the temperature on a display. Figure 78 shows the display, in this case the temperature was equal to 51.3°C.

Figure 78: Temperature display

8. Measurements

With the installation complete, measurements could be conducted. These measurements were done during the week of the 31st of May when the kitchen was operational. During this week, not only the water temperature was monitored, but the environmental temperature and the solar irradiation was also collected to later simulate the water temperature with the same conditions. The water temperature is measured directly from inside the water storage tank. The temperature in °C in shown in Table 21.

Table 21: Water temperature [°C] of the water in the storage tank (31/05/2021-04/06/2021)

Hour	Monday	Tuesday	Wednesday	Thursday	Friday
08:00	34.7	40.3	59.3	48.2	35.8
10:00	36.4	45.3	62.9	48.9	48.4
12:00	45.5	56.7	73.5	69.6	60.1
14:00	52.3	67.9	72.8	69.6	65.1
16:00	55.1	64.3	69.8	69.8	68.9

For the simulations, the outside temperature is needed. These temperatures during the week of the 31st of May is shown in Table 22.

Table 22: Outside temperature [°C] (31/05/2021-04/06/2021)

Hour	Monday	Tuesday	Wednesday	Thursday	Friday
00:00	26	26	25	26	26
01:00	26	26	25	25	26
02:00	27	26	25	24	25
03:00	28	26	25	24	25
04:00	29	27	25	23	25
05:00	30	27	25	23	25
06:00	30	27	25	23	25
07:00	30	28	26	23	25
08:00	30	28	26	25	26
09:00	30	28	27	27	28
10:00	30	29	28	28	28
11:00	30	29	29	29	29
12:00	30	30	29	30	30
13:00	30	29	30	30	30
14:00	30	30	30	30	30
15:00	30	30	30	30	30
16:00	29	30	29	29	29
17:00	28	29	28	28	28
18:00	27	28	27	27	27
19:00	27	27	27	26	26
20:00	26	26	26	26	26
21:00	26	26	26	26	26
22:00	26	25	25	26	26
23:00	26	25	25	26	26

In addition to the outdoor temperature, solar radiation will also have an effect on the simulations. This solar radiation is shown in Table 23 for the week of the 31st May.

Table 23: Hourly solar irradiation [W/m²] (31/05/2021-04/06/2021)

Hour	Monday	Tuesday	Wednesday	Thursday	Friday
00:00	0.0	0.0	0.0	0.0	0.0
01:00	0.0	0.0	0.0	0.0	0.0
02:00	0.0	0.0	0.0	0.0	0.0
03:00	0.0	0.0	0.0	0.0	0.0
04:00	0.0	0.0	0.0	0.0	0.0
05:00	0.0	0.0	0.0	0.0	0.0
06:00	0.0	0.0	0.0	0.0	0.0
07:00	95.51	100.43	104.22	93.4	84.07
08:00	237.5	337.77	342.43	328.08	328.3
09:00	532.82	554.31	543.7	548.21	563.41
10:00	674.42	478.25	714.85	717.15	744.86
11:00	745.92	684.75	804.01	749.27	863.29
12:00	760.42	812.94	806.73	526.58	912.13
13:00	652.99	653.96	667.64	324.97	847.52
14:00	780.39	704.27	794.18	249.88	601.38
15:00	676.72	689.36	662.95	133.94	613.08
16:00	389.19	421.59	482.55	267.08	325.96
17:00	237.0	251.82	239.25	178.95	231.22
18:00	13.99	14.99	14.99	13.99	13.99
19:00	0.0	0.0	0.0	0.0	0.0
20:00	0.0	0.0	0.0	0.0	0.0
21:00	0.0	0.0	0.0	0.0	0.0
22:00	0.0	0.0	0.0	0.0	0.0
23:00	0.0	0.0	0.0	0.0	0.0

Using the data above, the simulation can be adjusted to the correct environmental conditions. Then these simulations can be compared with the measured data from Table 21. From this, it can be decided if the simulations were a qualitative approximation of the real situation. In a perfect situation, both heat gain graphs should be similar throughout the day.

8.1 Heat gain during the day

The collected data can now be plotted to get a better view of the temperature progress during the day, this is show in Figure 79.

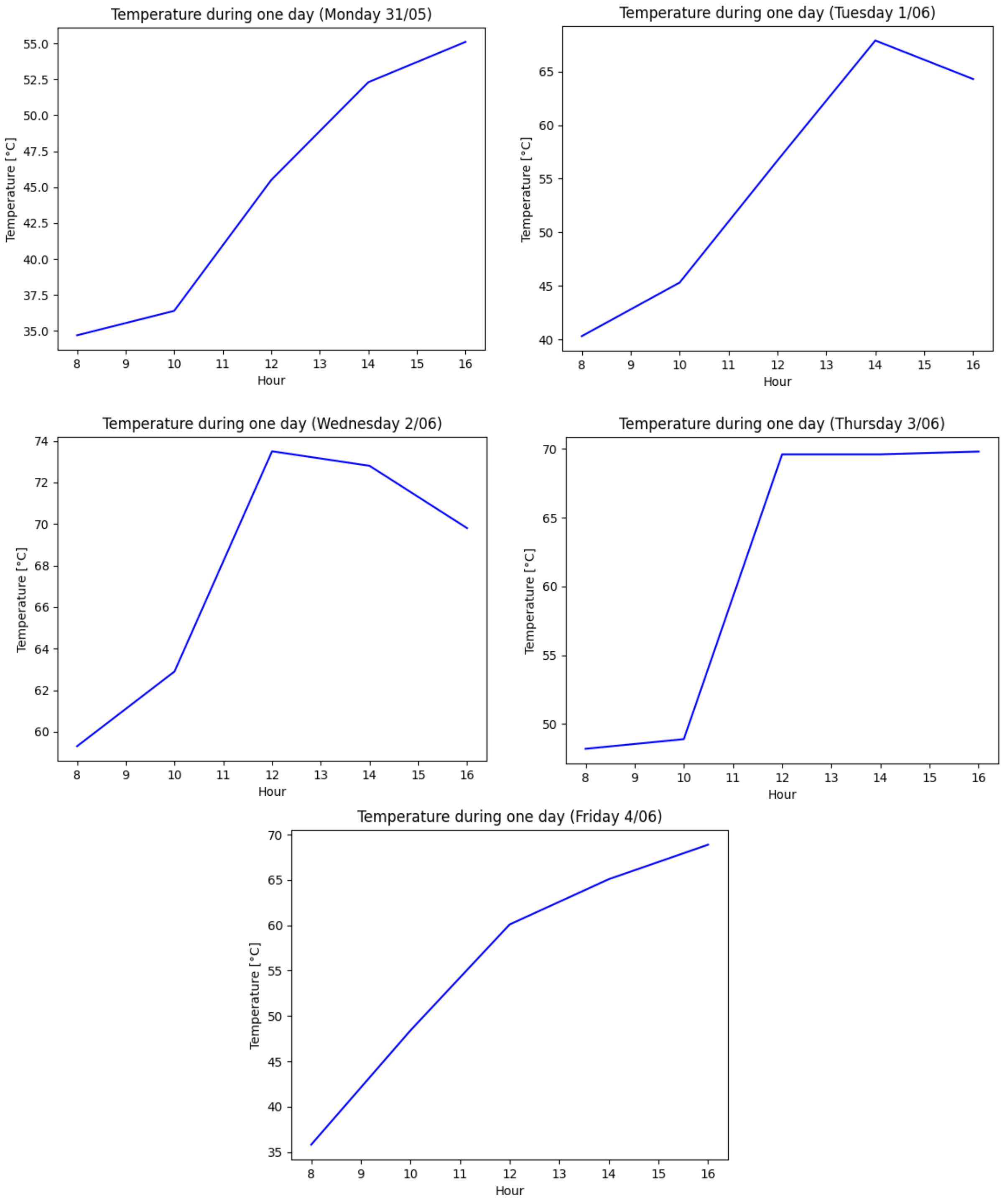

Figure 79: Measured water temperature progression (31/05/2021-04/06/2021)

During the measured interval, an average temperature gain of 21.92 °C is achieved. This sounds like a little gain, but we have to take in account that the timespan of taking data lays between 8 a.m. in the morning and 4 p.m. in the evening. The temperature gain before 8 a.m. and after 4 p.m. was not monitored so no data is available.

Around 12 p.m., a reduction in temperature gain usually occurs. This is due to the usage of hot water. The usual cooking times in the kitchen at the TUM are around 7 a.m. and 12 p.m. Due to the usage of hot water, cold water will be added in the water storage tank. This will cause the temperature of the water to decrease. Unfortunately, the exact cooking times and water usages were not monitored.

From the graphs in Figure 79 and the usual cooking times, the available water temperature can be estimated. The estimates are combined in Table 24 to get a better overview.

Table 24: Estimated water temperature during cooking times [°C] (31/05/2021-04/06/2021)

Hour	Monday	Tuesday	Wednesday	Thursday	Friday
7:00	34.7	40.3	59.3	48.2	35.8
12:00	45.5	56.7	73.5	69.6	68.9

In the morning, water with an average temperature of 43.7 °C is available for cooking. During noon, this average temperature is about 63.8 °C. When assuming the water starts from a temperature of 20 °C, this means a reduction in energy usage of 29.6% in the morning and 54.8% during noon.

8.2 Heat loss during the night

The heat loss during the night can be found by measuring the water temperature in the evening just after the sun sets and in the next morning just before the sun rises. Unfortunately, the collected data starts at 8 a.m., just after the sun rises and stops already at 4 p.m., a few hours before the sun sets. This makes it not possible to compare the actual temperature loss to the simulated temperature loss, so no conclusion can be made here.

However, the results of the simulation can be shown. Now that the correct weather data has been entered into the simulation, the temperature loss can be found. This loss includes the loss during the night as well as during the day and is shown in Table 25.

Table 25: Temperature loss during the day [°C] (31/05/2021-04/06/2021)

Day of the week	Temperature loss during the day [°C]
Monday	2.79
Tuesday	3.38
Wednesday	5.36
Thursday	3.61
Friday	3.05

An average loss of 3.64 °C occurs according to the simulations. The loss on Wednesday is considerably higher than the other days. This is however no surprise because the considerably higher water temperature that day.

8.3 Comparing results with simulations

To get an even better view of the performance of the installation, the collected data can be compared with the earlier performed simulations. This will also give an idea of how accurate the simulations were. These results are plotted in Figure 80.

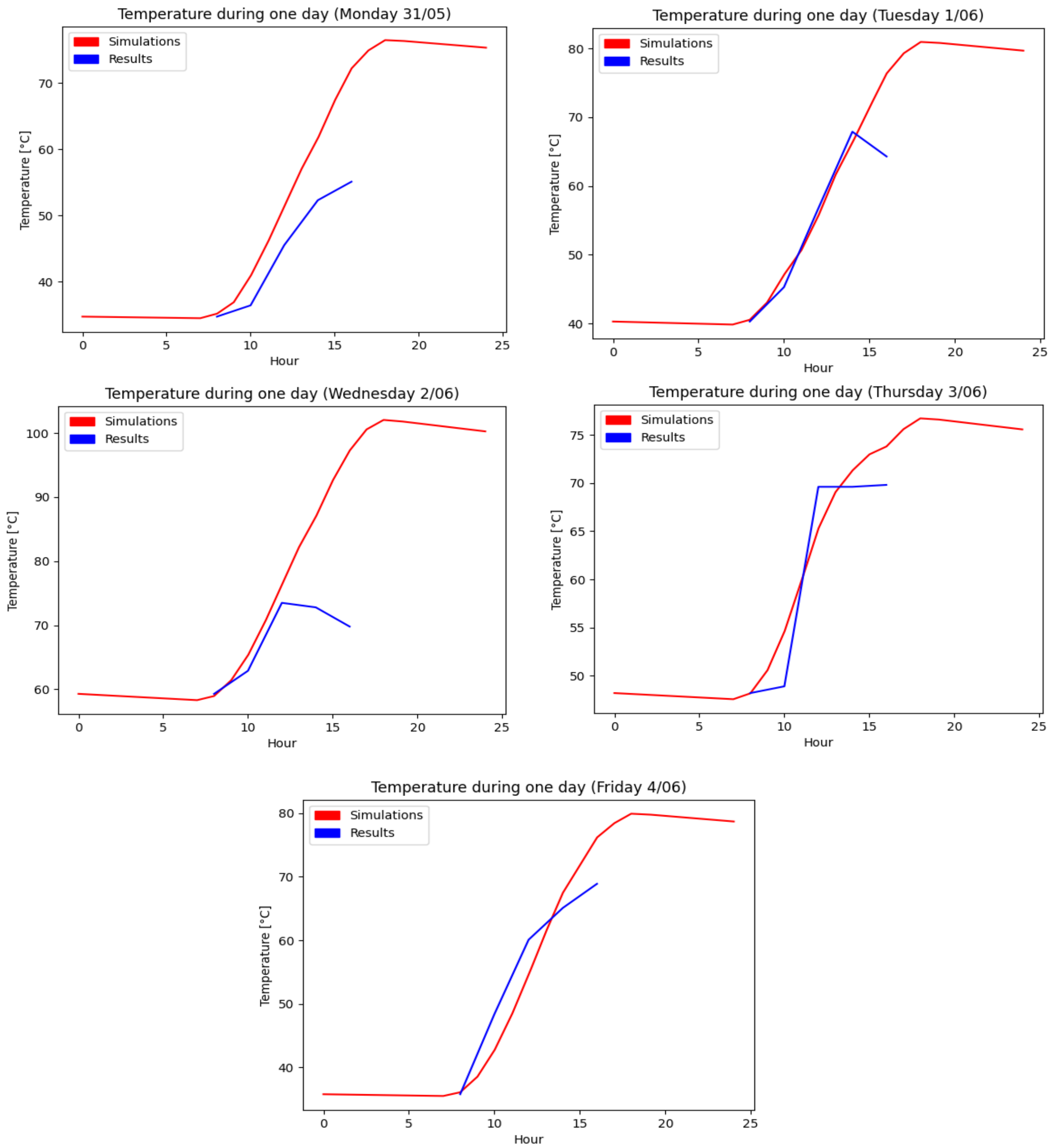

Figure 80: Measured and simulated water temperature progression (31/05/2021-04/06/2021)

As seen in Figure 80, the actual curves tend to follow the simulated ones. The curves also usually start to deviate from the simulated curve around 12 p.m. As explained earlier, this is a result of the usage of the hot water for cooking, which will cause the temperature in the water storage tank to decrease.

The simulations seem to be fairly accurate during the periods of no water usage. However, there is still room for improvement. For example, when the water usage is monitored, the simulation can account for the resulted temperature drop. The data collection also should be automated so that more data points during the day are achieved. This will also make it possible to collect data during the evening and night. This way, the temperature drop during the night can be found to further verify the simulations results.

9. Conclusion

This entire master thesis was a learning process for both of us. This went from determining the best possible solar collector based on a literature review and SWOT analysis. But also setting up the simulations to already get an idea of the performances of the installation. These simulations already gave very promising results where the main objective of 70 °C in the water storage tank was reached.

After these simulations, the real work began, as the installation was actually built. With this building process a lot has been learned about the effective operation of such a system but also what problems can occur that were not accounted for at the beginning. After 3.5 months abroad, the installation is finished and already in use. The question remained whether or not the simulations where accurate.

Based on the measurements in Table 21, a comparison could be made with the simulations. In this section, a brief overview of the obtained results will be given. In Table 26, the maximum water temperatures throughout the day are listed. This table shows that in 3 out of the 5 days, a water temperature of 70 °C is reached. Considering the main objective of reaching 70 °C, this is a positive result.

Table 26: Maximum water temperature [°C] (31/05/2021-04/06/2021)

Day of the week	Maximum water temperature [°C]
Monday	55
Tuesday	67
Wednesday	73.5
Thursday	70
Friday	70

In addition, not only the maximum value is important but also the evolution for the temperature through the day. The evolution of the measured situation was placed next to the simulation. Figure 80 gives a clear picture of these two graphs. It can be concluded that the simulations approach the reality. From this it can be concluded that the simulations are qualitative and therefore give reliable results.

Besides the values for the temperature, one can also look at the energy reduction of the existing cooking process. At the moments that cooking takes place, namely at 7.00 a.m. and 12 p.m., an energy reduction of respectively 29.6% and 54.8% is achieved. Obviously, the reduction will increase as the cooking is moved later in the day, because then the temperature of the water increased more.

From this master thesis it can be concluded that the project was a success all things considered. A reduction in energy costs has been made as well as progress on ecological and ergonomic fronts by reducing the use of fossil fuels.

9.1 The future work

With the solar collector installation almost completed, we can now look at the works that can be done in the future to push the system to its limits. First, the hot water is now stored in the storage tank on the solar collector, this water is then drained when needed. But there is a disadvantage that the water in the hot line cools quickly. When the tap is turned on, it will take a few seconds for the hot water from the storage tank to reach the tap. This could be solved by installing a second barrel. This barrel is then placed in the kitchen so that after the day is over, the water from the storage tank on the collector can run to the second barrel. In this way, the second container is directly at the place where the water is needed and so the hot water will flow instantly from the tap.

In addition, it was mentioned in section 1.3 that this thesis is part of a larger project. This larger project includes the installation of a solar collector but also the installation of a biogas plant. This installation can be coupled to the solar collector so that the entire installation is aligned. The works for linking these installations still needs to be done. From the moment these installations are linked together, the use of LPG and wood fire can be further reduced. The intention is then that the solar collector heats the water to a certain temperature depending on the irradiation. This water will then be used for cooking rice, vegetables or beans. The cooking itself will be done by using biogas. This biogas was extracted from a fermentation process. The digestion process itself takes place at the university in a digester that is fed by food waste from the school itself and local markets and restaurants in the vicinity. This process will release biogas that can be piped to the kitchen. In a perfect situation, the use of LPG and wood can be eliminated. But due to irregularities in feeding of the biogas plant, there will not always be enough biogas available for full biogas cooking. Nevertheless, this coupled system will give a considerable reduction in the use of LPG and wood and thus reduce the harmful gasses produced. The effective reduction cannot yet be determined as the systems have yet to be linked together.

The final work item includes starting lessons around sustainability and the reduction of harmful fuels. When the project is fully completed, lessons will be conducted around sustainability. This project will then give a perfect picture of how this can be done in practice. These lessons can be given not only in the technical university but also by other universities. The project can then receive income by giving these lessons which gives an opportunity to start a master education around sustainable energy inside TUM. In addition, these classes are not only useful for students but also for the local population to gain experience. This experience can then be useful for them when looking for a permanent job.

It can be concluded that this project is a start of something big. First of all, it has given us an experience and it has also learned us a lot. Secondly, the project gives opportunities to the local people and students at various levels. Lastly, it saves money in many areas, and this was the main objective of the project from the beginning.

Bibliography

[1] S. f. e. i. Afrika. [Online]. Available: https://studentsforenergyinafrica.com/nl/. [Accessed February 2021].

[2] S. and J. , *Masterthesis: Solar heater,* Hasselt University & royal university Leuven, 2016.

[3] W. Deferme and M. J. Saulo, *Project proposal,* 2020.

[4] T. u. o. Mombasa. [Online]. Available: https://www.tum.ac.ke/. [Accessed February 2021].

[5] T. u. o. Mombasa, "Fee structures, courses & application guide," [Online]. Available: https://www.tuko.co.ke/269916-technical-university-mombasa-fee-structure-courses-application-guide.html.. [Accessed Novembre 2020].

[6] Skygarden, "Chloride megasun solar water heater 300 litres for salty & hard water," [Online]. Available: https://sky.garden/product/PdZhHcvp. [Accessed March 2021].

[7] Apricus, "Apricus eco-energy," [Online]. Available: https://www.apricus.com/Solar-Hot-Water-Systems.html. [Accessed April 2021].

[8] D. watergroep, "Jouw drinkwater," [Online]. Available: https://www.dewatergroep.be/nl-be/drinkwater/jouw-drinkwater. [Accessed April 2021].

[9] E. B. Chebet, J. K. Kibet en D. Mbui, *The assessment of water quality in river Molo water basin,* Kenya: Applied Water Science, 2021.

[10] W. specialist, "Hoe werkt de restharheid bij een waterontharder," [Online]. Available: https://www.waterontharder-specialist.be/resthardheid. [Accessed April 2021].

[11] Wikipedia, "Uitzettingscoëfficiënt," [Online]. Available: https://nl.wikipedia.org/wiki/Uitzettingsco%C3%ABffici%C3%ABnt. [Accessed Novembre 2020].

[12] SCRIBD, "Density of liquid water from 0 °C to 100 °C: External pressure: 1 atm = 101 325 Pa," [Online]. Available: https://www.scribd.com/doc/131726829/Water-Density. [Accessed Novembre 2020].

[13] T. e. toolbox, "Engineering toolbox," [Online]. Available: https://www.engineeringtoolbox.com/ethylene-glycol-d_146.html. [Accessed 2021 April].

[14] J. D. Vree, „Convectie stroming," [Online]. Available: https://www.joostdevree.nl/shtmls/convectie.shtml. [Geopend November 2020].

[15] phys.ttu.edu, "Unit 19 reading B: Mirrors," [Online]. Available: http://www.phys.ttu.edu/~batcam/Courses/semester%202/Readings/UNIT%2019%20READING%20B%20OPTICS.htm. [Accessed November 2020].

[16] D. Standaard, „De comeback van een groene stroompionier,” 2018. [Online]. Available: https://www.standaard.be/cnt/dmf20180404_03446710. [Geopend September 2020].

[17] I. L. Mohammed, *Design and development of a parabolic dish solar collector,* International journal of engineering research and applications, 2012.

[18] R. Idlimam, A. Bah, M. Asbik, M. Malha en H. Kazdaba, *Impact of the parabolic solar concentrator's rim angle ont the quantity of reglected rays and concentrated fluw on the receiver,* Center for Research on Energy, Higher Normal School of Technical Education-ENSET Mohammed V universtity in Rabat, 2018.

[19] M. P. Collares en J. Chaves, *Improved design for linear fresnel reflector systems,* Advances in Concentrating Solar Thermal Research and Technology, 2017.

[20] K. Lovegrove en J. Pye, *Fundamental principles of concentrating solar power (CSP) systems,* Concentrating Solar Power Technology, 2012.

[21] V. Thakkar, A. Doshi en A. Rana, *Performance analysis methodology for parabolic dish solar concentrators for process heating using thermic fluid,* IOSR Journal of Mechanical and Civil Engineering (IOSR-JMCE), 2015.

[22] S. Tabassum, L. Sharmin, M. S. Bashar, M. Rahaman, S. C. Debnath en M. Khanam, *Design and Analysis of Parabolic Trough Solar Water Heating System,* Dhaka, Bangladesh: Institute of Fuel Research & Development, Bangladesh Council of Scientific and Industrial Research, 2019.

[23] Zwembadprijs, "Solar bol zwembadverwarming," [Online]. Available: https://www.zwembadprijs.nl/zonne-energie-solar-zwembadverwarming/17-solar-bol-zwembadverwarming-zonnecollector-voor-zwembaden-solar-collector-dome.html. [Accessed September 2020].

[24] R. compared, "Robot pool cleaners," [Online]. Available: https://roboticpoolcleanerscompared.com/best-solar-pool-heater-reviews/. [Accessed April 2021].

[25] T. duurzaam, "Soorten zonnecollectoren," [Online]. Available: https://www.technea.nl/product-categorie/leverancier-duurzame-installatietechniek/zonneboilersystemen/soorten-zonnecollectoren/. [Accessed September 2020].

[26] Centraleverwarmingscv, „Zonneboiler: werking, soorten en prijzen,” [Online]. Available: https://www.centraleverwarmingcv.be/zonneboiler-verwarming. [Geopend September 2020].

[27] M. S. Hossain, R. Saidur, H. Fayaz, N. A. Rahim, M. R. Islam, J. U. Ahamed en M. M. Rahman, *Review on solar collector collector and thermal energy performance of circulating pipe,* Elsevier Renewable and Sustainable Energy Reviews, 2011.

[28] R. Tang, Y. Yang en W. Gao, *Comparative studies on thermal performance of water-in-glass evacuated tube solar collectors with different collector tilt-angles,* Yunnan Normal University, Kunming, China: Laboratory of Advanced Technology and Preparation for Renewable Energy Materials, 2011.

[29] F. Struckmann, *Analysis of a Flat-plate Solar Collector,* Sweden: Dept. of Energy Sciences, Faculty of Engineering, Lund University, 2008.

[30] G. L. Morrison, I. Budihardio en M. Behnia, *Measurement and simulation of flow rate in a water-in-glass evacuated tube solar collector,* Sydney, Australia: School of Mechanical and Manufacturing Engineering, University of New South Wales, 2004.

[31] R. Daghigh en A. Shafieian, *Theoretical and experimental analysis of thermal performance of a solar water heating system with evacuated tube heat pipe collector,* Kurdistan, Iran: Department of Mechanical Engineering, University of Kurdistan, 2016.

[32] Wikipedia, "Batch solar thermal collector," [Online]. Available: https://en.wikipedia.org/wiki/File:Batch_solar_thermal_collectorColour.jpg. [Accessed September 2020].

[33] Pinterest, "Solar panels DIY," [Online]. Available: https://www.pinterest.com/bestdiyblog/solar-panels-diy/. [Accessed April 2021].

[34] J. Varghese, G. K. Awari en M. P. Singh, *Experimental analysis of distinct design of a batch solar collector with integrated collector storage system,* Thermal Science, 2007.

[35] B. O. Bolaji, *Flow design and collector performance of a natural circulation solar water heater,* Akure, Nigeria: Department of mechanical engineering, federal university of technology, 2006.

[36] A. Matveev , S. Shcheklein en V. Pahaluev, *Determination of consumption of heat-transfer agent and productivity of thermosyphon waterheating system with flat-plate solar collector,* Yeltsin, Russia: Department of Nuclear power plants and renewable energy sources, 2015.

[37] Werktuigbouw.nl, "Stromingsweerstand in pijpleiding," [Online]. Available: https://www.werktuigbouw.nl/calculators/pipeflow_fluid.htm. [Accessed November 2020].

[38] Wikipedia, „Warmteoverdracht," [Online]. Available: https://nl.wikipedia.org/wiki/Warmteoverdracht. [Geopend February 2021].

[39] T. Tiempo, "Solar radiation in Mombasa," [Online]. Available: https://en.tutiempo.net/solar-radiation/mombasa.html. [Accessed March 2021].

[40] T. Tiempo, "Solar radiation in Bilzen," [Online]. Available: https://en.tutiempo.net/solar-radiation/bilzen.html. [Accessed March 2021].

[41] P. Mwakio, „REREC now eyes partnership with counties to establish Energy Centres," *The standard,* 2019.

[42] C. Exide. [Online]. Available: https://www.chlorideexide.com/. [Accessed April 2021].

[43] Sollatek. [Online]. Available: https://sollatek.co.ke/. [Accessed April 2021].

[44] Remon, „Leidingen schoonmaken / reinigen," [Online]. Available: https://www.remon.com/waterzuivering/leidingen-schoonmaken-reinigen. [Geopend April 2021].

[45] Wikipedia, "Biofilm," [Online]. Available: https://nl.wikipedia.org/wiki/Biofilm. [Accessed April 2021].

[46] Livios, „Wat is levensduur van koperen verwarmingsbuizen?," [Online]. Available: https://www.livios.be/nl/bouwinformatie/technieken/verwarming-en-koeling/centrale-verwarming/vraag/30807/wat-is-levensduur-van-koperen-verwarmingsbuizen/. [Geopend April 2021].

[47] R. Biersteker, *Bepaling corrosiesnelheid van koperen leidingen voor en na de AquaCell waterontharder,* Den Helder: TNO Innovation for life, 2012.

[48] Farys, "Hoeveel water verbruiken wij gemiddeld?," [Online]. Available: https://www.farys.be/nl/hoeveel-water-verbruiken-wij-gemiddeld. [Accessed April 2021].

[49] W. advies, "Prijs waterontharder," [Online]. Available: https://www.waterontharder-advies.nl/prijs-waterontharder#:~:text=Gemiddelde%20prijs%20voor%20een%20waterontharder&text=Voor%20een%20instapmodel%20mag%20je,tussen%201.000%20en%202.000%20euro.. [Accessed April 2021].

[50] K. waterontharder, "Waterontharder," [Online]. Available: https://kosten-waterontharder.be/. [Accessed April 2021].

[51] P. P. systems, "Solar water Heating," Kenia.

[52] S. castings, "Magnesium anodes," [Online]. Available: https://www.specialistcastings.com/anodes/sacrificial-anodes/magnesium-anodes/. [Accessed April 2021].

[53] S. Pramudity, "Water thermodynamic properties," ITB Physics department , [Online]. Available: http://portal.fi.itb.ac.id/tecdoc/waterprop. [Accessed November 2020].

Attachments

Attachment A: Datasheet solar collector form company Sollatek

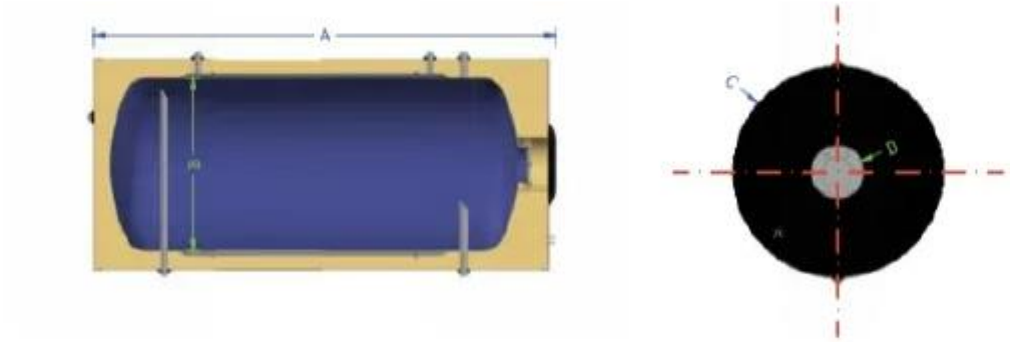

	ECO SXF TYPE	120	150	200	250	300
	Gross Capacity (lt)	116	144	199	242	295
A	Tank's Length (mm)	1065	1285	1285	1555	1785
B	Main Tank's Diameter (mm)	Ø400	Ø400	Ø480	Ø480	Ø480
C	External Diameter (mm)	Ø500	Ø500	Ø580	Ø580	Ø580
	Jacket's Surface (m²)	0,54	0,64	0,81	1,01	1,55
	Jacket's Capacity (lt)	6	8	9	12	19
D	Flange Diameter (mm)	Ø140	Ø140	Ø140	Ø140	Ø140
	Weight	44	54	68	84	100

TECHNICAL FEATURES	UNIT OF	COLLECTOR'S TECHNICAL STANDARDS H98			
TYPE		H81 - 12	H81 - 15	H81 - 20	H81 - 25
Outer dimensions (height x width x thickness)	mm	1250x960x80	1455x960x80	1960x960x80	1960x1210x80
Total surface	m²	1.20	1.40	1.88	2.38
Window surface	m²	1.15	1.35	1.83	2.33
Absorber capacity	m²	1.15	1.35	1.83	2.33
Χωρητικότητα απορροφητή	L	1.1	1.3	1.6	1.9
Frame / Thickness	mm	painted aluminum sheet / 0.5			
Glass panel		Tempered			
Thermal insulation(shoulders) Thickness/Density	mm / Kg/ m³	Stone wool / 30 / 50 A material properly designed for collectors, chemically inert, its qualities remain unchanged over time and it does not allow parasites to evolve			
Absorber		Harp-shaped bronze frame, aluminum selective coating on a panel **(Full face)** – laser welding			
• Absorption capacity	%	95			
• Transmission	%	5			
• Header Cu Ø / Thickness	mm	22 / 0,7			
• Riser Cu Ø /Thickness	mm	8 / 0,40			
• Risers	Pcs	8	8	8	11
• Cu welding Ø 22		4 or 2			
• Maximum operation pressure	Bar	10			
Means of heat transmittal		Mixture of water and anti-freeze (monopropylen-glycol)			
Layout		vertical			
Weight (Dry & Packaged)	Kg	21.5	24.5	32.5	40.5